PARALLEL STUDIES ON REPLICATION PATTERNS OF INFECTIOUS LARYNGOTRACHEITIS VIRUS (ILTV) IN THE RESPIRATORY TRACT AND THE ONSET OF LOCAL IMMUNITY IN THE HEAD-ASSOCIATED LYMPHOID TISSUE (HALT) OF INFECTED AND VACCINATED CHICKENS

by

LETICIA GABRIELA BELTRÁN GARZA

(Under the Direction of Maricarmen García)

ABSTRACT

Infectious laryngotracheitis (ILT) is an acute upper respiratory tract infection causes by *Gallid alpha herpesvirus type 1* (GaHV-1) given the common name - Infectious laryngotracheitis virus (ILTV). Currently vaccination, with either live-attenuated and/or recombinant viral vector vaccines, is the main tool used to control the disease. Both live attenuated vaccines, (of chicken embryo origin (CEO) and of tissue culture origin (TCO)) are administered by the mucosal route. Vaccines given on mucosal tissues in the head induce effective protection against infection. The head-associated lymphoid tissue (HALT) is comprised of nasal-associated lymphoid tissue (NALT), conjunctiva-associated lymphoid tissue (CALT) and the Harderian gland (HG). These are located in the anatomical site of ILTV entry, and are important for the initiation of immunity by interaction of virus with local organized lymphoid tissues after ocular vaccination of chickens. The focus of this dissertation was to demonstrate the dynamics of B and T cells (but not γδ T cells), and mononuclear phagocytes in the CALT and HG following vaccine or exposure to virulent ILTV. In summary, this study showed that entry of the virus onto mucosal

tissues of the head dictated the level ILTV replication in the upper and lower respiratory tract, and consequently influenced the outcome of infection. Further, the results of these experiments revealed important dynamic changes in the number of B cells, T cells and macrophages in HALT and HG following vaccination or exposure to virulent ILTV virus. Furthermore, this study underscored distinctive roles for CALT and HG during viral replication associated with CEO vaccination or virulent virus, and provided an indication that ILTV can circumvent the local immune activation, by delaying innate responses and downregulating MHC class II cellular expression. This knowledge will be critical to the future development of live attenuated vaccines and viral vector, or subunits vaccines that effectively trigger virus specific T cell responses after mucosal vaccination via eye-drop, in drinking water or by aerosol spray

INDEX WORDS: ILTV, CALT, HG, Cell-mediated immunity, Avian mononuclear phagocytes.

PARALLEL STUDIES ON REPLICATION PATTERNS OF INFECTIOUS LARYNGOTRACHEITIS VIRUS (ILTV) IN THE RESPIRATORY TRACT AND THE ONSET OF LOCAL IMMUNITY IN THE HEAD-ASSOCIATED LYMPHOID TISSUE (HALT) OF INFECTED AND VACCINATED CHICKENS

by

LETICIA GABRIELA BELTRÁN GARZA

Médico Veterinario Zootecnista, Universidad Autónoma de Nuevo León, México, 2008

A Dissertation Submitted to the Graduate Faculty of The University of Georgia in Partial Fulfillment of the Requirements for the Degree

DOCTOR OF PHILOSOPHY

ATHENS, GEORGIA

2018

PARALLEL STUDIES ON REPLICATION PATTERNS OF INFECTIOUS LARYNGOTRACHEITIS VIRUS (ILTV) IN THE RESPIRATORY TRACT AND THE ONSET OF LOCAL IMMUNITY IN THE HEAD-ASSOCIATED LYMPHOID TISSUE (HALT) OF INFECTED AND VACCINATED CHICKENS

by

LETICIA GABRIELA BELTRÁN GARZA

Major Professor:	Maricarmen García
Committee:	Guillermo Zavala
	Susan M. Williams
	David J. Hurley
	Stephen Spatz

Electronic Version Approved:

Suzanne Barbour
Dean of the Graduate School
The University of Georgia
December 2018

DEDICATION

I would like to dedicate this dissertation to my parents, Ignacio and Lety. Thank you very much for your love and for always having the words to encourage me to pursue my goals. I would also like to dedicate this work to my brothers, Nacho and Roberto, and my best friends Karina and Jason. I could not have achieved this without your love and support. Lastly, this work is dedicated to my lovely grandparents, Cipriano, Ramona, Raymundo and Socorro. Thank you for always believing in me and for your blessings; they come with me wherever I go.

ACKNOWLEDGEMENTS

First, I would like to acknowledge my advisor, Dr. Maricarmen García. Thank you very much for your guidance and for taking a chance on me as your graduate student without knowing much about me. Working in your laboratory was a life experience that I will always remember with gratitude and love.

I would also like to acknowledge the members of my committee, Dr. Zavala, Dr. Susan Williams, Dr. Hurley, and Dr. Steve Spatz. Thank you very much for the time you have taken serving on my committee and for your advice and feedback, which helped guide my research.

To my family and friends, thank you for your unconditional love and support through this experience.

Finally, I would like to thank Sylva Riblet, who was a key and essential element in the realization of this work. I could never finish this research without your help and for that I will always be very thankful

TABLE OF CONTENTS

Page

LIST OF TABLES

Page

LIST OF FIGURES

Page

CHAPTER 1

INTRODUCTION

Infectious laryngotracheitis (ILT) is a highly contagious acute respiratory disease of chickens. The disease is caused by *Gallid alpha herpesvirus 1 (GaHV-1)* commonly known as infectious laryngotracheitis virus (ILTV), a member of the genus *Iltovirus*, subfamily *alphaherpesviridae* of the *Herpesviridae* family within the order *Herpesvirales* (Davison, 2010). ILT is an economically significant disease of poultry that can result in severe losses due to mortality and/or decrease in egg production in areas with large poultry concentrations and intensive poultry production. The use of live-attenuated and/or recombinant viral vector vaccines expressing ILTV proteins are the major measures utilized to control the disease. Among live-attenuated vaccines there are two main types; the tissue culture origin (TCO) vaccine (Gelenczei & Marty, 1965); and chicken embryo origin (CEO) vaccines (Samberg et al., 1971). Both, CEO and TCO vaccines are administered through the ocular, oral and intranasal mucosal routes to elicit local immunity (Gelenczei & Marty, 1964; Fulton et al., 2000). Although these vaccines are routinely used in the field, little is known about the essential components associated with vaccine-induced protection.

When ILTV enters through the respiratory and ocular route both field virus and the vaccine strain establish a primary lytic infection in the epithelium of the conjunctiva, nasal cavity and the trachea (Bang & Bang, 1967; García et al., 2013). In a recent study, it was demonstrated that ILTV can cross the basal membrane of the conjunctiva and tracheal epithelium (Reddy et al., 2014). In addition to the conjunctiva and the respiratory tract, dissemination of the virus to other

tissues in the body has been documented (Purcell & McFerran, 1969; Oldoni et al., 2009; Wang et al., 2013; Zhao et al., 2013; Davidson et al., 2016). However, evidence of productive ILTV replication in peripheral blood lymphocytes has not yet been described, but it has been demonstrated that monocyte-derived macrophages support a semi-productive ILTV infection. This semi-productive infection is characterized by a low level production of viral particles with significant expression of viral antigen and the production of syncytia (Calnek et al., 1986; Coppo et al., 2018). Apart from this finding, not much is currently know about the interaction of ILTV with macrophages during the course of acute infection. The original studies of ILTV immunity demonstrated a central role for cell-mediated immunity, particularly T cells in vaccine protection and the resistance to development of disease. Immunized bursectomized chickens were protected against disease after challenge, but immunized-thymectomized chickens were not (Fahey et al., 1983; Fahey et al., 1984; Honda et al., 1994). Recent findings highlight the pivotal role of ILTV interactions with the immune system and their association with viral virulence and disease outcome. For example evidence that ILTV down-regulates type I interferon, delays transcription of inflammatory genes (Coppo et al., 2018; Vagnozzi et al., 2018), and eventually modulates the development of the adaptive immune response in the trachea appears to favor viral replication and induction of disease (Coppo et al., 2013). These findings highlight ILTV interactions with the immune system and the pivotal role of viral immune modulation in viral pathogenesis.

One of the primary differences between the avian and mammalian immune systems is the absence of lymph nodes and lymphatic vessels in birds (Balic et al., 2014). In chickens lymphocytes transit through the blood to secondary central and mucosal lymphoid tissues. These are: spleen (as the primary central secondary immune site), and a network of mucosal-associated

lymphoid tissues (MALT), and a diffused system of small local lymphoid aggregates (Balic et al., 2014).

The head of the chicken has a large network of mucosal-associated lymphoid tissues. These contribute to the function of mucosal vaccination of poultry. This netwrok is defined as head-associated lymphoid tissue (HALT) and is primarily comprised by the nasal-associated lymphoid tissue (NALT), the conjunctiva-associated lymphoid tissue (CALT) and the Harderian gland (HG). The chicken NALT harbors organized lymphoid structures and it has been identified as a site for antigen uptake (by antigen presenting cells) in the head (de Geus et al., 2015). The eye associated lymphoid tissues; CALT and HG are involved in the generation of innate mucosal and cell-mediated immune responses in support of the upper airways (van Ginkel et al., 2009; Toro et al., 2011; Gurjar et al., 2013). The development of immune responses in these mucosal tissues is under the control of a complex network of mononuclear phagocytes (MNP) comprised monocytes, macrophages, and conventional dendritic cells (Paul, 2013). An indication that both dendritic cells (DC's) and avian macrophages can function as antigen-presenting cells (APCs) is supported by the fact that both cell types express pathogen recognition receptors (PRRs) (Wu & Kaiser, 2011). In addition to PRRs, both chicken macrophages and dendritic cells express colony-stimulating factor 1 receptor (CSF1R), a key component of avian APC function (Sutton et al., 2018).

After infection or vaccination via the respiratory system, antigens is recognized and taken up by phagocytic cells - macrophages and dendritic cells. In contrast to mammals, where DCs and macrophages are found in high numbers in the alveolar spaces and in the lung parenchyma (de Heer et al., 2005), avian lung macrophages are primarily found lining the parabronchi (Maina, 2002) and sequestered in the connective tissue (Klika et al., 1996). Sampling of

exogenous antigen on the mucosa-associated lymphoid tissues of the upper respiratory tract occurs across the mucosal surface through the actions of a specialized follicle-associated epithelium (FAE) that contains epithelial microfold cells (M cells) and by mucosal dendritic cells (Fix & Arp, 1991; Kang et al., 2013; Paul, 2013). It appears that chicken FAE display the same characteristics as mammalian M cells and aid in the rapid localization and active transport of antigens from the luminal space to the lamina propria of the mucosal-associated lymphoid tissues (de Geus et al 2015).

Although it has been clearly documented that respiratory mucosal vaccination with ILTV live attenuated vaccines induces robust protection against development of disease (Fulton et al., 2000; Vagnozzi et al., 2012), the level of post-vaccinal ILTV replication in the mucosal tissues of the conjunctiva, nasal cavity and Harderian gland have not been fully studied. Furthermore, the elements of the cell-mediated immune responses that provide protection in the head, and their dynamics in associated lymphoid tissue (HALT) remain unknown. This knowledge is necessary to allow the development of better and more effective live attenuated, viral vector, or subunits vaccines. Further, this understanding could be used to develop novel adjuvants that would effectively target the mucosal tissues during eye-drop, drinking water or aerosol vaccination.

Our central hypothesis was that immune responses initiated in the head-associated lymphoid tissues (HALT) would direct and regulate the level of ILTV replication in the upper and lower respiratory tract, and influence the overall outcome of infection. The first objective of this thesis was to evaluate the replication patterns of the virulent strain 63140 and the CEO vaccine virus in the conjunctiva, (HG), upper and lower respiratory tract after mucosal exposure by the ocular, oral, intranasal or intra-tracheal routes. The second objective was the assessment

of the innate and adaptive cell-mediated immune responses elicited in the eye-associated lymphoid tissues (CALT and HG) after ocular inoculation with CEO and 63140 viruses. This was accomplished by monitoring dynamics of B and T cell populations relative to ILTV exposure in the tissues. Cellular expression of the major histocompatibility complex (MHC) type I and II antigens, and levels of cytokines transcription associated with the dynamics of immune cells were evaluated. A third objective was added, to assess the dynamics of mononuclear phagocyte (MNP) in the CALT and HG after ocular exposure to CEO and 63140 virus by quantifying the surface expression on CSF1R positive cells. As a further test of viral-MNP interaction, monocyte-derived macrophages (MDM) cultures were used to assess the replication of CEO and 63140 viruses, and to determine if these viruses induced apoptosis in MDMs

REFERENCES

Balic, A., Garcia-Morales, C., Vervelde, L., Gilhooley, H., Sherman, A., Garceau, V., Gutowska, M. W., Burt, D. W., Kaiser, P., Hume, D. A., Sang, H.M. (2014). Visualisation of chicken macrophages using transgenic reporter genes: Insights into the development of the avian macrophage lineage. *Development, 141*, 3255-3265.

Bang, B.G., & Bang, F.B. (1967). Laryngotracheitis virus in chickens. A model for study of acute nonfatal desquamating rhinitis. *The Journal of Experimental Medicine, 125*, 409-428.

Calnek, B.W., Fahey, K.J., & Bagust, T.J. (1986). In vitro infection studies with infectious laryngotracheitis virus. *Avian Diseases, 30*, 327-336.

Coppo, M.J., Hartley, C.A., & Devlin, J.M. (2013). Immune responses to infectious laryngotracheitis virus. *Developmental and Comparative Immunology, 41*, 454-462.

Coppo, M.J.C., Devlin, J.M., Legione, A.R., Vaz, P.K., Lee, S.W., Quinteros, J.A., Gilkerson, J. R., Ficorilli, N., Reading, P. C., Noormohammadi, A. H., Hartley, C.A. (2018). Infectious laryngotracheitis virus viral chemokine-binding protein glycoprotein g alters transcription of key inflammatory mediators in vitro and in vivo. *Journal of Virology, 92*.

Davidson, I., Raibshtein, I., Altori, A., & Elkin, N. (2016). Infectious laryngotracheitis virus (ILTV) vaccine intake evaluation by detection of virus amplification in feather pulps of vaccinated chickens. *Vaccine, 34*, 1630-1633.

Davison, A.J. (2010). Herpesvirus systematics. *Veterinary Microbiology, 143*, 52-69.

de Geus, E.D., Degen, W.G., van Haarlem, D.A., Schrier, C., Broere, F., & Vervelde, L. (2015). Distribution patterns of mucosally applied particles and characterization of the antigen presenting cells. *Avian Pathology, 44*, 222-229.

de Heer, H.J., Hammad, H., Kool, M., & Lambrecht, B.N. (2005). Dendritic cell subsets and immune regulation in the lung. *Seminars in Immunology, 17*, 295-303.

Fahey, K.J., Bagust, T.J., & York, J.J. (1983). Laryngotracheitis herpesvirus infection in the chicken: The role of humoral antibody in immunity to a graded challenge infection. *Avian Pathology, 12*, 505-514.

Fahey, K.J., York, J.J., & Bagust, T.J. (1984). Laryngotracheitis herpesvirus infection in the chicken. Ii. The adoptive transfer of resistance with immune spleen cells. *Avian Pathology, 13*, 265-275.

Fix, A.S., & Arp, L.H. (1991). Quantification of particle uptake by conjunctiva-associated lymphoid tissue (CALT) in chickens. *Avian Diseases, 35*, 174-179.

Fulton, R.M., Schrader, D.L., & Will, M. (2000). Effect of route of vaccination on the prevention of infectious laryngotracheitis in commercial egg-laying chickens. *Avian Diseases, 44*, 8-16.

García, M., Spatz, S., & Guy, J. (2013). Infectious laryngotracheitis. In D. E. Swayne, J. R. Glisson, L. R. McDougland, L.K. Nolan, D. L. Suarez & V. L. Nair (Eds.), *Diseases of poultry 13th edn* (pp. 161-179): Ames, Iowa: Wiley-Blackwell.

Gelenczei, E.F., & Marty, E.W. (1964). Studies on a tissue-culture-modified infectious laryngotracheitis virus. *Avian Diseases, 8*, 105-122.

Gelenczei, E.F., & Marty, E.W. (1965). Strain stability and immunologic characteristics of a tissue-culture-modified infectious laryngotracheitis virus. *Avian Diseases, 9*, 44-56.

Gurjar, R.S., Gulley, S.L., & van Ginkel, F.W. (2013). Cell-mediated immune responses in the head-associated lymphoid tissues induced to a live attenuated avian coronavirus vaccine. *Developmental and Comparative Immunology, 41*, 715-722.

Honda, T., Okamura, H., Taneno, A., Yamada, S., & Takahashi, E. (1994). The role of cell-mediated immunity in chickens inoculated with the cell-associated vaccine of attenuated infectious laryngotracheitis virus. *The Journal of Veterinary Medical Science, 56*, 1051-1055.

Kang, H., Yan, M., Yu, Q., & Yang, Q. (2013). Characteristics of nasal-associated lymphoid tissue (nalt) and nasal absorption capacity in chicken. *PLoS One, 8*, e84097.

Klika, E., Scheuermann, D.W., De Groodt-Lasseel, M.H., Bazantova, I., & Switka, A. (1996). Pulmonary macrophages in birds (barn owl, tyto tyto alba), domestic fowl (gallus gallus f. Domestica), quail (coturnix coturnix), and pigeons (columbia livia). *The Anatomical Record, 246*, 87-97.

Maina, J.N. (2002). Some recent advances on the study and understanding of the functional design of the avian lung: Morphological and morphometric perspectives. *Biological Reviews of the Cambridge Philosophical Society, 77*, 97-152.

Oldoni, I., Rodriguez-Avila, A., Riblet, S.M., Zavala, G., & García, M. (2009). Pathogenicity and growth characteristics of selected infectious laryngotracheitis virus strains from the united states. *Avian Pathology, 38*, 47-53.

Paul, W.E. (2013). Fundamental immunology. *Philadelphia : Wolters Kluwer Health/Lippincott Williams & Wilkins*.

Purcell, D.A., & McFerran, J.B. (1969). Influence of method of infection on the pathogenesis of infectious laryngotracheitis. *Journal of Comparative Pathology, 79*, 285-291.

Reddy, V.R., Steukers, L., Li, Y., Fuchs, W., Vanderplasschen, A., & Nauwynck, H.J. (2014). Replication characteristics of infectious laryngotracheitis virus in the respiratory and conjunctival mucosa. *Avian Pathology, 43*, 450-457.

Samberg, Y., Cuperstein, E., Bendheim, U., & Aronovici, I. (1971). The development of a vaccine against avian infectious laryngotracheitis. Iv. Immunization of chickens with a modified laryngotracheitis vaccine in the drinking water. *Avian Diseases, 15*, 413-417.

Sutton, K., Borowska, D., Katrina, M., Balic, A., & Vervelde, L. (2018). Identification and characterisation of antigen-presenting cells in the chicken spleen. *XV Avian Immunology Research Group (AIRG) Meeting*.

Toro, H., Suarez, D.L., Tang, D.C., van Ginkel, F.W., & Breedlovea, C. (2011). Avian influenza mucosal vaccination in chickens with replication-defective recombinant adenovirus vaccine. *Avian Diseases, 55*, 43-47.

Vagnozzi, A., Zavala, G., Riblet, S., Mundt, A., & Garcia, M. (2012). Protection induced by commercially available live-attenuated and recombinant viral vector vaccines against infectious laryngotracheitis virus in broiler chickens. *Avian Pathology, 41*, 21-31.

Vagnozzi, A.E., Beltran, G., Zavala, G., Read, L., Sharif, S., & Garcia, M. (2018). Cytokine gene transcription in the trachea, harderian gland, and trigeminal ganglia of chickens inoculated with virulent infectious laryngotracheitis virus (ILTV) strain. *Avian Pathology*, 1-12.

van Ginkel, F.W., Tang, D.C., Gulley, S.L., & Toro, H. (2009). Induction of mucosal immunity in the avian harderian gland with a replication-deficient ad5 vector expressing avian influenza h5 hemagglutinin. *Developmental and Comparative Immunology, 33*, 28-34.

Wang, L.G., Ma, J., Xue, C.Y., Wang, W., Guo, C., Chen, F., Cao, Y.C. (2013). Dynamic distribution and tissue tropism of infectious laryngotracheitis virus in experimentally infected chickens. *Archives of Virology, 158*, 659-666.

Wu, Z., & Kaiser, P. (2011). Antigen presenting cells in a non-mammalian model system, the chicken. *Immunobiology, 216*, 1177-1183.

Zhao, Y., Kong, C., Cui, X., Cui, H., Shi, X., Zhang, X., Hu, S., Hao, L.,. Wang, Y. (2013). Detection of infectious laryngotracheitis virus by real-time pcr in naturally and experimentally infected chickens. *PLoS One, 8*, e67598.

CHAPTER 2

LITERATURE REVIEW

ETIOLOGICAL AGENT

Classification

Gallid alpha herpesvirus type 1 (GaHV-1) also known as Infectious laryngotracheitis virus (ILTV) is a member of the genus *Iltovirus*, subfamily *alphaherpesviridae* of the *Herpesviridae* family (Davison et al., 2010).

Viral Structure and Genome

Electron microscopy revealed that ILTV particles exhibit the typical morphology of herpesvirus virions consisting of an icosahedral nucleocapsid surrounded by a tegument layer containing proteins that are encapsulated by an outer envelope with integrated viral glycoproteins on its surface (Cruickshank et al., 1963; Roizman & Pellett, 2001).

The ILTV genome is a single linear double-stranded molecule which is enclosed in the nucleocapsid. The ILTV genome contains a unique long (U_L) and unique short (U_S) regions flanked by two 11 kb inverted repeats (internal repeat and terminal repeat) (Leib et al., 1987; M. A. Johnson et al., 1991). Full genome sequence of four virulent United States (U.S.) isolates determined that on average, the total length of the ILTV genome is 151,607 nucleotides (nt) with unique long and unique short regions of 111,275 and 13,094 nt, respectively, and 13,619 nt comprising the inverted repeats (Spatz et al., 2012). The ILTV genome also contains 79 open reading frames (ORFs) of which 64 are located within the U_L, eight within the U_S, six within the

inverted repeats, and one spanning the U_S/TR_S junction (Ziemann et al., 1998; García et al., 2013).

With the exception of eight ORFs (ORFs A, B, C, D, E, F, U_L-0 and U_L-1) that are unique to the members of the *Iltoviruses* genus, the U_L1 to U_L54, U_S2 to U_S8, U_S10, and 12 ORFs genes encode glycoproteins homologous to *Herpes Simplex Virus-1* (HSV-1) (gB, gC, gD, gE, gG, gH, gI, gJ, gK, gL, gN and gM) (McGeoch et al., 1988). These glycoproteins are involved in viral attachment and entry, cell fusion and viral egress. The ILTV U_L47 gene (tegument protein) is located in the U_S region rather than in the UL as in other alphaherpesviruses. Also the ILTV genome contains a unique large internal inversion of a conserved gene cluster from U_L22 (envelop glycoprotein H) to U_L44 (envelope glycoprotein C) (Fuchs et al., 2007).

In addition to their role in host range and pathogenicity, the glycoproteins of ILTV are immunogenic and stimulate the humoral and cell-mediated immune responses (York et al., 1989; Fahey & York, 1990). Twelve glycoprotein-coding genes have been identified in the ILTV genome and are designated gB, gC, gD, gE, gG, gH, gI, gJ, gK, gL, gM and gN (Thureen & Keeler, 2006). Based on antibody responses and monoclonal antibodies, the envelope glycoprotein J and C are the most abundantly expressed surface glycoproteins of ILTV (Fuchs et al., 2005). The gB (Poulsen et al., 1991; Poulsen & Keeler, 1997), gC (Spear, 1993; Kingsley et al., 1994), gN (Fuchs & Mettenleiter, 2005) and gJ (Veits et al., 2003) were characterized as functional HSV-1 homologues. The glycoprotein G (gG) of ILTV functions as a broad-spectrum chemokine binding protein (vCKBP) and as a virulence factor. The secreted form of viral gG binds to host chemokines blocking the interaction between the chemokine and its receptor,

consequently inhibiting the chemokine activity, which alters the type of cells that are recruited to the trachea (Devlin et al., 2010).

MicroRNAs are a class of small non-coding RNA molecules found in plants, animal, and viral genomes. These molecules play an important role in regulating the expression of many viral and cellular genes at the post-transcriptional level. The ILTV genome encodes 10 microRNAs (miRNAs) of approximately 22 nt long (Rachamadugu et al., 2009). Four of the ILTV microRNAs, the miR-I1, miR-I2, miR-I3, and miR-I4 are located at the extreme 5` terminus of the genome and they are not associated with any annotated ORFs (Yao & Nair, 2014). The miR-I5 and miR-I6 are the two most highly expressed miRNAs by ILTV and are mapped in the repeat regions within ICP4. The ILTV miR-I7 is mapped in the replication origin (*OriL*) located near the binding site of the origin-binding-protein U_L9 (Yao & Nair, 2014). The regulatory roles of these microRNAs in viral or host transcription/translation processes are still unknown.

Virus Life Cycle

The replication cycle of ILTV initiates with the viral attachment to the cell receptor following fusion of the viral envelope with the cell plasma membrane (García et al., 2013). For other herpesviruses the major glycoproteins associated with viral attachment are gB and gC, which interact with heparan sulfate receptor in the cell membrane (Shukla & Spear, 2001). The ILTV glycoprotein C is shorter than that of the HSV-1 and lacks the heparan sulfate binding domain. Although the cellular receptor responsible for ILTV attachment to t is still not known, it is believed that gC promotes initial attachment through a different mechanism than that utilized by HSV-1 (Kingsley & Keeler, 1999).

Following viral envelope and cell plasma membrane fusion, the nucleocapsids are released into the cytoplasm and transported to the nuclear membrane (García et al., 2013). The viral DNA is released from the nucleocapsid and transported to the nucleus through nuclear pores. Once inside the nucleus, transcription and replication of ILTV DNA occurs (Guo et al., 1994; García et al., 2013). The transcription of ILTV happens in an ordered sequential pattern as follows: immediate-early (IE), early (E), early-late (E/L), and late (L). Assessment of ILTV genes transcription kinetics classified the ICP4 as the only immediate-early gene, 30 genes were classified as early; 28 genes were classified as late, and 15 genes showed features of both early and late genes and were classified as early/late (Mahmoudian et al., 2012). The newly synthetized viral DNA is further cleavage and packaged into nucleocapsids which obtain an envelope by migrating through the inner lamellae of the nuclear membrane. The enveloped particles then migrate through the endoplasmic reticulum and accumulate within vacuoles in the cytoplasm where mature capsids are formed by the incorporation of the tegument material and a final envelop step. Mature virions are released from the cells by exocytosis (Guo et al., 1994; Fuchs et al., 2007).

PRODUCTIVE, SEMI-PRODUCTIVE AND LATENT INFECTIONS

Upon ILTV entry through the respiratory and ocular routes both field and vaccine strains establish a primary lytic infection in the epithelium of the conjunctiva, nasal cavity and the trachea (Bang & Bang, 1967; García et al., 2013). Other than the conjunctiva and the respiratory tract, dissemination of the virus to other organs such as the brain, spleen, kidney, thymus, esophagus, lungs, pancreas, and ceca has been documented (Purcell & McFerran, 1969; Oldoni et al., 2009; Wang et al., 2013; Zhao et al., 2013; Davidson et al., 2016). Based on the wide tissue distribution of viral DNA, these studies suggest that ILTV establishes some levels of

viremia (Davidson et al., 2016). However, evidence of productive ILTV replication in peripheral blood lymphocytes has not yet been described. On the other hand, ILTV attenuated and virulent strains establish a poor productive infection in cultures of monocyte derived macrophages (MDM). This was demonstrated through the expression of viral antigens, increased transcription of viral genes, generation of cytopathic effect but low yield of virions were produced and released to culture supernatants (Calnek et al., 1986; Loudovaris et al., 1991; Coppo et al., 2018).

It was recently demonstrated that ILTV can block apoptosis of infected epithelial cells and induce apoptosis of neighboring uninfected cells. Therefore it was suggested that the prolonged survival of ILTV infected cells favor further mucosal invasion and ultimately the establishment of latency (Reddy et al., 2014). Like other alphaherpesvirus ILTV possesses the ability of establishing lifelong latent infection in the sensory ganglia of chickens following acute disease. During this period ILTV remains dormant in the trigeminal ganglia (TRG) of the ocular sensory nerve. Sporadic viral genome reactivation can occur leading to the establishment of lytic replication in the respiratory epithelium resulting in virus shedding and infection of susceptible animals (García et al., 2013). Stressful conditions such as re-housing and onset of reproduction are associated with ILTV genome reactivation in latently infected birds (Hughes et al., 1989). Under experimental conditions, reactivation of ILTV genome from the trigeminal ganglia was demonstrated when trigeminal ganglia explants from infected chickens were co-cultured with trachea explants from non-infected chickens (Bagust et al., 1986). Furthermore, recovered or vaccinated asymptomatic chickens become carriers and can contribute to virus shedding (Bagus et al., 2000; Hughes et al., 1991), which can further infect susceptible chickens.

PATHOLOGY

During ILTV infection gross lesion may be found in the conjunctiva and throughout the respiratory tract (García et al., 2013). In severe forms of the disease the most common clinical signs include conjunctivitis, nasal discharge, lethargy, sneezing and gasping. During severe epizootic forms of the disease severe dyspnea, expectoration of blood stained mucus and elevated mortality are detected (Bagust et al., 2000; García et al., 2013). Catarrhal inflammation in the trachea is observed early after infection and can progress to degeneration, necrosis, and hemorrhage of the trachea and conjunctiva mucosa. The histopathological changes in the trachea and the conjunctiva vary with the stage of the disease. Under experimental conditions, from 0 to 72 hours post-infection, there is a mild infiltration of lymphocytes and polymorphonuclear cells, presumably heterophils, into the lamina propria of the trachea and conjunctival epithelium. From 3 to 5 days post infection increased edema and infiltration of numerous lymphocytes, histiocytes and plasma cells throughout the lamina propria and areas where syncytia and intranuclear inclusion bodies are detected in the trachea and conjunctiva epithelium is observed. Regeneration of the damaged epithelium is observed as early as day five post-infection and by day nine the mucosal epithelial of the trachea and conjunctiva regain its normal structure (Purcell, 1971).

MUCOSA-ASSOCIATED LYMPHOID TISSUES

Different from mammals, the chicken immune system lacks encapsulated lymph nodes and lymphatic vessels. Instead, it possesses central primary lymphoid organs such as the bursa and thymus responsible for the maturation and differentiation of B and T lymphocytes, respectively (Oláh et al., 2014). In addition, chickens develop peripheral or secondary lymphoid organs. The spleen and highly developed mucosa-associated lymphoid tissue (MALT) (Oláh et al., 2014). In mammals, all MALT structures resemble lymph nodes (LNs) with variable T-cell

zones, B-cell follicles and numerous antigen-presenting cells (APCs) (Brandtzaeg & Pabst, 2004). The anatomical distribution of mammalian MALT reflects the local abundance of foreign materials and microorganisms (Neutra et al., 2001). The mammalian mucosa-associated lymphoid tissues lack afferent lymphatics, thus sampling of exogenous antigens is performed directly from the mucosal surface through a specialized follicle-associated epithelium (FAE) that contains epithelial microfold cells, also known as M cells and by mucosal dendritic cells (Paul, 2013). Specialized M cells are of epithelial origin and are joined to adjacent epithelial cells with tight junctions and desmosomes (Paul, 2013). In chickens, M like cells have been found within the follicle-associated epithelium that covers organized lymphoid tissue such as cecal tonsils, Peyer´s patches, Meckel´s diverticulum, bronchus-associated lymphoid tissue (BALT), conjunctival associated lymphoid tissue (CALT), and nasal-associated lymphoid tissue (NALT) (Befus et al., 1980; Burns & Maxwell, 1986; A. S. Fix & L. H. Arp, 1991b; Jeurissen et al., 1999; H. Kang et al., 2013; Sutton et al., 2018). Chicken M like cells have a very efficient pinocytic activity allowing the transport of specific antigens from the intestinal lumen to the underlying antigen presenting cells (APCs) (Burns, 1982). Therefore similar to the M cells in mammals, in the chicken cells from the follicle-associated epithelium (FAE) might aid in the rapid localization and transport of antigens from the luminal space to regions were conventional antigen-presenting cells (macrophages, dendritic cells and B cells) are located in the mucosal-associated lymphoid tissues. This mechanism allows for activation of primary or memory immune responses without the need for systemic involvement.

In chickens, the MALT associated with the respiratory tract can be divided into upper and lower components (Olah et al., 1996). The Harderian gland and the nasal associated-lymphoid tissue (NALT) constitute the upper components, while the bronchus-associated lymphoid tissue

(BALT) constitutes the lower components. Both the conjunctiva-associated lymphoid tissue (CALT) of the upper and lower eyelid and the Harderian gland are the major eye-associated lymphoid tissues that despite the lack of direct anatomic connection with the respiratory system, they are necessary for the generation of local immunity in the upper airways (Smialek et al., 2011).

Conjunctiva-associated Lymphoid Tissue (CALT). The CALT is situated in the upper and lower eye conjunctivas of turkeys and chickens (Fix & Arp, 1989; Fix & Arp et al., 1991). The upper eye conjunctiva of chickens contains scattered distribution of small lymphoid nodules primarily situated in close proximity to the lacrimal duct, while the lymphoid nodules located in the lower eyelid are more prominent and are associated with the folds and fissures of the eye conjunctiva epithelium (A. S. Fix & L. H. Arp, 1991a). The development and maturation of CALT is age dependent (A. S. Fix & L. H. Arp, 1991a). During early development, CALT contains isolated clusters of lymphocytes and as chickens age they become prominent lymphoid nodules harboring lymphocytes, lymphoblasts, macrophages, and germinal centers. A flat layer of specialized lymphoid-epithelium (LE) containing short irregular microvilli, M-like cells and intraepithelial lymphocytes (IEL) overlays the developed lymphoid nodules (A. S. Fix & L. H. Arp, 1991b) which resembles the follicle-associated epithelium (FAE) of the gut-associated lymphoid tissue (GALT) in chickens (Befus et al., 1980; Burns & Maxwell, 1986; Jeurissen et al., 1999).

The CALT in chickens has the ability to endocytose macromolecules that come in contact with the lymphoid epithelium (LE) (A. S. Fix & L. H. Arp, 1991b). This function is age dependent and significantly increases between 3 and 5 weeks of age. More recently, following

ocular stimulation with a replication-deficient adenovirus serotype 5 (Ad5) or infectious bronchitis virus (IBV), B cells, γδ T cells, and T effector cells ($CD3^+$, $CD44^+$) were detected in the CALT indicating that both T and B cells responses were mounted in the CALT after ocular stimulation with two completely different viruses (van Ginkel et al., 2009; Gurjar et al., 2013). These results underscore the role of the CALT as a site were effective mucosal cell-mediated responses are generated.

Harderian gland (HG). The second major eye-associated lymphoid tissue is the Harderian gland (HG). It was first described in 1694 by Johann Jacob Harder and is found in most vertebrates except fish and aquatic amphibians. The chicken Harderian gland has diverse functions including lubrication of the eye and the nictitating membrane, nourish the avascular cornea, and it is a site of immune responses (Payne, 1994). In the domestic fowl the Harderian gland is larger than the lacrimal gland covering much of the posteriomedial surface of the eye (Wight et al., 1971). The Harderian gland is surrounded by a connective tissue capsule, which subdivides the gland into lobules. The cells lining the Harderian gland tubules are uniform at all ages and consists of columnar epithelial cells, often bipolar in that they contain two distinct accumulations of vesicles: 1) a basal group of vesicles which contains lipid material; 2) an apical group whose vesicles are probably bounded and filled with mucoid and which are released by exocytotic mechanism (Payne, 1994). However, Rothwell et al*.,* (1972) described a more complex epithelium and classified the cells in three different types based on the development of the Golgi apparatus (more developed in type II cells), rough endoplasmic reticular lamellae (type III) or secretory granules (type IV). Nevertheless, it is not clear if in fact these are distinct cell types or these cells reflect different stages of activity or secretory cycle.

The lymphoid tissue of the HG can be divided in two histologically different areas, a head and a body. The structure of the head resembles a typical secondary lymphoid organ with a follicle-associated epithelium (FAE) containing B cell-dependent germinal centers, and T cell-dependent inter-follicular regions with scattered T cells and macrophages (Oláh et al., 2014). The body of the HG contains numerous plasma cells at different stages of maturation (Smialek et al., 2011; Oláh et al., 2014). The concentration of plasma cells in the HG is age dependent reaching the highest numbers at four weeks of age thereafter the number did not change (Niedorf & Wolters, 1978). Kowalski et al., (1978) demonstrated that IgA, IgM and IgY immunoglobulin were not present in tears and serum of bursectomized chickens as compared to non-bursectomized control chickens, indicating that B cells in the HG are of Bursa of Fabricious origin.

Discrepancies exist regarding the proportion of resident IgM, IgA, and IgY- producing B cells in the un-stimulated HG of the chicken. Early studies described high frequency of IgM and IgY expressing cells in the HG and very few cells expressing IgA (Bienenstock et al., 1973). In disagreement with Bienenstock et al (1973), Albini & Wick (1973) reported a high concentration of B cells and plasma cells expressing IgM by four weeks of age, and between 4 to 9 weeks of age IgY and IgA expressing cells became more prominent, switching to mainly IgA expressing cells after 9 weeks of age. Whereas, Oláh et al., (1992) described high number of IgM and IgA, and only a few IgY expressing cells in the HG of 8 and 10 week-old chickens. It has been documented that upon antigen stimulation, the Harderian gland plasma cells can undergo a rapid isotype switching resulting in a change of secretion from IgM to IgA or IgY antibodies (Mansikka et al., 1989). Also it has been suggested that the proportions of Ig-expressing B cells in the Harderian gland could be influenced by the chicken`s age but most importantly by the

microbial environment and the overall health of the chickens (Ohshima & Hiramatsu, 2002). Thus the immune responses generated in the HG of chickens will vary depending on the stimuli that it receives.

Synthesis of specific antibodies by Harderian gland plasma cells can occur after antigen stimulation and can be readily detected in the chicken´s lacrimal fluid. Ocular exposure with bovine serum albumen (BSA) or infectious bronchitis virus (IBV) resulted in synthesis of specific antibodies that were detected in tears of stimulated chickens (Burns, 1976; Davelaar et al., 1982). Furthermore, ocular administration of adenovirus (Ad5) expressing the hemagglutinin H5 protein of avian influenza virus induced synthesis of specific antibodies in tears, while ocular stimulation with Infectious bronchitis virus (IBV) resulted in generation of effector T cells in the gland (van Ginkel et al., 2009; Gurjar et al., 2013). These findings highlight the role of the HG in the induction of mucosal immunity.

Nasal-associated Lymphoid Tissue (NALT). During inhalation, the nasal mucosa lining of the upper respiratory tract is the first structure to come in contact with aerosols or microorganisms. In humans and mice, the nasal associated-lymphoid tissue (NALT) is considered the first site were immune responses are triggered after inhalation of an infectious agent (Hiller et al., 1998; Brandtzaeg & Pabst, 2004). In chickens the NALT harbors lymphoid accumulations consisting of B cell areas occasionally displaying germinal centers (GC) surrounded by a $CD4^+$ T cells, while $CD8^+$ T cells are widely distributed in the epithelium and the lamina propria of the nasal mucosa (Ohshima & Hiramatsu, 2000). Similar to CALT and HG, the development of the chicken NALT is age dependent. Lymphocyte aggregations under NALT mucosa are absent in 1-day-old chickens. However, an increase in number of lymphocytes and the development of

secondary lymphoid follicles was observed around 14 days of age reaching fully maturity around 35 days of age (H. Kang et al., 2013). NALT is also a site of antigen uptake by phagocytic cells such as macrophages and dendritic cells, indicating that this lymphoid structure is an important inductive site of mucosal immune responses (de Geus et al., 2015).

Bronchus-associated Lymphoid Tissue (BALT). The lungs of chickens contain organized lymphoid structures called bronchus-associated lymphoid tissue (BALT) located at each opening of the secondary bronchi (Sutton et al., 2018). The lymphoid follicles and the number of follicles associated to BALT increase in size and number as chickens age (Fagerland & Arp, 1990). Fully mature BALT is observed from 4 weeks of age onwards and consists of a layer of follicle-associated epithelium (FAE) (Bienenstock, 1980), with B and T cell areas and germinal centers (Sutton et al., 2018). Limited knowledge about M cells in the BALT is available, however a recent study described these cells within the follicle-associated epithelium overlaying the BALT of chickens (Sutton et al., 2018).

Lymphoid Aggregates in the Chicken Trachea. The normal trachea of chickens is lined by ciliated pseudostratified columnar epithelium containing large numbers of simple alveolar mucous glands. The ciliated epithelium, mucus, and mucous secreting cells of the trachea form the mucociliary blanket constitutes an important barrier mechanism for the entrapment and clearance of particulate material from the respiratory tract (Fletcher et al., 2008). Development of lymphoid aggregates in the trachea of chickens has been recently described as early as 1 week of age, whereas highly organized lymphoid tissues appear from 4 weeks onward (Sutton et al., 2018). In the lamina propria leukocytes consist mainly of macrophages and an occasional $CD4^+$ and $CD8^+$ T cells and B cells (Krunkosky et al., 2018). Lymphoid cells can also be recruited to

the trachea upon antigen stimulation. Interaction between the respiratory epithelial cells and antigens results in the production of antiviral molecules and pro-inflammatory cytokines leading to the recruitment and activation of macrophages as well as B and T cells to the trachea mucosa (Majumder & Silbart, 2015).

The trachea bifurcates into two bronchi that subsequently branches into secondary bronchi. The gas exchange in birds occurs at the tertiary bronchi or parabronchi, which originates from the secondary bronchi, whereas in mammals the gas exchange takes place in the alveoli (de Geus et al., 2012). The epithelium lining the respiratory tract of chickens is the target for many avian respiratory viruses including ILTV and infectious bronchitis virus (IBV) (García et al., 2013; Jackwood & Sjaak, 2013). Either ILTV or IBV infections cause extensive necrosis of the trachea epithelium causing sloughing of epithelial cells (García et al., 2013; Jackwood & Sjaak, 2013). As ILTV establish lytic replication in the nucleus of epithelial cells. ILTV infected epithelial cells express high levels of viral glycoproteins that induce cell fusion and formation of large multinucleated syncytial epithelial cells with intranuclear inclusions in the mucosa of the respiratory and conjunctiva epithelium (Fletcher et al., 2016). Whereas the tracheal mucosa of chickens infected with IBV becomes edematous, showing rounding of epithelial cells and loss of cilia with less involvement of the conjunctival epithelium (Jackwood & Sjaak, 2013). Another important avian respiratory pathogen whose primary site of colonization is the respiratory epithelium is *Mycoplasma gallisepticum* (MG). Upon colonization, MG is confined to the luminal surface of the tracheal epithelium, causing swelling of epithelial cells and interferes with cillia function (Ferguso, 2013).

Migration of inflammatory cells to the lamina propria of the trachea mucosa is commonly observed after infection with either ILTV, IBV or MG. The degree of cellular infiltration varied depending on the process of the infections. Upon MG colonization inflammatory cells infiltrate to the lamina propria causing thickening of the trachea mucosa. This microscopic change, particularly the increased mucosal thickness, has been used as an indication of MG infection (Nunoya et al., 1987). Diffuse infiltration of lymphocytes is typically caused by IBV infection, depending on the virulence of the virus. Whereas ILTV infection can cause multifocal to diffuse infiltration of inflammatory cells to the trachea mucosa and the level of infiltration will depend on the virus or vaccine strain.

MONONUCLEAR PHAGOCYTE SYSTEM (MNP)

Development of rapid immune responses at the mucosal surfaces is required to protect the host against invading pathogens. This process is under the control of a complex network of mononuclear phagocytes (MNP) (Paul, 2013). The differentiation, proliferation and survival of mammalian macrophages are controlled primarily by the cytokine macrophage colony-stimulating factor (CSF1) by interacting with its receptor (CSF1R) (Balic et al., 2014). Recently, it was discovered that in contrast to mammals, chicken express the colony stimulating factor 1 receptor (CSF1R) not only on macrophages, but also on dendritic cells (Sutton et al., 2018), and at low levels by heterophils (Balic et al., 2014). New technology has allowed for a more in-depth visualization of cells of the mononuclear phagocytes system in the lung where lymphoid aggregates were detected in the bronchi associated lymphoid tissue (BALT) and in the air sacs as early as 1 week of age, and in the trachea highly organized lymphoid tissues were detected from 4 weeks onward (Sutton et al., 2018).

In contrast to mammals where DCs and macrophages are found free in the alveolar space and in the lung parenchyma (de Heer et al., 2005), the respiratory tract of chickens contains fewer macrophages outside of the tissue matrix and are known as avian respiratory phagocytes (ARP) (de Geus et al., 2012). In the avian lungs, macrophages are located in the atria, atrial connective tissue and infundibulae (Klika et al., 1996; Maina, 2002). Thus, it has been suggested that epithelial cells located at the gas-exchange tissue (tertiary bronchi) are able to phagocytose, process and present antigens to macrophages located in the connective tissue compartments (Klika et al., 1996; Sutton et al., 2018).

INNATE IMMUNE RESPONSES TO ILTV INFECTION

The innate immune system is the first line of defense against invading pathogens. It is designed to efficiently fight respiratory pathogens in a rapid and non-specific response resulting in pathogen clearance (Vareille et al., 2011). A coat of mucous overlaying the airway epithelium provides the first specialized innate immune defense barrier. This mucus overlay consists of large glycoproteins called mucins, which form a structural frame barrier by interacting with mucus components, such as IgA, collectins, and defensins in order to prevent pathogens to reach the airway epithelium. During respiratory infections, the production of airway mucus increases allowing the trapping and clearance of pathogens. However, mucin overproduction and excessive formation of mucus can result in obstruction of the airways turning what is supposed to be an efficient innate cleaning defense system into a harmful mechanism (Vareille et al., 2011). Mucins are the major components of the respiratory mucus. It has been documented that the chicken genome codes for three membrane-bound mucin genes (MUC4, MUC13, and MUC16), and four gel-forming mucins (MUC6, MUC2, MUC5AC, and MUC5B) (Lang et al., 2006). As ILTV infection frequently led to the formation of mucus/plug casts resulting in chicken

suffocation and death (García et al., 2013), it was suggested that ILTV stimulates the hypersecretion of mucus in the trachea. However, Reddy et al., (2017) demonstrated that the production of gel-forming mucins (MUC5AC and MUC5B) during ILTV infection was not significantly increased in the trachea. Whereas mucus plug/cast generated during acute ILTV infection were mainly composed of DNA fibrous structures probably generated by heterophils and other inflammatory cells. Heterophils, the counterpart of mammalian neutrophils, are considered a main innate immune effector cell, as is the first cell type to respond and migrate to a site of infection in response to chemokines (Kaiser, 2010). Heterophils have phagocytic capabilities; they can kill pathogens by the release of toxic oxygen metabolites (oxidative burst), lytic enzymes, and antimicrobial peptides (degranulation) (Kogut et al., 2005). In addition, activated heterophils can induce programmed cell death different from apoptosis or necrosis called HETosis. The result of this process is the production of heterophils extracellular traps (HETs). HETs released from activated chicken heterophils cytoplasmic granules consist of net-like structures comprised by DNA, histone-DNA complex and elastase (Chuammitri et al., 2009). Based on Reddy et al., (2017) findings, tracheal plugs induced by ILTV infection are most likely caused by HETs. Therefore, the possibility exists that uncontrolled innate inflammatory responses may exacerbate the disease and precipitate mortalities.

When viruses penetrate the physical barriers, they met with important components of the host immune system that rapidly trigger an innate antiviral immune response. The first response is initiated by pathogen recognition receptors (PRRs) that respond to conserved pathogen-associated molecular patters (PAMPs). The main families of PRRs in chickens are the Toll-like receptors (TLR), retinoic acid-inducible gene I (RIG-I)-like receptors (RLRs), the nucleotide

oligomerization domain (NOD)-like receptors (NLRs), and C-type lectin receptors (Juul-Madsen et al., 2014).

Chicken Toll-like receptors (chTLRs): TLRs are type I integral membrane glycoproteins (Akira & Takeda, 2004). TLRs are widely expressed in many cell types including respiratory epithelial cells (Whitsett & Alenghat, 2015), dendritic cells, macrophages, B-lymphocytes and heterophils (Iqbal et al., 2005; Kogut et al., 2005). With the exception of chTLR3, 7 and 21, which are expressed in endosomal compartments, all other chTLRs are expressed on the cell surface (Juul-Madsen et al., 2014). Chicken TLR3 can sense double-stranded RNA (dsRNA), chTLR4 senses lipopolysaccharide (LPS), chTLR5 responds to bacteria flagellin, while chTLR7 and chTLR8 respond to single stranded RNA (Juul-Madsen et al., 2014). The chicken TLR15 and TLR21 respond to yeast and DNA containing deoxycytidylate-phosphate-deoxyguanylate (CpG) motifs, respectively (Boyd et al., 2012; Juul-Madsen et al., 2014). The chicken TLR2 type 1 forms a functional heterodimer complex with chTLR1LB and with chTLR1LA in the cell surface. The formation of these complexes is triggered by sensing of tri-acylated and di-acylated lipoproteins (Higuchi et al., 2008). With the exception of TLR3, all chicken TLRs trigger a signaling pathway via MyD88 adapter leading to nuclear factor κB (NF-κB) activation, which result in the production of inflammatory responses. Chicken TLR3 senses dsRNA and triggers the production of Type I IFN through the TRIF-dependent pathway, and establishes an antiviral state around infected cells (Akira & Takeda, 2004; Keestra et al., 2013).

Global transcriptional analysis of chicken embryo lung cells infected with a virulent ILTV strain provided some initial indication of genes associated with innate immune responses stimulated by ILTV. Particularly the increased transcription of genes involved in the pro-

inflammatory processes, such as interleukin-8 (IL-8) and IL-1β, chemokine (CXC-K60), and IL-6 genes were identified as associated with ILTV immune responses (J. Y. Lee et al., 2010).

Activation of chicken TLRs with synthetic ligands has also been investigated in their potential to limit ILTV replication. Stimulation of the macrophage cell line (MQ-NCSU) with the chTLR2 ligand lipoteichoic acid (LTA) resulted in significantly increased transcription of MyD88 and IL-1β (Haddadi et al., 2015). While, stimulation with the chTLR4 ligand lipopolysaccharide (LPS) (Haddadi et al., 2013) resulted in increased expression of TLR4 and CD14 cell surface markers, and the generation of pro-inflammatory responses. In these studies, stimulation of both TLR2 and TLR4 signaling pathways resulted in the generation of antiviral responses against ILTV infection. Furthermore, *in ovo* delivery of TLR2 ligand LTA or TLR21 ligand CpG DNA produced up regulation of genes associated with pro-inflammatory responses such as MyD88, iNOS and IL-1β that mediated antiviral activity against ILTV infection by the recruitment and activation of macrophages into the lungs of chickens after hatch (Thapa, Cader, et al., 2015; Thapa, Nagy, et al., 2015). Even though synthetic ligands were utilized rather than the virus itself to induce immune response, these studies corroborate the importance of effective sensing by the innate immune system to properly activate TLRs signaling cascades that consequently induce antiviral responses.

The interaction between TLRs and herpes simplex virus-1 (HSV-1) has been widely studied. Recognition of HSV-1 by TLR2 leads to expression of inflammatory cytokines in the brain of infected mice resulting in lethal encephalitis (Kurt-Jones et al., 2004). In addition, patients lacking a functional endoplasmic reticulum protein (UNC-93B) required for TLR3, 7 and 9 signaling, were not able to produce type I interferon (IFNα, and IFNβ) after HSV-1

infection resulting in increased susceptibility to herpes simplex encephalitis (HSE) (Zhang et al., 2007). HSV-1 DNA contains abundant CpG motifs, which activate TLR9 signaling, and consequently an effective production of IFNα (Krug et al., 2004).

Since IFNs are essential for the activation of antiviral responses, most herpesviruses have developed immune evasion mechanisms that target the PRRs and IFN dependent signaling pathways resulting in either the reduction of IFNs and interferon stimulated genes (ISGs) expression (Vandevenne et al., 2010). For example, ICP34.5, ICP0 and ICP27 HSV-1 proteins prevent the activation of interferon regulatory factor-3 (IRF3) subsequently blocking the transcription of type I IFNs and ISGs (Verpooten et al., 2009; K. E. Johnson & Knipe, 2010; Paladino et al., 2010). It has been speculated that ILTV infection inhibits early Type I IFN responses. The level of transcription of the IFN-β gene in the trachea after intratracheal inoculation with ILTV virulent strain remained unaltered from days 1 to 9 post-infection. Whereas IFN-α gene transcription was up regulated from days 3 to 5 post-infection after the virus already established a productive lytic infection in the trachea (Coppo et al., 2018; Vagnozzi et al., 2018). These studies suggest that ILTV similarly to other herpesviruses hampers the type I interferon antiviral innate responses. Therefore, better understanding of which viral components activate more effective innate antiviral responses will be important for the development of suitable adjuvants for ILTV vaccination.

ADAPTIVE IMMUNE RESPONSES TO ILTV INFECTION

The second line of defense consists of elements of the antibody-mediated and adaptive immune responses. Early adaptive immune responses are modulated by activated APCs through the production of IL-12, which stimulate natural killer (NK) and T cells to produce IFN- γ. In

humans and mice bioactive IL-12 is composed by two subunits, p40 and p35. Subunit p35 is expressed by many cell types, whereas p40 is expressed mainly by APCs (Balu & Kaiser, 2003). Similar to activated $CD8^+$ cells, activated NK cells are capable of inducing cytotoxic activity by the production of serine proteases such as granzyme A (Sarson et al., 2008). More pertinent, NK cells participate in the maturation of professional APCs, enhance antigen specific cytotoxic $CD8^+$ T cell responses, assists in the polarization of $CD4^+$ T cells (Lam & Lanier, 2017) and in the absence of a $CD4^+$ T cells can participate as helpers in the genesis of functional $CD8^+$ T cell responses (Nandakumar et al., 2008; Morandi et al., 2009). Although the role that NK cells play during the early adaptive ILTV immune response is not clearly understand. Recent evidence obtained after intratracheal inoculation with a virulent ILTV strain showed an early upregulation of the IFN-γ gene at 1 day post-infection in the Harderian gland. In striking contrast in the mucosal epithelium of the trachea increased transcription of IL-2 and IFN-γ genes were detected late at 5 to 9 days post-infection (Vagnozzi et al., 2018). The early increase of the IFN-γ gene transcription hints an early adaptive immune response probably triggered by activated NK cells in the Harderian gland. While the late upregulation of IL-2 and IFN-γ genes transcription suggests the expansion of the adaptive immune response in the trachea.

Although the components of the adaptive immune responses to ILTV infection are still unclear, early seminal studies demonstrated that protection against ILTV infection was conferred by cell-mediated immunity rather than humoral responses. This claim was supported by evidence that ILTV immunized chickens that were previously subjected to surgical and chemical bursectomy were properly protected against challenge (Fahey et al., 1983). In addition, passive transfer of hyperimmune serum to chickens provided no evidence that circulating antibodies conferred protection against ILTV challenge (Fahey et al., 1983). Otherwise, transfer of

hyperimmune spleen cells from immunized chickens did confer protection to bursectomized chickens after challenge. This demonstrated that bursectomized chickens were able to recover from ILTV challenge even in the absence of IgA or IgY producing cells in the tracheal mucosa (Fahey et al., 1984, Fahey et al., 1990). In addition, York et al., (1989) found that after ILTV intratracheal inoculation IgA^+ synthetizing cells in the trachea peaked by day 7 pi when virus replication was no longer detected. The onset of protection after challenge of chickens vaccinated with a cell-associated ILTV vaccine did not correlated with the arrival of virus-neutralizing antibodies in serum and in tracheal washes in after challenge (Honda et al., 1994). Furthermore, Honda et al., (1994) showed that thymectomized/immunized chickens were poorly protected after challenge, implying that live attenuated vaccinal protection was principally mediated by the cellular arm of the immune system, particularly by T cells.

Under experimental conditions the peak of viral replication, for either vaccine strains or field isolates, is between 3 to 5 days post-inoculation (Oldoni et al., 2009; M. J. Coppo et al., 2012; S. W. Lee et al., 2015; A. Vagnozzi et al., 2015; Beltrán et al., 2017). By this stage of infection multinucleated epithelial cells (syncytia cell formation) accompanied by significant influx of lymphocytes, histiocytes and plasma cells to the lamina propria of the trachea (Purcell, 1971) and conjunctival epithelium (Beltrán et al., 2017) is observed. It has been suggested that the types of inflammatory cells recruited to the site of infection influence the outcome of the disease and modulates the adaptive immune responses (Devlin et al., 2010). Like other alphaherpesviruses, both virulent and live attenuated vaccine strains of ILTV, encode a glycoprotein G (gG) gene which functions as a broad-spectrum chemokine binding protein (vCKBP) (Gonzalez-Motos et al., 2016). The secreted form of gG binds to host chemokines blocking the interaction between the chemokine and its receptor, consequently inhibiting the

chemokine activity. This results in the increased recruitment of B cells, and limits the number of heterophils, $CD4^+$ T, and $CD8^+$ T cells that migrate to the trachea. It was suggested that the increase of B cells recruited to the trachea would eventually direct the host immune response away from cell-mediated immunity and towards antibody-mediated responses allowing viral survival (Devlin et al., 2010). More recently Coppo et al., (2018) demonstrated that ILTV expressing gG downregulates the transcription of chicken chemokine homolog CCLi4 and the interleukin (IL)-6; but despite the immunomodulatory effect of viral gG, increased transcription of pro-inflammatory, chCXLi1, chCXCLi2 and IL-1β and anti-inflammatory IL-10 cytokine genes were detected in the trachea (Coppo et al., 2018; Vagnozzi et al., 2018). Increased transcription of inflammatory cytokines and IL-10 after intratracheal inoculation of a virulent ILTV strain coincided with the recruitment of inflammatory cells, extensive mucosa damage, decreased virus replication, and ultimately repair of the trachea mucosa (Vagnozzi et al., 2018).

Major histocompatibility complex (MHC) I and II processing and presentation pathways play a critical role in induction and regulation of adaptive immune responses to pathogens. The MHC class I complex present antigenic peptides by an intracellular route to $CD8^+$ T cells, whereas MHC class II complex presents peptides to $CD4^+$ T cells (Paul, 2013). In mammals, expression of MCH class I and MHC class II varies among tissue types, for example certain reproductive and developmental tissues as well as the cells of the nervous system and the eye lack expression of MHC class I molecules. The highest levels of MHC class I gene expression occur in tissues and cells of the immune system (van den Elsen et al., 2004). The chicken MHC class I is expressed in all nucleated cells (Kaufman, 2014). Whereas MHC class II molecules are constitutively expressed in antigen-presenting cells such as dendritic cells, macrophages and B cells, and in bursal and thymic epithelial cells (LeibundGut-Landmann et al., 2004). However, in

response to cytokines such as IL-2 and interferon (IFN)-γ, other cell types, including chicken γδ T cells and fibroblasts, as well as human, bovine, and canine T cells express the MHC class II complex (Kasahara et al., 1993; Ting & Trowsdale, 2002; Reith et al., 2005). In addition, the assessment of high and low levels of MHC class II surface expression in chickens has been utilized as a marker for the identification of different subsets of antigen presenting cells, and as a marker for their activation (de Geus et al., 2012).

The nature of vaccine induced protection elicited after ILTV immunization with live attenuated vaccines is still not completely understood. Chickens immunized via the ocular/nasal route with a CEO vaccine showed transcription up regulation of MHC class I and MHC class II genes in the trachea indicating that ILTV vaccination induce the activation of antigen processing and presentation pathways (Luo et al., 2014). Up regulation of IFN-γ gene transcription was detected in the trachea of CEO vaccinated chickens as early as six hours post-challenge (Vagnozzi et al., 2016). Therefore, early expression of IFN-γ in CEO vaccinated chickens may trigger pathways of antiviral responses necessary to diminishing early viral replication in vaccinated chickens.

INFECTIOUS LARYNGOTRACHEITIS VIRUS VACCINES

Live Attenuated Vaccines

Live attenuated vaccines have been in used since the early 1960´s to control outbreaks of the disease. Live attenuated vaccines originated from virulent field viruses that were attenuated by either serial passages in embryonated eggs which gave rise to the chicken embryo origin (CEO) vaccines (Samberg et al., 1971), or by serial passages in cell culture which gave rise to the tissue culture origin (TCO) vaccine (Gelenczei & Marty, 1964). The CEO vaccines can be

given individually via the eye drop or by mass vaccination via the drinking water or by coarse spray, while the TCO vaccine can be given only individually via eye drop (Gelenczei & Marty, 1964; Garcia, 2016). Since their early use both the CEO and the TCO vaccines had proven to induce effective protection against the disease. Protection has been defined by the ability of the vaccine to prevent clinical signs, reduce replication of the challenge virus in the trachea, and maintain body weight gain after challenge (Vagnozzi et al., 2012).

Poor mass administration (water or spray) particularly with the CEO vaccine can enhance the potential for virus shedding, transmit to unvaccinated chickens and regain virulence (Clarke et al., 1980; Fulton et al., 2000; Garritty, 2008). Furthermore, similar to field viruses, live attenuated ILTV vaccines have the potential to establish long-term latent infections as determined by intermittent shedding of vaccine viruses in the trachea of vaccinated clinically normal chickens (Bagust et al., 1986; Hughes et al., 1991).

Recombination events allow alphaherpesviruses to evolve over time and become more virulent (Loncoman et al., 2017). Recombination events between two live attenuated vaccines occurred in Australia after the administration of the European Serva vaccine in previously vaccinated flocks with local produced vaccines (SA2 and A2) (Lee et al., 2012). Emergence of new recombinant field viruses, that causes severe outbreaks of the disease still occurring in Australia (Augnew-Crumpton et al., 2016). Vaccination with the U.S. CEO vaccine (Trachivax® MERCK, Animal Health, Summit, NJ) prevented recombination of two virulent ILTV strains after co-administration under experimental conditions. Therefore, vaccination with a single live attenuated vaccine prevented the recombination of virulent viral strains (Loncoman et al., 2018).

Recombinant Vaccines

As a response to the drawbacks associated with the use of live attenuated ILTV vaccines, a new generation of viral vectored vaccines also known as recombinant vaccines were developed. These new generations of vaccines utilize the fowl-pox virus (FPV) and serotype 3 Marek´s disease virus (MDV), also known as herpesvirus of turkeys (HVT) as vectors to express exogenous viral proteins. The commercial available FPV vector vaccine carries the ILTV glycoprotein B and UL32 genes. Two HVT vector products are commercially available, one expressing the ILTV glycoproteins I and D and a second HVT vector vaccine expressing the ILTV glycoprotein B (Garcia, 2016). Unlike ILTV live attenuated vaccines, administration of recombinant vaccines, particularly the HVT vector vaccines, is performed in the hatchery using highly automatized equipment. HVT viral vector vaccines are applied between 18 to 19 days of embryonation or via the subcutaneous route at 1-day of age. Whereas the FPV vector vaccine is administered subcutaneously at 1-day of age and in the wing web at 6 to 8 weeks of age in the case of long lived chickens (Davison et al., 2006).

Both HVT and FPV vectored vaccines can improve bird performance, reducing to some degree clinical signs, and challenge virus replication in the trachea. However, it has been demonstrated that vaccination with ILTV viral vector vaccines is not as effective as CEO vaccination in reducing shedding of the challenge virus (A. Vagnozzi et al., 2012). This observation has raised the hypothesis that ILTV recombinant vaccines induce weak mucosal immune responses as compared to the live attenuated vaccines (Gimeno et al., 2011).

REFERENCES

Akira, S., & Takeda, K. (2004). Toll-like receptor signalling. *Nature Reviews Immunology, 4*, 499-511.

Albini, B., & Wick, G. (1973). Immunoglobulin determinants on the surface of chicken lymphoid cells. *International archives of allergy and immunology, 44*, 804-822.

Agnew-Crumpton, R., Vaz, P.K., Devlin, J.M., O'Rourke, D., Blacker-Smith, H.P., Konsak-Ilievski, B., Noormohammadi, A.H. (2016). Spread of the newly emerging infectious laryngotracheitis viruses in australia. *Infection, Genetics and Evolution, 43*, 67-73

Bagust, T.J., Calnek, B.W., & Fahey, K.J. (1986). Gallid-1 herpesvirus infection in the chicken. 3. Reinvestigation of the pathogenesis of infectious laryngotracheitis in acute and early post-acute respiratory disease. *Avian Diseases, 30*, 179-190.

Bagust, T.J., Jones, R.C., & Guy, J.S. (2000). Avian infectious laryngotracheitis. *Revue Scientifique et Technique, 19*, 483-492.

Balic, A., Garcia-Morales, C., Vervelde, L., Gilhooley, H., Sherman, A., Garceau, V., Gutowska, M. W., Burt, D. W., Kaiser, P., Hume, D. A., Sang, H.M. (2014). Visualisation of chicken macrophages using transgenic reporter genes: Insights into the development of the avian macrophage lineage. *Development, 141*, 3255-3265.

Balu, S., & Kaiser, P. (2003). Avian interleukin-12beta (p40): Cloning and characterization of the cdna and gene. *Journal of Interferon & Cytokine Research, 23*, 699-707.

Bang, B.G., & Bang, F.B. (1967). Laryngotracheitis virus in chickens. A model for study of acute nonfatal desquamating rhinitis. *The Journal of Experimental Medicine, 125*, 409-428.

Befus, A.D., Johnston, N., Leslie, G.A., & Bienenstock, J. (1980). Gut-associated lymphoid tissue in the chicken. I. Morphology, ontogeny, and some functional characteristics of peyer's patches. *Journal of Immunology, 125*, 2626-2632.

Beltrán, G., Williams, S.M., Zavala, G., Guy, J.S., & García, M. (2017). The route of inoculation dictates the replication patterns of the infectious laryngotracheitis virus (ILTV) pathogenic strain and chicken embryo origin (CEO) vaccine. *Avian Pathology, 46*, 585-593.

Bienenstock, J. (1980). Bronchus-associated lymphoid tissue and the source of immunoglobulin-containing cells in the mucosa. *Environmental Health Perspectives, 35*, 39-42.

Bienenstock, J., Gauldie, J., & Perey, D.Y. (1973). Synthesis of IgG, IgA, IgM by chicken tissues: Immunofluorescent and 14c amino acid incorporation studies. *Journal of Immunology, 111*, 1112-1118.

Boyd, A.C., Peroval, M.Y., Hammond, J.A., Prickett, M.D., Young, J.R., & Smith, A.L. (2012). Tlr15 is unique to avian and reptilian lineages and recognizes a yeast-derived agonist *Journal of Immunology, 189*, 4930-4938.

Brandtzaeg, P., & Pabst, R. (2004). Let's go mucosal: Communication on slippery ground. *Trends in Immunology, 25*, 570-577.

Burns, R.B. (1976). Specific antibody production against a soluble antigen in the harderian gland of the domestic fowl. *Clinical and Experimental Immunology, 26*, 371-374.

Burns, R.B. (1982). Histology and immunology of peyer's patches in the domestic fowl (gallus domesticus). *Research in Veterinary Science, 32*, 359-367.

Burns, R.B., & Maxwell, M.H. (1986). Ultrastructure of peyer's patches in the domestic fowl and turkey. *Journal of Anatomy, 147*, 235-243.

Calnek, B.W., Fahey, K.J., & Bagust, T.J. (1986). In vitro infection studies with infectious laryngotracheitis virus. *Avian Diseases, 30*, 327-336.

Chuammitri, P., Ostojic, J., Andreasen, C.B., Redmond, S.B., Lamont, S.J., & Palic, D. (2009). Chicken heterophil extracellular traps (HETs): Novel defense mechanism of chicken heterophils. *Veterinary Immunology and Immunopathology, 129*, 126-131.

Clarke, J.K., Robertson, G.M., & Purcell, D.A. (1980). Spray vaccination of chickens using infectious laryngotracheitis virus. *Australian Veterinary Journal, 56*, 424-428.

Coppo, M.J., Devlin, J.M., & Noormohammadi, A.H. (2012). Comparison of the replication and transmissibility of an infectious laryngotracheitis virus vaccine delivered via eye-drop or drinking-water. *Avian Pathology, 41*, 99-106.

Coppo, M.J.C., Devlin, J.M., Legione, A.R., Vaz, P.K., Lee, S.W., Quinteros, J.A., Gilkerson, J. R., Ficorilli, N., Reading, P. C., Noormohammadi, A. H., Hartley, C.A. (2018). Infectious laryngotracheitis virus viral chemokine-binding protein glycoprotein g alters transcription of key inflammatory mediators in vitro and in vivo. *Journal of Virology, 92*.

Cruickshank, J.G., Berry, D.M., & Hay, B. (1963). The fine structure of infectious laryngotracheitis virus. *Virology, 20*, 376-378.

Davelaar, F.G., Noordzij, A., & Vanderdonk, J.A. (1982). A study on the synthesis and secretion of immunoglobulins by the jarderian gland of the fowl after eyedrop vaccination against infectious bronchitis at 1-day-old. *Avian Patholoy, 11*, 63-79.

Davidson, I., Raibshtein, I., Altori, A., & Elkin, N. (2016). Infectious laryngotracheitis virus (ILTV) vaccine intake evaluation by detection of virus amplification in feather pulps of vaccinated chickens. *Vaccine, 34*, 1630-1633.

Davison, A.J. (2010). Herpesvirus systematics. *Veterinary Microbiology, 143*, 52-69.

Davison, S., Gingerich, E.N., Casavant, S., & Eckroade, R.J. (2006). Evaluation of the efficacy of a live fowlpox-vectored infectious laryngotracheitis/avian encephalomyelitis vaccine against ilt viral challenge. *Avian Diseases, 50*, 50-54.

de Geus, E.D., Degen, W.G., van Haarlem, D.A., Schrier, C., Broere, F., & Vervelde, L. (2015). Distribution patterns of mucosally applied particles and characterization of the antigen presenting cells. *Avian Pathology, 44*, 222-229.

de Geus, E.D., Rebel, J.M., & Vervelde, L. (2012). Induction of respiratory immune responses in the chicken; implications for development of mucosal avian influenza virus vaccines. *The Veterinary Quarterly, 32*, 75-86.

de Geus, E.D., Jansen, C.A., & Vervelde, L. (2012). Uptake of particulate antigens in a nonmammalian lung: Phenotypic and functional characterization of avian respiratory phagocytes using bacterial or viral antigens. *Journal of Immunology, 188*, 4516-4526.

de Heer, H.J., Hammad, H., Kool, M., & Lambrecht, B.N. (2005). Dendritic cell subsets and immune regulation in the lung. *Seminars in Immunology, 17*, 295-303.

Devlin, J.M., Viejo-Borbolla, A., Browning, G.F., Noormohammadi, A.H., Gilkerson, J.R., Alcami, A., & Hartley, C.A. (2010). Evaluation of immunological responses to a glycoprotein g deficient candidate vaccine strain of infectious laryngotracheitis virus. *Vaccine, 28*, 1325-1332.

Fagerland, J.A., & Arp, L.H. (1990). A morphologic study of bronchus-associated lymphoid tissue in turkeys. *The American Journal of Anatomy, 189*, 24-34.

Fahey, K.J., Bagust, T.J., & York, J.J. (1983). Laryngotracheitis herpesvirus infection in the chicken: The role of humoral antibody in immunity to a graded challenge infection. *Avian Pathology, 12*, 505-514.

Fahey, K.J., & York, J.J. (1990). The role of mucosal antibody in immunity to infectious laryngotracheitis virus in chickens. *The Journal of General Virology, 71 (Pt 10)*, 2401-2405.

Fahey, K.J., York, J.J., & Bagust, T.J. (1984). Laryngotracheitis herpesvirus infection in the chicken. Ii. The adoptive transfer of resistance with immune spleen cells. *Avian Pathology, 13*, 265-275.

Ferguson, N. M. (2013). Mycoplasmosis. In D. E. Swayne, J. R. Glisson, L. R. McDougland, L.K. Nolan, D. L. Suarez & V. L. Nair (Eds.), *Diseases of poultry 13th edn* (pp. 875-941): Ames, Iowa: Wiley-Blackwell.

Fix, A.S., & Arp, L.H. (1989). Conjunctiva-associated lymphoid tissue (calt) in normal and bordetella avium-infected turkeys. *Veterinary Pathology, 26*, 222-230.

Fix, A.S., & Arp, L.H. (1991a). Morphologic characterization of conjunctiva-associated lymphoid tissue in chickens. *American Journal of Veterinary Research, 52*, 1852-1859.

Fix, A.S., & Arp, L.H. (1991). Particle uptake by conjunctiva-associated lymphoid tissue (CALT) in turkeys. *Avian Diseases, 35*, 100-106.

Fix, A.S., & Arp, L.H. (1991b). Quantification of particle uptake by conjunctiva-associated lymphoid tissue (CALT) in chickens. *Avian Diseases, 35*, 174-179.

Fletcher, O. J., Abdul-Aziz, T., (2016). Respiratory system. In. Abdul-Aziz, T., Fletcher, O. J., Barnes, J. H. (Eds.), *Avian Histopathology 4th ed* (pp. 195 – 269): *The American Association of Avian Pathologists*.

Fuchs, W., & Mettenleiter, T.C. (2005). The nonessential ul49.5 gene of infectious laryngotracheitis virus encodes an o-glycosylated protein which forms a complex with the non-glycosylated ul10 gene product. *Virus Research, 112*, 108-114.

Fuchs, W., Wiesner, D., Veits, J., Teifke, J.P., & Mettenleiter, T.C. (2005). In vitro and in vivo relevance of infectious laryngotracheitis virus gj proteins that are expressed from spliced and nonspliced mrnas. *Journal of Virology, 79*, 705-716.

Fuchs, W., Veits, J., Helferich, D., Granzow, H., Teifke, J.P., & Mettenleiter, T.C. (2007). Molecular biology of avian infectious laryngotracheitis virus. *Veterinary Research, 38*, 261-279.

Fulton, R.M., Schrader, D.L., & Will, M. (2000). Effect of route of vaccination on the prevention of infectious laryngotracheitis in commercial egg-laying chickens. *Avian Diseases, 44*, 8-16.

García, M. (2016). Current and future vaccines and vaccination strategies against infectious laryngotracheitis (ILT) respiratory disease of poultry. *Veterinary Microbiology, 206*, 157-162.

García, M., Spatz, S., & Guy, J. (2013). Infectious laryngotracheitis. In D. E. Swayne, J. R. Glisson, L. R. McDougland, L.K. Nolan, D. L. Suarez & V. L. Nair (Eds.), *Diseases of poultry 13th edn* (pp. 161-179): Ames, Iowa: Wiley-Blackwell.

Garritty, A.D. (2008). ILTV vaccination-challenging the dogma. *The Poultry Informed Professional*, 1-5.

Gelenczei, E.F., & Marty, E.W. (1964). Studies on a tissue-culture-modified infectious laryngotracheitis virus. *Avian Diseases, 8*, 105-122.

Gimeno, I.M., Cortes, A.L., Guy, J.S., Turpin, E., & Williams, C. (2011). Replication of recombinant herpesvirus of turkey expressing genes of infectious laryngotracheitis virus in specific pathogen free and broiler chickens following in ovo and subcutaneous vaccination. *Avian Pathology, 40*, 395-403.

Gonzalez-Motos, V., Kropp, K.A., & Viejo-Borbolla, A. (2016). Chemokine binding proteins: An immunomodulatory strategy going viral. *Cytokine & Growth Factor Reviews, 30*, 71-80.

Guo, P., Scholz, E., Maloney, B., & Welniak, E. (1994). Construction of recombinant avian infectious laryngotracheitis virus expressing the beta-galactosidase gene and DNA sequencing of the insertion region. *Virology, 202*, 771-781.

Gurjar, R.S., Gulley, S.L., & van Ginkel, F.W. (2013). Cell-mediated immune responses in the head-associated lymphoid tissues induced to a live attenuated avian coronavirus vaccine. *Developmental and Comparative Immunology, 41*, 715-722.

Haddadi, S., Kim, D.S., Jasmine, H., van der Meer, F., Czub, M., & Abdul-Careem, M.F. (2013). Induction of toll-like receptor 4 signaling in avian macrophages inhibits infectious laryngotracheitis virus replication in a nitric oxide dependent way. *Veterinary Immunology and Immunopathology, 155*, 270-275.

Haddadi, S., Thapa, S., Kameka, A.M., Hui, J., Czub, M., Nagy, E., Muench, G., Abdul-Careem, M.F. (2015). Toll-like receptor 2 ligand, lipoteichoic acid is inhibitory against infectious laryngotracheitis virus infection in vitro and in vivo. *Developmental and Comparative Immunology, 48*, 22-32.

Hamzic, E., Pinard-van der Laan, M.H., Bed'Hom, B., & Juul-Madsen, H.R. (2015).

Annotation and genetic diversity of the chicken collagenous lectins. *Molecular Immunology, 65*, 277-286.

Higuchi, M., Matsuo, A., Shingai, M., Shida, K., Ishii, A., Funami, K., Suzuki, Y., Oshiumi, H., Matsumoto, M., Seya, T. (2008). Combinational recognition of bacterial lipoproteins and peptidoglycan by chicken toll-like receptor 2 subfamily. *Developmental and Comparative Immunology, 32*, 147-155.

Hiller, A.S., Tschernig, T., Kleemann, W.J., & Pabst, R. (1998). Bronchus-associated lymphoid tissue (BALT) and larynx-associated lymphoid tissue (LALT) are found at different frequencies in children, adolescents and adults. *Scandinavian Journal of Immunology, 47*, 159-162.

Honda, T., Okamura, H., Taneno, A., Yamada, S., & Takahashi, E. (1994). The role of cell-mediated immunity in chickens inoculated with the cell-associated vaccine of attenuated infectious laryngotracheitis virus. *The Journal of Veterinary Medical Science, 56*, 1051-1055.

Honda, T., Taneno, A., Sakai, E., Yamada, S., & Takahashi, E. (1994). Immune response and in vivo distribution of the virus in chickens inoculated with the cell-associated vaccine of attenuated infectious laryngotracheitis (ILT) virus. *The Journal of Veterinary Medical Science, 56*, 691-695.

Hughes, C.S., Gaskell, R.M., Jones, R.C., Bradbury, J.M., & Jordan, F.T. (1989). Effects of certain stress factors on the re-excretion of infectious laryngotracheitis virus from latently infected carrier birds. *Research in Veterinary Science, 46*, 274-276.

Hughes, C.S., Williams, R.A., Gaskell, R.M., Jordan, F.T., Bradbury, J.M., Bennett, M., & Jones, R.C. (1991). Latency and reactivation of infectious laryngotracheitis vaccine virus. *Archives of Virology, 121*, 213-218.

Iqbal, M., Philbin, V.J., & Smith, A.L. (2005). Expression patterns of chicken toll-like receptor mrna in tissues, immune cell subsets and cell lines. *Veterinary Immunology and Immunopathology, 104*, 117-127.

Jackwood, M., & Sjaak, W. (2013). Infectious Bronchitis. In D.E. Swayne, J. R. Glisson, L. R. McDougland, L. K. Nolan, D. L. Suarez & V. L. Nair (Eds.), *Diseases of Poultry 13th ed* (pp. 139-159): Ames, Iowa: Willey-Blackwell.

Jeurissen, S.H., Wagenaar, F., & Janse, E.M. (1999). Further characterization of m cells in gut-associated lymphoid tissues of the chicken. *Poultry Science, 78*, 965-972.

Johnson, K.E., & Knipe, D.M. (2010). Herpes simplex virus-1 infection causes the secretion of a type i interferon-antagonizing protein and inhibits signaling at or before Jak-1 activation. *Virology, 396*, 21-29.

Johnson, M.A., Prideaux, C.T., Kongsuwan, K., Sheppard, M., & Fahey, K.J. (1991). Gallid herpesvirus 1 (infectious laryngotracheitis virus): Cloning and physical maps of the sa-2 strain. *Archives of Virology, 119*, 181-198.

Juul-Madsen, H.R., Viertlböeck, B., Härtle, S., Smith, A.L., & Göbel, T.W. (2014). Chapter 7 - innate immune responses. In B. Kaspers & P. Kaiser (Eds.), *Avian immunology (second edition)* (pp. 121-147). Boston: Academic Press.

Kaiser, P. (2010). Advances in avian immunology--prospects for disease control: A review. *Avian Pathology, 39*, 309-324.

Kang, H., Yan, M., Yu, Q., & Yang, Q. (2013). Characteristics of nasal-associated lymphoid tissue (NALT) and nasal absorption capacity in chicken. *PLoS One, 8*, e84097.

Kasahara, Y., Chen, C.H., & Cooper, M.D. (1993). Growth requirements for avian gamma delta t cells include exogenous cytokines, receptor ligation and in vivo priming. *European Journal of Immunology, 23*, 2230-2236.

Kaufman, J. (2014). Chapter 8 - the avian mhc. In K. A. Schat, B. Kaspers & P. Kaiser (Eds.), *Avian Immunology (second edition)* (pp. 149-167). Boston: Academic Press.

Keestra, A.M., de Zoete, M.R., Bouwman, L.I., Vaezirad, M.M., & van Putten, J.P. (2013). Unique features of chicken toll-like receptors. *Developmental and Compparative Immunology, 41*, 316-323.

Kingsley, D.H., Hazel, J.W., & Keeler, C.L., Jr. (1994). Identification and characterization of the infectious laryngotracheitis virus glycoprotein C gene. *Virology, 203*, 336-343.

Kingsley, D.H., & Keeler, C.L., Jr. (1999). Infectious laryngotracheitis virus, an alpha herpesvirus that does not interact with cell surface heparan sulfate. *Virology, 256*, 213-219.

Klika, E., Scheuermann, D.W., De Groodt-Lasseel, M.H., Bazantova, I., & Switka, A. (1996). Pulmonary macrophages in birds (barn owl, tyto tyto alba), domestic fowl (gallus gallus f. Domestica), quail (coturnix coturnix), and pigeons (columbia livia). *The Anatomical Record, 246*, 87-97.

Kogut, M.H., Iqbal, M., He, H., Philbin, V., Kaiser, P., & Smith, A. (2005). Expression and function of toll-like receptors in chicken heterophils. *Developmental and Compparative Immunology, 29*, 791-807.

Kowalski, W.J., Malkinson, M., Leslie, G.A., & Small, P.A. (1978). The secretory immunological system of the fowl. Vi. The effect of chemical bursectomy on immunoglobulin concentration in tears. *Immunology, 34*, 663-667.

Krug, A., Luker, G.D., Barchet, W., Leib, D.A., Akira, S., & Colonna, M. (2004). Herpes simplex virus type 1 activates murine natural interferon-producing cells through toll-like receptor 9. *Blood, 103*, 1433-1437.

Krunkosky, M., Garcia, M., Beltran Garza, L.G., Karpuzoglu-Belgin, E., Levin, J., Williams, R.J., & Gogal, R.M., Jr. (2018). Seeding of the mucosal leukocytes in the halt and trachea of white leghorn chickens. *Journal of Immunoassay and Immunochemistry, 39*, 43-57.

Kurt-Jones, E.A., Chan, M., Zhou, S., Wang, J., Reed, G., Bronson, R., Finberg, R.W. (2004). Herpes simplex virus 1 interaction with toll-like receptor 2 contributes to lethal encephalitis. *Proceedings of the National Academy of Science of U S A, 101*, 1315-1320.

Lam, V.C., & Lanier, L.L. (2017). NK cells in host responses to viral infections. *Current Opinion in Immunology, 44*, 43-51.

Lang, T., Hansson, G.C., & Samuelsson, T. (2006). An inventory of mucin genes in the chicken genome shows that the mucin domain of muc13 is encoded by multiple exons and that ovomucin is part of a locus of related gel-forming mucins. *BMC Genomics, 7*, 197.

Lee, J.Y., Song, J.J., Wooming, A., Li, X., Zhou, H., Bottje, W.G., & Kong, B.W. (2010). Transcriptional profiling of host gene expression in chicken embryo lung cells infected with laryngotracheitis virus. *BMC Genomics, 11*, 445.

Lee, S.W., Hartley, C.A., Coppo, M.J., Vaz, P.K., Legione, A.R., Quinteros, J.A., Noormohammadi, A. H., Markham, P. F. Browning, G. F. Devlin, J.M. (2015). Growth kinetics and transmission potential of existing and emerging field strains of infectious laryngotracheitis virus. *PLoS One, 10*, e0120282.

Lee, S.W., Markham, P.F., Coppo, M.J., Legione, A.R., Markham, J.F., Noormohammadi, A.H., Devlin, J.M. (2012). Attenuated vaccines can recombine to form virulent field viruses. *Science, 337*, 188.

Leib, D.A., Bradbury, J.M., Hart, C.A., & McCarthy, K. (1987). Genome isomerism in two alphaherpesviruses: Herpesvirus saimiri-1 (herpesvirus tamarinus) and avian infectious laryngotracheitis virus. Brief report. *Archives of Virology, 93*, 287-294.

LeibundGut-Landmann, S., Waldburger, J.M., Krawczyk, M., Otten, L.A., Suter, T., Fontana, A., Reith, W. (2004). Mini-review: Specificity and expression of ciita, the master regulator of MHC class II genes. *European Journal of Immunology, 34*, 1513-1525.

Loncoman, C.A., Hartley, C.A., Coppo, M.J.C., Browning, G.F., Beltran, G., Riblet, S., freitas, C. O., García, M., Devlin, J.M. (2018). The snp genotyping assay shows that vaccination can limit the number and diversity of recombinant progeny of infectious laryngotracheitis viruses from the USA. *Applied and Environmental Microbiology*.

Loncoman, C.A., Hartley, C.A., Coppo, M.J., Vaz, P.K., Diaz-Mendez, A., Browning, G.F.,Devlin, J.M. (2017). Development and application of a taqman single nucleotide polymorphism genotyping assay to study infectious laryngotracheitis virus recombination in the natural host. *PLoS One, 12*, e0174590.

Loudovaris, T., Calnek, B.W., Yoo, B.H., & Fahey, K.J. (1991). Genetic susceptibility of chicken macrophages to in vitro infection with infectious laryngotracheitis virus. *Avian Pathology, 20*, 291-302.

Luo, J., Carrillo, J.A., Menendez, K.R., Tablante, N.L., & Song, J. (2014). Transcriptome analysis reveals an activation of major histocompatibility complex I and II pathways in chicken trachea immunized with infectious laryngotracheitis virus vaccine. *Poultry Science, 93*, 848-855.

Lynn, D.J., Higgs, R., Lloyd, A.T., O'Farrelly, C., Herve-Grepinet, V., Nys, Y., Brinkman, F. S., Yu, P. L., Soulier, A., Kaiser, P., Zhang, G., Lehrer, R.I. (2007). Avian beta-defensin nomenclature: A community proposed update. *Immunology Letters, 110*, 86-89.

Mahmoudian, A., Markham, P.F., Noormohammadi, A.H., & Browning, G.F. (2012). Kinetics of transcription of infectious laryngotracheitis virus genes. *Comparative Immunology, Microbiology and Infectious Diseases, 35*, 103-115.

Maina, J.N. (2002). Some recent advances on the study and understanding of the functional design of the avian lung: Morphological and morphometric perspectives. *Biological Reviews of the Cambridge Philosophical Society, 77*, 97-152.

Majumder, S., & Silbart, L.K. (2015). Interaction of mycoplasma gallisepticum with chicken tracheal epithelial cells contributes to macrophage chemotaxis and activation. *Infection and Immunity, 84*, 266-274.

Mansikka, A., Sandberg, M., Veromaa, T., Vainio, O., Granfors, K., & Toivanen, P. (1989). B cell maturation in the chicken harderian gland. *Journal of Immunology, 142*, 1826-1833.

McGeoch, D.J., Dalrymple, M.A., Davison, A.J., Dolan, A., Frame, M.C., McNab, D., Perry, L. J., Scott, J. E., Taylor, P. (1988). The complete DNA sequence of the long unique region in the genome of herpes simplex virus type 1. *The Journal of General Virology, 69 (Pt 7)*, 1531-1574.

Morandi, B., Mortara, L., Carrega, P., Cantoni, C., Costa, G., Accolla, R.S., Ferlazzo, G. (2009). NK cells provide helper signal for CD8+ T cells by inducing the expression of membrane-bound IL-15 on DCs. *International Immunology, 21*, 599-606.

Nandakumar, S., Woolard, S.N., Yuan, D., Rouse, B.T., & Kumaraguru, U. (2008). Natural killer cells as novel helpers in anti-herpes simplex virus immune response. *Journal of Virology, 82*, 10820-10831.

Neutra, M.R., Mantis, N.J., & Kraehenbuhl, J.P. (2001). Collaboration of epithelial cells with organized mucosal lymphoid tissues. *Nature Immunology, 2*, 1004-1009.

Niedorf, H.R., & Wolters, B. (1978). Dvelopment of the harderian gland in the chicken: Light and electron microscopic investigations. *Investigative and Cell Pathology, 1*, 205-215.

Nunoya, T., Tajima, M., Yagihashi, T., & Sannai, S. (1987). Evaluation of respiratory lesions in chickens induced by mycoplasma gallisepticum. *Nihon Juigaku Zasshi. The Japanese Journal of Veterinary Science, 49*, 621-629.

Ohshima, K., & Hiramatsu, K. (2000). Distribution of t-cell subsets and immunoglobulin-containing cells in nasal-associated lymphoid tissue (NALT) of chickens. *Histology and Histopathology, 15*, 713-720.

Ohshima, K., & Hiramatsu, K. (2002). Immunohistochemical localization of three different immunoglobulin classes in the harderian gland of young chickens. *Tissue & Cell, 34*, 129-133.

Olah, I., Kupper, A., & Kittner, Z. (1996). The lymphoid substance of the chicken's harderian gland is organized in two histologically distinct compartments. *Microscopy Research and Techniques, 34*, 166-176.

Oláh, I., Nagy, N., & Vervelde, L. (2014). Chapter 2 - structure of the avian lymphoid system. In B. Kaspers & P. Kaiser (Eds.), *Avian immunology (second edition)* (pp. 11-44). Boston: Academic Press.

Olah, I., Scott, T.R., Gallego, M., Kendall, C., & Glick, B. (1992). Plasma cells expressing immunoglobulins m and a but not immunoglobulin g develop an intimate relationship with central canal epithelium in the harderian gland of the chicken. *Poultry Science, 71*, 664-676.

Oldoni, I., Rodriguez-Avila, A., Riblet, S.M., Zavala, G., & García, M. (2009). Pathogenicity and growth characteristics of selected infectious laryngotracheitis virus strains from the united states. *Avian Pathology, 38*, 47-53.

Paladino, P., Collins, S.E., & Mossman, K.L. (2010). Cellular localization of the herpes simplex virus icp0 protein dictates its ability to block irf3-mediated innate immune responses. *PLoS One, 5*, e10428.

Paul, W.E. (2013). Fundamental immunology. *Philadelphia : Wolters Kluwer Health/Lippincott Williams & Wilkins,*.

Payne, A.P. (1994). The harderian gland: A tercentennial review. *Journal of Anatomy, 185 (Pt 1)*, 1-49.

Poulsen, D.J., Burton, C.R., O'Brian, J.J., Rabin, S.J., & Keeler, C.L., Jr. (1991). Identification of the infectious laryngotracheitis virus glycoprotein gb gene by the polymerase chain reaction. *Virus Genes, 5*, 335-347.

Poulsen, D.J., & Keeler, C.L., Jr. (1997). Characterization of the assembly and processing of infectious laryngotracheitis virus glycoprotein b. *The Journal of General Virology, 78 (Pt 11)*, 2945-2951.

Purcell, D.A. (1971). The ultrastructural changes produced by infectious laryngotracheitis virus in tracheal epithelium of the fowl. *Research in Veterinary Science, 12*, 455-458.

Purcell, D.A., & McFerran, J.B. (1969). Influence of method of infection on the pathogenesis of infectious laryngotracheitis. *Journal of Comparative Pathology, 79*, 285-291.

Rachamadugu, R., Lee, J.Y., Wooming, A., & Kong, B.W. (2009). Identification and expression analysis of infectious laryngotracheitis virus encoding micrornas. *Virus Genes, 39*, 301-308.

Reddy, V.R., Steukers, L., Li, Y., Fuchs, W., Vanderplasschen, A., & Nauwynck, H.J. (2014). Replication characteristics of infectious laryngotracheitis virus in the respiratory and conjunctival mucosa. *Avian Pathology, 43*, 450-457.

Reddy, V.R., Trus, I., & Nauwynck, H.J. (2017). Presence of DNA extracellular traps but not muc5ac and muc5b mucin in mucoid plugs/casts of infectious laryngotracheitis virus (ILTV) infected tracheas of chickens. *Virus Research, 227*, 135-142.

Reith, W., LeibundGut-Landmann, S., & Waldburger, J.M. (2005). Regulation of mhc class ii gene expression by the class ii transactivator. *Nature Reviews Immunology, 5*, 793-806.

Roizman, B., & Pellett, P.E. (2001). The family herpesviridae: A brief introduction. *In: Fields Virology. D. M. Knipe and P. M. Howley, eds. Lippincott Williams & Wilkins, Philadelphia.*, 2381-2397.

Rothwell, B., Wight, P.A., Burns, R.B., & Mackenzie, G.M. (1972). The harderian glands of the domestic fowl. 3. Ultrastructure. *Journal of Anatomy, 112*, 233-250.

Samberg, Y., Cuperstein, E., Bendheim, U., & Aronovici, I. (1971). The development of a vaccine against avian infectious laryngotracheitis. Iv. Immunization of chickens with a modified laryngotracheitis vaccine in the drinking water. *Avian Diseases, 15*, 413-417.

Sarson, A.J., Abdul-Careem, M.F., Read, L.R., Brisbin, J.T., & Sharif, S. (2008). Expression of cytotoxicity-associated genes in marek's disease virus-infected chickens. *Viral Immunology, 21*, 267-272.

Shukla, D., & Spear, P.G. (2001). Herpesviruses and heparan sulfate: An intimate relationship in aid of viral entry. *The Journal of Clinical Investigation, 108*, 503-510.

Smialek, M., Tykalowski, B., Stenzel, T., & Koncicki, A. (2011). Local immunity of the respiratory mucosal system in chickens and turkeys. *Polish Journal of Veterinary Science, 14*, 291-297.

Spatz, S.J., Volkening, J.D., Keeler, C.L., Kutish, G.F., Riblet, S.M., Boettger, C.M., Clark, K. F., Zsak, L., Afonso, C. L., Mundt, E. S., Rock, D. L.,. García, M. (2012). Comparative full genome analysis of four infectious laryngotracheitis virus (gallid herpesvirus-1) virulent isolates from the united states. *Virus Genes, 44*, 273-285.

Spear, P.G. (1993). Entry of alphaherpesviruses into cells. *Seminars in Virology, 4*, 167-180.

Sutton, K., Costa, T., Alber, A., Bryson, K., Borowska, D., Balic, A., Kaiser, P., Stevens, M., Vervelde, L. (2018). Visualisation and characterisation of mononuclear phagocytes in the

chicken respiratory tract using CSF1R-transgenic chickens. *Veterinary Research, 49*, 104.

Thapa, S., Cader, M.S., Murugananthan, K., Nagy, E., Sharif, S., Czub, M., & Abdul-Careem, M.F. (2015). In ovo delivery of cpg DNA reduces avian infectious laryngotracheitis virus induced mortality and morbidity. *Viruses, 7*, 1832-1852.

Thapa, S., Nagy, E., & Abdul-Careem, M.F. (2015). In ovo delivery of toll-like receptor 2 ligand, lipoteichoic acid induces pro-inflammatory mediators reducing post-hatch infectious laryngotracheitis virus infection. *Veterinary Immunology and Immunopathology, 164*, 170-178.

Thureen, D.R., & Keeler, C.L., Jr. (2006). Psittacid herpesvirus 1 and infectious laryngotracheitis virus: Comparative genome sequence analysis of two avian alphaherpesviruses. *Journal of Virology, 80*, 7863-7872.

Ting, J.P., & Trowsdale, J. (2002). Genetic control of mhc class II expression. *Cell, 109 Suppl*, S21-33.

Vagnozzi, A., Riblet, S., Williams, S.M., Zavala, G., & Garcia, M. (2015). Infection of broilers with two virulent strains of infectious laryngotracheitis virus: Criteria for evaluation of experimental infeccions. *Avian Diseases, 59*, 394-399.

Vagnozzi, A., Riblet, S., Zavala, G., Ecco, R., Afonso, C.L., & Garcia, M. (2016). Evaluation of the transcriptional status of host cytokines and viral genes in the trachea of vaccinated and non-vaccinated chickens after challenge with the infectious laryngotracheitis virus. *Avian Pathology, 45*, 106-113.

Vagnozzi, A., Zavala, G., Riblet, S.M., Mundt, A., & Garcia, M. (2012). Protection induced by commercially available live-attenuated and recombinant viral vector vaccines against infectious laryngotracheitis virus in broiler chickens. *Avian Pathology, 41*, 21-31.

Vagnozzi, A.E., Beltran, G., Zavala, G., Read, L., Sharif, S., & Garcia, M. (2018). Cytokine gene transcription in the trachea, harderian gland, and trigeminal ganglia of chickens inoculated with virulent infectious laryngotracheitis virus (ILTV) strain. *Avian Pathology*, 1-12.

van den Elsen, P.J., Holling, T.M., Kuipers, H.F., & van der Stoep, N. (2004). Transcriptional regulation of antigen presentation. *Current Opinion in Immunology, 16*, 67-75.

van Ginkel, F.W., Tang, D.C., Gulley, S.L., & Toro, H. (2009). Induction of mucosal immunity in the avian harderian gland with a replication-deficient ad5 vector expressing avian influenza h5 hemagglutinin. *Developmental and Comparative Immunology, 33*, 28-34.

Vandevenne, P., Sadzot-Delvaux, C., & Piette, J. (2010). Innate immune response and viral interference strategies developed by human herpesviruses. *Biochemical Pharmacology, 80*, 1955-1972.

Vareille, M., Kieninger, E., Edwards, M.R., & Regamey, N. (2011). The airway epithelium: Soldier in the fight against respiratory viruses. *Clinical Microbiology Reviews, 24*, 210-229.

Veits, J., Kollner, B., Teifke, J.P., Granzow, H., Mettenleiter, T.C., & Fuchs, W. (2003). Isolation and characterization of monoclonal antibodies against structural proteins of infectious laryngotracheitis virus. *Avian Diseases, 47*, 330-342.

Verpooten, D., Ma, Y., Hou, S., Yan, Z., & He, B. (2009). Control of tank-binding kinase 1-mediated signaling by the gamma(1)34.5 protein of herpes simplex virus 1. *The Journal of Biological Chemistry, 284*, 1097-1105.

Wang, L.G., Ma, J., Xue, C.Y., Wang, W., Guo, C., Chen, F., Qin, J. P., Huang, N. H., Bi, Y. Z., Cao, Y.C. (2013). Dynamic distribution and tissue tropism of infectious laryngotracheitis virus in experimentally infected chickens. *Archives of Virology, 158*, 659-666.

Whitsett, J.A., & Alenghat, T. (2015). Respiratory epithelial cells orchestrate pulmonary innate immunity. *Nature Immunology, 16*, 27-35.

Wight, P.A., Burns, R.B., Rothwell, B., & Mackenzie, G.M. (1971). The harderian gland of the domestic fowl. I. Histology, with reference to the genesis of plasma cells and russell bodies. *Journal of Anatomy, 110*, 307-315.

Yao, Y., & Nair, V. (2014). Role of virus-encoded micrornas in avian viral diseases. *Viruses, 6*, 1379-1394.

York, J.J., & Fahey, K.J. (1990). Humoral and cell-mediated immune responses to the glycoproteins of infectious laryngotracheitis herpesvirus. *Archive of Virology, 115*, 289-297.

York, J.J., Sonza, S., & Fahey, K.J. (1987). Immunogenic glycoproteins of infectious laryngotracheitis herpesvirus. *Virology, 161*, 340-347.

York, J.J., Young, J.G., & Fahey, K.J. (1989). The appearance of viral antigen and antibody in the trachea of naive and vaccinated chickens infected with infectious laryngotracheitis virus. *Avian Pathology, 18*, 643-658.

Zhang, S.Y., Jouanguy, E., Ugolini, S., Smahi, A., Elain, G., Romero, P., Segal, D., Sancho-Shimizu, V., Lorenzo, L., Puel, A., Picar, C., Chapigier, A., Plancoulaine, S., Titeux, M., Cognet, C., Von Bernuth, H., Ku, C. L., Casrouge, A., Zhang, X. X., Barreiro, L., Leonard, J., Hamilton, C., Lebon, P., Heron, B., Vallee, L., Quintanta-Murci, L., Hovnanian, A., Rozenberg, F., Vivier, E., Geissmann, F., Tardieu, M., Abel, L., Casanova, J.L. (2007). Tlr3 deficiency in patients with herpes simplex encephalitis. *Science, 317*, 1522-1527.

Zhao, Y., Kong, C., Cui, X., Cui, H., Shi, X., Zhang, X., Hu, S., Hao, L.,. Wang, Y. (2013). Detection of infectious laryngotracheitis virus by real-time pcr in naturally and experimentally infected chickens. *PLoS One, 8*, e67598.

Ziemann, K., Mettenleiter, T.C., & Fuchs, W. (1998). Infectious laryngotracheitis herpesvirus expresses a related pair of unique nuclear proteins which are encoded by split genes located at the right end of the UL genome region. *Journal of Virology, 72*, 6867-6874.

CHAPTER 3

The route of inoculation dictates replication patterns of infectious laryngotracheitis virus (ILTV) pathogenic strain and chicken embryo origin (CEO) vaccine

Gabriela Beltrán[1], S. M. Williams, Guillermo Zavala, James S. Guy Maricarmen García. 2017. Avian Pathology. 46:585-593. Reprinted here with permission of the publisher

ABSTRACT

Infectious laryngotracheitis virus (ILTV) has a high affinity to replicate in the larynx and trachea causing severe lesions. Apart from the trachea, lack of knowledge exists on the ability of ILTV to replicate in other respiratory associated tissues. The objective of this study was to investigate how tissues that first encounter the virus dictate further sites of viral replication during the lytic stage of infection. Replication patterns of pathogenic strain 63140 and the chicken embryo origin (CEO) vaccine in conjunctiva, Harderian gland, nasal cavity and trachea were evaluated after ocular, oral, intranasal or intratracheal inoculation of specific pathogen free chickens. Viral replication was assessed by detection of microscopic cytolytic lesions, detection of viral antigen and viral genome load. The route of viral entry greatly influenced virus replication of both strain 63140 and CEO vaccine in conjunctiva and trachea, while replication in the nasal cavity was not affected. In the Harderian gland independently of the route of viral entry, microscopic lesions characteristic of lytic replication were absent, whereas viral antigen and genome were detected for either virus, suggesting that the Harderian gland may be a key site of antigen uptake. Findings from this study suggest that interactions of the virus with nasal cavity, conjunctiva and Harderian gland epithelial-lymphoid tissues would dictate patterns of ILTV lytic replication.

INTRODUCTION

Infectious laryngotracheitis (ILT) is a highly contagious acute respiratory disease of chickens that results in severe losses due to mortality and/or decrease in egg production. The disease is caused by the avian alphaherpesvirus *Gallid alpha herpesvirus 1* (GaHV-1) commonly known as infectious laryngotracheitis virus (ILTV). Independent studies aimed to assess the levels of pathogenicity among field isolates and vaccines found that evaluation of microscopic lesions in the trachea after intratracheal inoculation did not necessarily correlated with the severity of the clinical presentation. When vaccines were administered intratracheally, although not severe clinical signs were observed, few birds showed severe microscopic lesions in the trachea (Guy *et al*., 1990). After intratracheal inoculation microscopic lesions in the trachea were not reliable indicators of pathogenicity since isolates that induced high mortality rates produced moderate pathological changes in the trachea (Kirkpatrick *et al*., 2006). Furthermore in two independent studies after intra-tracheal inoculation of the standard USDA challenge strain and more recent outbreak-related ILTV strains, the presence of tracheal lesions not necessarily correlated with clinical signs of disease (Koski *et al*., 2015) and neither microscopic lesions nor clinical signs revealed differences in pathogenicity between strains (Vagnozzi *et al*., 2015). On the other hand, when various US field isolates were inoculated by the ocular-nasal route differences in disease severity and viral tissue distribution were revealed (Oldoni *et al*., 2009), suggesting that the route of viral entry significantly influences the disease outcome.

Infectious laryngotracheitis is mainly controlled by vaccination with either live attenuated or recombinant viral vector vaccines (García *et al*., 2013). There are two types of live attenuated ILTV vaccines used to control the disease: the tissue culture origin (TCO) and the chicken embryo origin (CEO) (García et al., 2013) vaccines. The CEO vaccines are recommended for

mass administration by the drinking water, spray, or for individual administration by eye drop vaccination while the TCO vaccine is recommended solely for eye drop administration (Gelenczei & Marty, 1964). The method of administration of live attenuated vaccines plays a crucial role in the degree of protection elicited by vaccination (Fulton *et al*., 2000). Despite this knowledge, how the route of viral entry influences viral replication in the upper respiratory tract and in mucosal tissues of the nasal cavity, conjunctiva and Harderian gland has not been studied. The nasal cavity, conjunctiva and Harderian gland are structures that, although not anatomically connected to the respiratory system in concurrence with the trachea, are the first to come into contact with the virus during vaccination or natural infection (Härtle & Kaspers, 2014). In this study potential routes of viral entry, accessible during mass vaccination or natural infection, were reproduced by individually inoculating chickens via the ocular, intranasal, oral or intratracheal routes. The specific objective of this study was to determine how the route of viral entry influences the pattern of replication for pathogenic strain 63140 and the CEO vaccine. Viral replication in tissues was assessed by detection of microscopic lesions characteristic of ILTV lytic replication, detection of viral antigen by immunohistochemistry (IHC) and quantification of viral genome load. Findings from this study showed that the route of inoculation greatly influences the replication patterns of ILTV and revealed that tissues of the nasal cavity and conjunctiva, as well as the Harderian gland play a key role in early virus replication and consequently will dictate the outcome of infection.

MATERIALS AND METHODS

ILTV strains

The Georgia broiler strain 63140 (Vagnozzi *et al*., 2015) and the CEO vaccine (Trachivax® MERCK, Animal Health, NJ, USA) were utilized in this study. The pathogenic strain 63140 was propagated in chicken kidney cells obtained from 3 to 4-week-old specific pathogen free (SPF) chickens (Rodriguez-Avila *et al*., 2008). The CEO vaccine was reconstituted as recommended by the manufacturers. After inoculation both viruses were titrated in chicken kidney cells as previously described (Rodriguez-Avila *et al*., 2008) to confirm the median tissue culture infective dose ($TCID_{50}$) administered.

Experimental Design

Two independent studies were performed. In study I the replication of the pathogenic strain 63140 was examined and in study II the replication of CEO vaccine was evaluated. Replication in trachea, conjunctiva, nasal cavity and Harderian gland was evaluated when administered via the ocular (OC), oral (OR), intranasal (IN) or intratracheal (IT) routes. SPF fertile eggs were obtained from Sunrise (Stuarts Draft, VA, USA), and incubated for a total of 506 hours at the Poultry Diagnostic Research Center, University of Georgia hatchery facilities.

Study I. A total of 128 SPF chickens were divided into eight groups of 16 chickens per group. Chickens were housed in isolation units, eight chickens per unit, with filtered air and negative pressure, and provided with feed and water *ad libitum*. At three weeks of age four groups of chickens were inoculated with pathogenic strain 63140 by the OC, OR, IN, or IT route. Four additional groups of chickens were mock inoculated with cell culture media by the same routes and used as negative controls. All groups of chickens received a dose of $10^{3.5}$ $TCID_{50}$ per

chicken. The OC and IN inoculated group of chickens received the dose in a 60µl volume, 30µl per eye or per naris, respectively. The IT and OR inoculated groups of chickens received the dose in a 100µl volume. For oral inoculation the inoculum was placed in the palatine cleft of chickens. Mock-inoculated groups of chickens received cell culture media in a similar manner.

Study II. A total of 195 SPF one-day-old chickens were divided in eight groups of 26 to 24 chickens per group and housed and fed as described above. At two-weeks of age four groups of chickens were inoculated with the CEO vaccine by the OC, OR, IN, or IT routes as described above. Four additional groups of chickens were mock inoculated with cell culture media by OC, OR, IN, or IT routes and served as negative controls. All groups inoculated with the CEO vaccine received five times (5X) the recommended commercial dose.

All animal experiments conducted in this study were performed under the Animal Use Proposal A2015 05-001-Y2-A0 approved by the Animal Care and Use Committee (IACUC) in accordance with regulations of the Office of the Vice President for Research at the University of Georgia.

Tissue collection

Conjunctiva, nasal cavity swabs, trachea and Harderian gland were collected from four (Study I) and six chickens (Study II) per group at 3 and 5 days post-inoculation for PCR analysis. Eye-conjunctiva swabs were collected by rubbing the internal surface of the eyelids with sterile polyester tipped applicators (Puritan®, Guilford, ME. USA). Nasal cavity swabs were collected from the ciliated pseudo-stratified columnar epithelium of the nasal cavity after making a transversal cut at half way down the beak and wiping the nasal cavity 3 to 4 times with a swab.

One inch transverse sections of proximal tracheas were aseptically dissected and fat and connective tissue removed from serosa. Collection of Harderian gland was performed as previously described (Neumann, 1976). Conjunctiva, nasal cavity swabs, trachea and Harderian gland tissues were immediately placed in tubes containing 1.4 mm ceramic spheres (Lysing matrix D, MP Biomedicals, Santa Ana, CA. USA) with 2 ml of sterile phosphate-buffered saline solution (0.0067M PO_4 pH 7.0-7.2, Hyclone), 2% antibiotic-antimicotic and 2% foetal bovine serum (Atlanta®, Biological, Flowery Branch, GA. USA) and stored at -80 C° until processed for DNA extraction.

For histopathological examination trachea, conjunctiva, nasal cavity and Harderian glands were collected at three and five days post-inoculation from four chickens (Study I) and seven to six chickens (Study II) per group. Trachea and Harderian glands were collected as described above. The conjunctiva was collected by making a transversal cut of the upper and lower eyelids (left and right). Nasal cavity tissue was obtained by making a transversal cut of the distal portion of the beak, followed by a second cut of the central nasal fossa containing the ciliated, pseudo-stratified columnar epithelium. All tissues were immediately placed in 10% buffered neutral formalin and fixed for 24 hours.

Histopathology

Four-micrometer sections from formalin fixed paraffin-embedded, trachea, conjunctiva, nasal cavity and Harderian gland (right and left) were made and stained with haematoxylin and eosin (H&E). All H&E stained sections were examined for the presence of microscopic lesions typical of ILTV cytolitic replication (syncytial cell formation and intranuclear inclusion bodies).

Immunohistochemistry

Detection of ILTV antigen was performed in tissue sections where microscopic lesions typical of ILTV lytic replication were disputable. Viral antigen was detected by immunohistochemistry staining (IHC) of formalin-fixed, paraffin-embedded tissue sections using ILTV monoclonal antibody (Guy *et al*., 1992). Briefly, deparaffinized 4μm tissue sections were placed on positively charged slides. Sections were incubated with 3% hydrogen peroxide for 5 min to block endogenous peroxidase activity, followed by incubation with Proteinase K (Dako, Carpinteria, CA. USA) for five minutes at room temperature. Between 3% hydrogen peroxide and Proteinase K treatments sections were washed three times with a 1:10 phosphate-buffered saline (PBS) (NaPO4 monobasic, NaPO4 dibasic and NaCl, pH 7.2) for 1 min per rinse. Sections were then incubated with a 1:3000 dilution of ILTV monoclonal antibody in PBS (Guy *et al*., 1992) and incubated at room temperature in a humidity chamber for one hour. Sections were then incubated with a secondary antibody mouse and rabbit UnoVue™ polymer (Diagnostic BioSystem, Pleasanton, CA. USA) for 15 min. After incubation with primary and secondary antibody tissue sections were washed five times with a 0.1% solution of Tween® 20 (Sigma-Aldrich®, St. Louis, MO. USA) in PBS for one min per wash. Finally, diaminobenzidene (DAB) (Diagnostic Biosystem, Pleasanton, CA. USA) was added to the sections according to manufacturer´s instructions and incubated for five min at room temperature. Sections were carefully washed using distilled H_2O, counterstained with Gill´s haematoxilyn and 1% ammonium hydroxide for 1 min, dehydrated, and mounting media (Flo-Texx®, Thermo Fisher Scientific, Waltham, MA. USA) was added for microscopic examination. A brown precipitate indicative of the peroxidase conjugated antibody reaction with the DAB substrate was observed in tissue sections positive for ILTV antigen. Conjunctiva, nasal cavity and trachea tissues with

unequivocal microscopic lesions characteristics of ILTV replication and sections where ILTV antigen was detected by IHC were tallied and reported as percentages. All Harderian gland sections were stained by IHC. Cells in the Harderian gland positive for ILTV antigen were counted and the average of ILTV positive cells collected at days 3 and 5 post-inoculation with 63140 or CEO were estimated for groups of chickens inoculated via the ocular, oral, intranasal or intratracheal routes.

DNA Extraction

Total DNA was extracted from trachea, eye-conjunctiva swabs, nasal cavity swabs and Harderian glands using the MegaZorb® DNA extraction mini-prep 96-well kit (Promega, Madison, WI. USA) as previously described by (Vagonzzi *et al*., 2010).

Duplex real-time PCR

Duplex real time PCR assay that amplifies a fragment of the UL44 viral gene and a fragment of the chicken α2-collagen gene was performed as previously described (Vagnozzi *et al*., 2012). Briefly, each sample was normalized to the chicken α2-collagen gene and the relative amount of viral DNA in each sample was estimated as ΔΔCt = ΔCt ITLV inoculated - ΔCt mock inoculated expressed as $\log_{10} 2^{-\Delta\Delta Ct}$.

Statistical Analysis

The one-way analysis of variance Kruskal-Wallis test ($P<0.05$) was utilized to determine the effect of route of inoculation on viral replication. Genome load of 63140 or CEO vaccine for each tissue were compared among routes of inoculation (OC, OR, IN, IT) at day 3 or 5 post-inoculation.

The non-parametric Mann-Whitney U-test ($P<0.05$) was utilized to emphasize differences in the number of cells stained positive to ILTV antigen in Harderian glands from groups of chickens inoculated with either 63140 or CEO vaccine via the OC, OR, IN or IT route. The statistical analysis software used was the GraphPad PRISM 5.0 (GraphPad Software, Inc., La Jolla, CA) http://www.graphpad.com/company/

RESULTS

Histopathology examination and IHC in conjunctiva, nasal cavity and trachea

The percentage of conjunctiva, nasal cavity and trachea with unequivocal microscopic lesions characteristics of ILTV lytic replication (syncytial cell formation, and intranuclear inclusion bodies) and tissue sections where ILTV antigen was detected by IHC were tallied and reported as a percentage (Table 3.1). At five days post-inoculation via the ocular route with strain 63140 evidence of lytic replication was observed in 100% of the conjunctiva samples collected (Figure 3.1a). For groups of chickens inoculated with CEO vaccine via the ocular route, vaccine replication in conjunctiva was detected in 64% and 21% of the tissues collected at days three and five post-inoculation, respectively (Figure 3.1b). After intratracheal inoculation replication of either 63140 or CEO vaccine in the conjunctiva was absent, while replication of either virus was evident in tracheas collected at three and five days post-inoculation (Table 3.1). After ocular inoculation replication in the trachea was only detected in chickens inoculated with pathogenic strain 63140 (Figure 3.1c) but not in chickens inoculated with the CEO vaccine (Figure 3.1d).

Both viruses replicated extensively in the nasal cavity after oral or intranasal inoculations (Table 3.1). However after oral or intranasal inoculation with 63140 no viral lytic replication was observed in the conjunctiva (Figure 3.1e) and trachea (Figure 3.1g). In groups of chickens inoculated with the CEO vaccine strain via the oral or intranasal routes absence of viral replication was observed in the trachea (Figure 3.1h), while replication in the conjunctiva was detected when the vaccine was administered via the oral (15%) or intranasal (25%) routes of inoculation (Figure 3.1f).

Microscopic examination and IHC staining of Harderian gland

Neither microscopic lesions characteristic of ILTV lytic replication nor massive lymphocytic infiltration were identified in Harderian glands after inoculation via the OC, OR, IN or IT routes with either 63140 (Figure 3.2a) or CEO (Figure 3.2b). Instead ILTV antigen was detected in Harderian glands from chickens inoculated with 63140 or CEO vaccine. ILTV antigen was detected in cells scattered throughout the stroma of the gland (Figures 3.2c and 3.2d).

The average number of ILTV antigen positive cells per Harderian gland was tallied (Table 3.2). Independently of the route of inoculation no differences in the number of ILTV antigen positive cells was found in Harderian glands from chickens inoculated with either 63140 strain or CEO vaccine.

Viral genome load

As expected no viral genome load was detected in mock-inoculated groups of chickens (data not shown). Figure 3.3 shows the individual genome load of 63140 (Figure 3.3a to 3.3d) and CEO (Figure 3.3e to 3.3h) at days 3 and 5 post-inoculation in conjunctiva (3.3a & 3.3e), nasal cavity (3.3b & 3.3f), Harderian gland (3.3c & 3.3g) and trachea (3.3d & 3.3h) when chickens received the viruses via the ocular, oral, intranasal or intratracheal routes. Genome load per tissue was compared among routes of inoculation for each virus. Genome load in conjunctiva at day five post-inoculation from chickens inoculated with the 63140 strain via the ocular route was higher but not statistically different to genome load detected in the conjunctiva from chickens that received the virus via the OR, IN or IT routes. Chickens that received the CEO vaccine via the ocular route showed significantly high ($P< 0.05$) genome load in conjunctiva at

days 3 and 5 post-ocular inoculation (Fig. 3.3e), while chickens inoculated via the oral route showed significantly high ($P< 0.05$) genome load in the nasal cavity (Figure 3.3f). In both instances CEO genome load correlated with the presence of lesions in conjunctiva and nasal cavity epithelium. The levels of 63140 and CEO genome load in nasal cavity from chickens inoculated via the OC, IN, and IT did not correlated with microscopic lesions detected in the epithelium of the nasal cavity. Groups of chickens inoculated intratracheally with either 63140 or CEO showed significantly higher ($P<0.05$) genome load in trachea than when administered via the OC, OR, or IN routes (Figure 3.3d and 3.3h) which correlated with the presence of tracheal lesions. Genome load of 63140 in the Harderian gland was no different among chickens inoculated by the OC, OR, IN or IT routes (Figure 3.3c). While in the Harderian gland from chickens that received the CEO vaccine via the oral route at days 3 and 5 post-inoculation, the genome load of vaccine was significantly higher ($P<0.05$) than that detected in groups of chickens inoculated via the OC, IN and IT routes.

DISCUSSION

After exposure to ILTV microscopic changes in the respiratory epithelium and conjunctiva varied with the stage of infection. Early microscopic changes in the trachea mucosa were observed by two days post-infection, including the loss of goblet cells and infiltration of the mucosa with inflammatory cells. As the viral infection progresses, epithelial cells of the trachea and the conjunctiva enlarge and become oedematous. Multinucleated cells (syncytia) and inclusion bodies are formed and lymphocytes, histiocytes and plasma cells migrate into the mucosa and sub-mucosa of the trachea epithelium, lesions that are characteristic of ILTV lytic infection. Inclusion bodies disappear as infection progresses due to necrosis and desquamation of the epithelium (García *et al*., 2013). Several studies had shown that after intra-tracheal inoculation with pathogenic ILTV strains, moderate to severe lesions, as those described above, are produced in the trachea mucosa (Guy *et al*., 1990; Kirkpatrick *et al*., 2006; Vagnozzi *et al*., 2015), while live attenuated vaccines produce milder lesions in the trachea (Guy *et al*., 1990).

Similar to the trachea, after intranasal inoculation with pathogenic ILTV strains, viral replication in the nasal cavity produces acute sloughing, desquamation and formation of syncytia in the epithelium (Bang & Bang, 1967; Purcell & McFerran, 1969), while milder lesions were detected in the nasal epithelium after administration of the SA2 vaccine by the drinking water, eye drop (Robertson & Egerton, 1981) or spray (Clarke *et al*., 1980). In all instances replication of the SA2 vaccine strain was rarely detected in the larynx and was absence in the trachea.

The conjunctiva, eyes and nasal cavity contain structures like the conjunctiva – associated lymphoid tissue (CALT) (van Ginkel *et al*., 2012), the paranasal gland, the nasal associated lymphoid tissue (NALT) (Kang *et al*., 2013; de Geus *et al*., 2015) and the paraocular

Harderian gland (van Ginkel *et al*., 2009). These structures although not anatomically connected to the respiratory system harbour organized lymphoid follicles and intraepithelial lymphocytes which act as innate barriers to antigens and are functionally important components of the upper respiratory local immunity (Härtle & Kaspers, 2014). Upon exposure to antigen, strong mucosal and systemic immune responses are generated in the Harderian gland (van Ginkel *et al*., 2009) and CALT (van Ginkel *et al*., 2012). The lymphoid epithelium in CALT (Fix & Arp, 1991) and NALT (Kang *et al*., 2013) has the ability to uptake antigens. Full maturity of the CALT was signaled by an increased particle uptake as early as three weeks of age (van Ginkel *et al*., 2012), while NALT was considered fully developed by two weeks of age (Kang *et al*., 2013). When fully developed the uptake of antigen by the NALT was significantly more effective than antigen uptake by CALT (de Geus *et al*., 2015).

In the field when chickens are placed in an infected environment they are immediately expose to ILTV through multiple routes: oral, nasal, ocular and intratracheal, by ingesting infected material or inhaling aerosol virus-containing droplets. In this study we wanted to control the route of viral entry to investigate how tissues that first encounter the virus dictate further sites of viral replication during the lytic stage of infection. The viral dose necessary to elicit lesions indicative of lytic infection in trachea has been previously determined for 63140 (Vagnozzi *et al*., 2015) but is not known for CEO vaccine. In this experiment the CEO vaccine was administer at a (5X) dose per bird to increase the likelihood to detect lesions characteristic of lytic infection by the vaccine virus. Although is known that maturation of CALT and NALT is age dependent. In these experiments SPF birds were inoculated with CEO vaccine at two weeks of age since in the field vaccination at three weeks of age is not practiced, while inoculation with 63140 was performed at three-weeks of age to prevent increased mortality at an early age.

Results from this experiment clearly showed that the route of viral entry greatly influenced replication patterns of the pathogenic strain 63140 and the attenuated CEO vaccine in the trachea and conjunctiva but not in the nasal cavity. Both viruses showed high affinity to replicate in the conjunctiva epithelium when administer via the ocular route as indicated by ILTV cytolytic lesions. It is possible that after administration via the ocular route the decreased ability of the CALT to uptake antigen allowed the virus easy access to permissive epithelial cells favoring lytic replication in the conjunctiva. However, when strain 63140 was administered via the oral or intranasal routes replication in the conjunctiva and trachea were absent. One possibility is that through oral or intranasal routes of viral entry the virus is propelled into the NALT where local immune responses will eventually diminished lytic replication in the conjunctiva and trachea. In contrast to chickens inoculated with 63140, microscopic lesions were detected in the conjunctiva of chickens inoculated via the oral or intranasal routes with the CEO vaccine, an indication that the CALT of two-week old chickens was not able to halt virus replication in the conjunctiva. On the other hand the absence of microscopic lesions in the trachea after ocular, oral, or intranasal inoculation suggests that interaction of the CEO vaccine with a mature NALT eventually prevented the establishment of lytic replication in trachea.

In contrast to histological changes induced by Newcastle disease virus (Survashe *et al*., 1979) and infectious bronchitis virus (Toro *et al*., 1996) no evidence of lesions characteristic of ILTV lytic replication were detected in the Harderian gland where only viral antigen and nucleic acid were detected. Therefore during ILTV infections in the absence of tissue damage the Harderian gland may function as a key site of virus uptake. Further analysis is warranted to identify the cells in the gland that uptake ILTV antigen.

Viral genome load was a reliable indicator of lytic viral replication only in the trachea when viruses were administered intratracheally, in the conjunctiva when the CEO vaccine was administered via the ocular route, or in the nasal cavity when the CEO vaccine was administered via the oral route. However, when strain 63140 was administered via ocular, oral or intranasal routes, the viral genome load in conjunctiva and nasal cavity were not as predictable of lytic replication. Increase incidence of microscopic lesions and moderate levels of 63140 genome load in the conjunctiva and the nasal cavity may be an indicator of pathogenicity.

Overall the route of inoculation, particularly viral entry through the ocular, oral and intranasal routes greatly influenced lytic replication patterns of pathogenic strain 63140 and the CEO vaccine in the trachea and conjunctiva. Findings from this study suggest that interactions of the virus with nasal cavity, conjunctiva, and Harderian gland epithelial-lymphoid tissues would dictate patterns of ILTV lytic replication, which consequently will determine the outcome of infection. Furthermore, this study suggests that after mucosal administration (oral, ocular and intranasal) lytic replication of the CEO vaccine in trachea may not be necessary to induce protection. Further studies then are warranted to examine interactions of the CEO vaccine with cells of the CALT and NALT in order to unmask the mechanism by which CEO elicits a local immune response in these sites. Subsequently this information will aid in the development of new live attenuated vaccines against the disease.

Acknowledgements

This study is supported by Agriculture and Food Research Initiative Competitive Grant no. (2015-68004-23131) from the USDA National Institute of Food and Agriculture.

REFERENCES

Bang, B.G., & Bang, F.B. (1967). Laryngotracheitis virus in chickens. A model for study of acute nonfatal desquamating rhinitis. *The Journal of Experimental Medicine, 125*, 409-428.

Clarke, J.K., Robertson, G.M., & Purcell, D.A. (1980). Spray vaccination of chickens using infectious laryngotracheitis virus. *Australian Veterinary Journal, 56*, 424-428.

de Geus, E.D., Degen, W.G., van Haarlem, D.A., Schrier, C., Broere, F., & Vervelde, L. (2015). Distribution patterns of mucosally applied particles and characterization of the antigen presenting cells. *Avian Pathology, 44*, 222-229.

Fix, A.S., & Arp, L.H. (1991). Particle uptake by conjunctiva-associated lymphoid tissue (calt) in turkeys. *Avian Diseases, 35*, 100-106.

Fulton, R.M., Schrader, D.L., & Will, M. (2000). Effect of route of vaccination on the prevention of infectious laryngotracheitis in commercial egg-laying chickens. *Avian Diseases, 44*, 8-16.

García, M., Spatz, S., & Guy, J. (2013). Infectious laryngotracheitis. In D. E. Swayne & J. R. Glisson (Eds.), *Diseases of poultry 13th edn* (pp. 161-179). Wiley-Blackwell: Ames, Iowa.

Gelenczei, E.F., & Marty, E.W. (1964). Studies on a tissue-culture-modified infectious laryngotracheitis virus. *Avian Diseases, 8*, 105-122.

Guy, J.S., Barnes, H.J., & Morgan, L.M. (1990). Virulence of infectious laryngotracheitis viruses: Comparision of modified-live vaccine viruses and north carolina field isolates. *Avian Diseases, 34*, 106-113.

Guy, J.S., Barnes, H.J., & Smith, L.G. (1992). Rapid diagnosis of infectious laryngotracheitis using a monoclonal antibody-based immunoperoxidase procedure. *Avian Pathology, 21*, 77-86.

Härtle, S., & Kaspers, B. (2014). The avian respiratory immune system. In K. A. Schat, B. Kaspers & P. Kaiser (Eds.), *Avian immunology (2nd edn)* (pp. 251-263). Boston: Academic Press.

Kang, H., Yan, M., Yu, Q., & Yang, Q. (2013). Characteristics of nasal-associated lymphoid tissue (nalt) and nasal absorption capacity in chicken. *PLoS One, 8*, e84097.

Kirkpatrick, N.C., Mahmoudian, A., Colson, C.A., Devlin, J.M., & Noormohammadi, A.H. (2006). Relationship between mortality, clinical signs and tracheal pathology in infectious laryngotracheitis. *Avian Pathology, 35*, 449-453.

Koski, D.M., Predgen, A.S., Trampel, D.W., Conrad, S.K., Narwold, D.R., & Hermann, J.R. (2015). Comparison of the pathogenicity of the usda challenge virus strain to a field strain of infectious laryngotracheitis virus. *Biologicals, 43*, 232-237.

Neumann, U. (1976). The surgical removal of the harderian gland of the hen. *Zentralblatt Für Veterinärmedizin. Reihe A, 23*, 323-330.

Oldoni, I., Rodriguez-Avila, A., Riblet, S.M., Zavala, G., & García, M. (2009). Pathogenicity and growth characteristics of selected infectious laryngotracheitis virus strains from the united states. *Avian Pathology, 38*, 47-53.

Purcell, D.A., & McFerran, J.B. (1969). Influence of method of infection on the pathogenesis of infectious laryngotracheitis. *Journal of Comparative Pathology, 79*, 285-291.

Robertson, G.M., & Egerton, J.R. (1981). Replication of infectious laryngotracheitis virus in chickens following vaccination. *Australian Veterinary Journal, 57*, 119-123.

Rodriguez-Avila, A., Oldoni, I., Riblet, S., & García, M. (2008). Evaluation of the protection elicited by direct and indirect exposure to live attenuated infectious laryngotracheitis virus vaccines against a recent challenge strain from the united states. *Avian Pathology, 37*, 287-292.

Survashe, B.D., Aitken, I.D., & Powell, J.R. (1979). The response of the harderian gland of the fowl to antigen given by the ocular route. I. Histological changes. *Avian Pathology, 8*, 77-93.

Toro, H., Godoy, V., Larenas, J., Reyes, E., & Kaleta, E.F. (1996). Avian infectious bronchitis: Viral persistence in the harderian gland and histological changes after eyedrop vaccination. *Avian Diseases, 40*, 114-120.

Vagnozzi, A., Riblet, S., Williams, S.M., Zavala, G., & M., G. (2015). Infection of broilers with two virulent strains of infectious laryngotracheitis virus: Criteria for evaluation of experimental infeccions. *Avian Diseases, 59*, 394-399.

Vagnozzi, A., Riblet, S.M., Zavala, G., & García, M. (2012). Optimization of a duplex real-time pcr method for relative quantitation of infectious laryngotracheitis virus. *Avian Diseases, 56*, 406-410.

Vagonzzi, A., García, M., Riblet, S., & Zavala, G. (2010). Protection induced by infectious laryngotracheitis virus vaccines alone and combined with newcastle disease virus and/or infectious bronchitis virus vaccines. *Avian Diseases, 54*, 1210-1219.

van Ginkel, F.W., Gulley, S.L., Lammers, A., Hoerr, F.J., Gurjar, R., & Toro, H. (2012). Conjunctiva-associated lymphoid tissue in avian mucosal immunity. *Developmental & Comparative Immunology, 36*, 289-297.

van Ginkel, F.W., Tang, D.C., Gulley, S.L., & Toro, H. (2009). Induction of mucosal immunity in the avian harderian gland with a replication-deficient ad5 vector expressing avian influenza h5 hemagglutinin. *Developmental & Comparative Immunology, 33*, 28-34.

TABLES

Table 3.1. *Percentage of ILTV positive samples as indicated by histopathology examination and antigen detection by immunohistochemistry.*

Virus	Tissues	Route of inoculation							
		OC[c]		OR		IN		IT	
Pathogenic 63140[a]		D3[d]	D5	D3	D5	D3	D5	D3	D5
	Conjunctiva	0	100	0	0	0	0	0	0
	Nasal cavity	100	100	25	100	50	75	0	100
	Trachea	0	100	0	0	0	0	100	100
CEO[b]									
	Conjunctiva	64	21	15	14	0	25	0	0
	Nasal cavity	14	57	100	86	67	100	33	50
	Trachea	0	0	0	0	0	0	100	100

[a] n=4

[b] n=6

[c]Ocular (OC), Oral (OR), Intranasal (IN) or Intratracheal (IT).

[d]3 and 5 days (D) post-inoculation.

Table 3.2. *Mean number of positive cells per Harderian gland where ILTV antigen was detected.*

Route	Virus strain	
	Pathogenic strain 63140	CEO vaccine
Ocular	20.89(±5.18)[a]	12.53(±3.66)
Oral	8.75(±1.90)	26(±11.42)
Intranasal	6.2(±2.88)	6.3(±2.58)
Intra-tracheal	5.6(±1.85)	5.2(±0.96)

[a]Mean number of ILTV antigen positive cells (standard error of the mean).

FIGURES

63140	*CEO*
a) 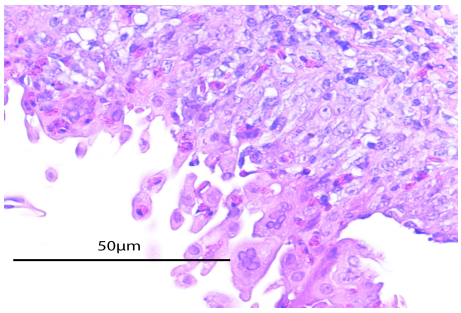	*b)* 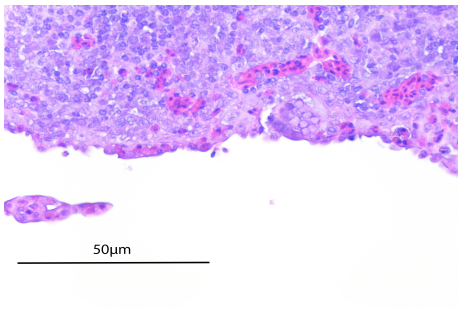
c) 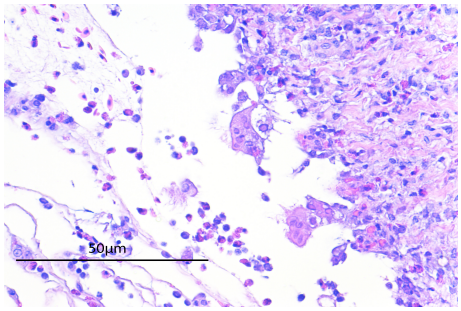	*d)* 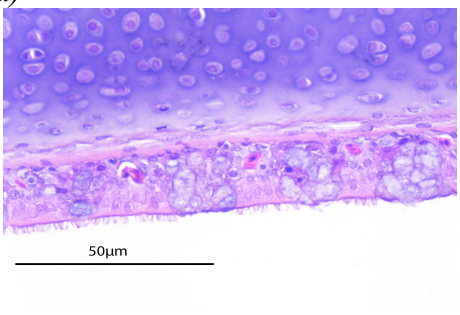
e) 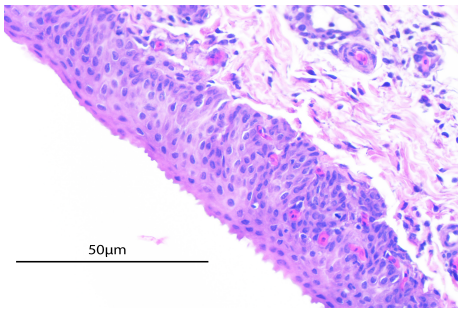	*f)* 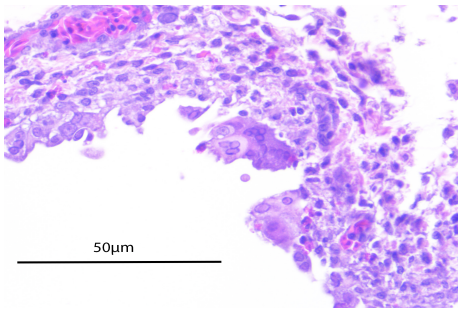
g) 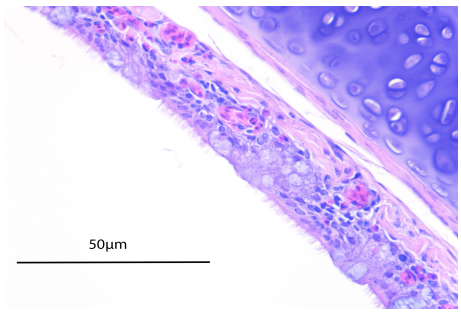	*h)* 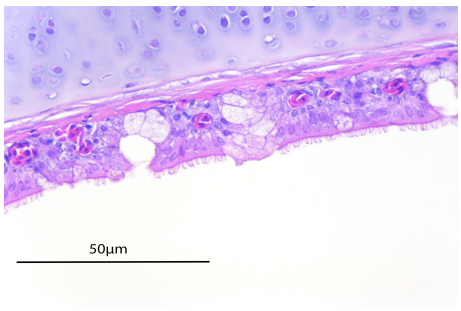

Figure 3.1. Haematoxylin and eosin (H&E) staining of conjunctiva and trachea sections from chickens inoculated with ILTV pathogenic strain 63140 (Figure 3.1 a, c, e, g) or CEO vaccine strain (Figure 3.1 b, d, f, h) and collected at five days post-inoculation. Presence of syncytial cell formation and intranuclear inclusion bodies in the conjunctiva (Figure 3.1a) and trachea (Figure 3.1c) of chickens inoculated with strain 63140 via the ocular route, and in the conjunctiva of chickens inoculated with the CEO strain via the ocular (Figure 3.1b) and intranasal (Figure 3.1f) route. Absence of lesions in the conjunctiva (Figure 3.1e) and trachea (Figure 3.1g) of 63140-inoculated chickens and in the trachea (Figure 3.1h) and conjunctiva (Figure 3.1d) of chickens inoculated with the CEO strain via the intranasal and ocular routes respectively. 156x249mm (72 x 72 DPI).

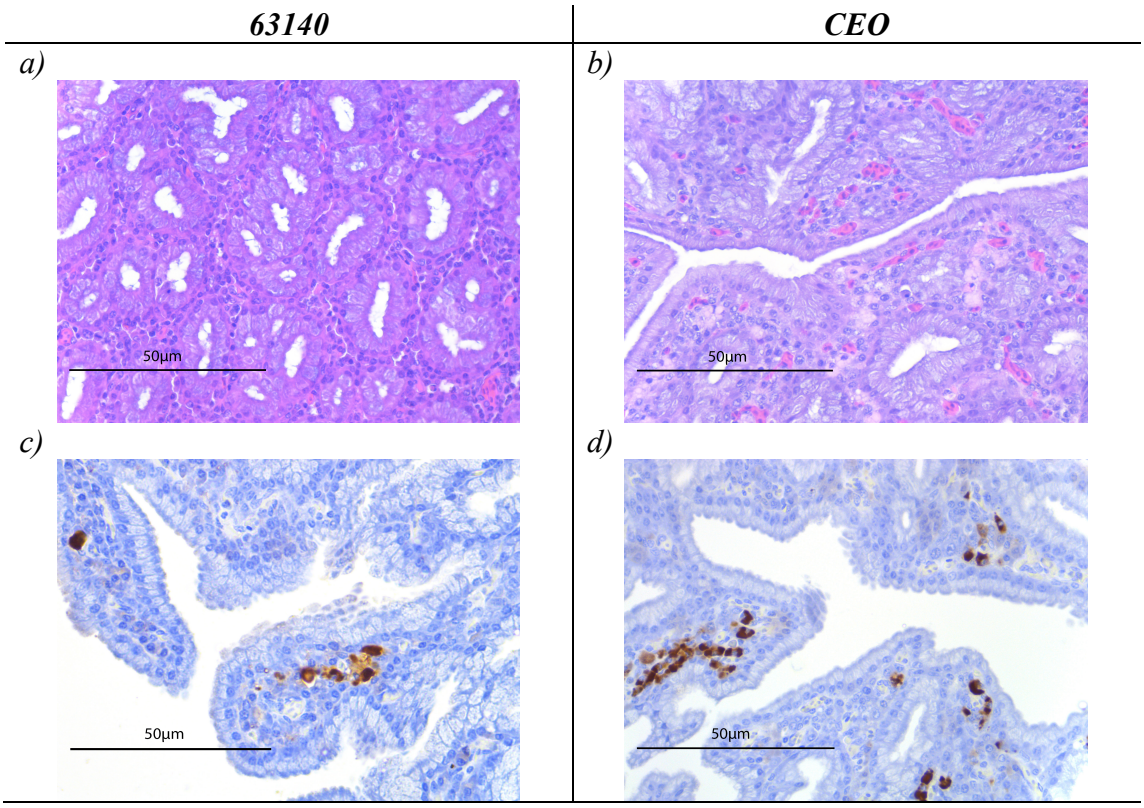

Figure 3.2. Haematoxylin and eosin (H&E) and Immunohistochemistry (IHC) staining of Harderian gland sections collected at five days post-inoculation of chickens that received ILTV pathogenic strain 63140 or the CEO vaccine strain via the ocular route. Absence of syncytial cell formation, intranuclear inclusion bodies and lymphocyte infiltration in Harderian gland sections (Figure 3.2a and 3.2b). Viral antigen detection in Harderian gland sections (Figure 3.2c and 3.2d) 156x133mm (72 x 72 DPI).

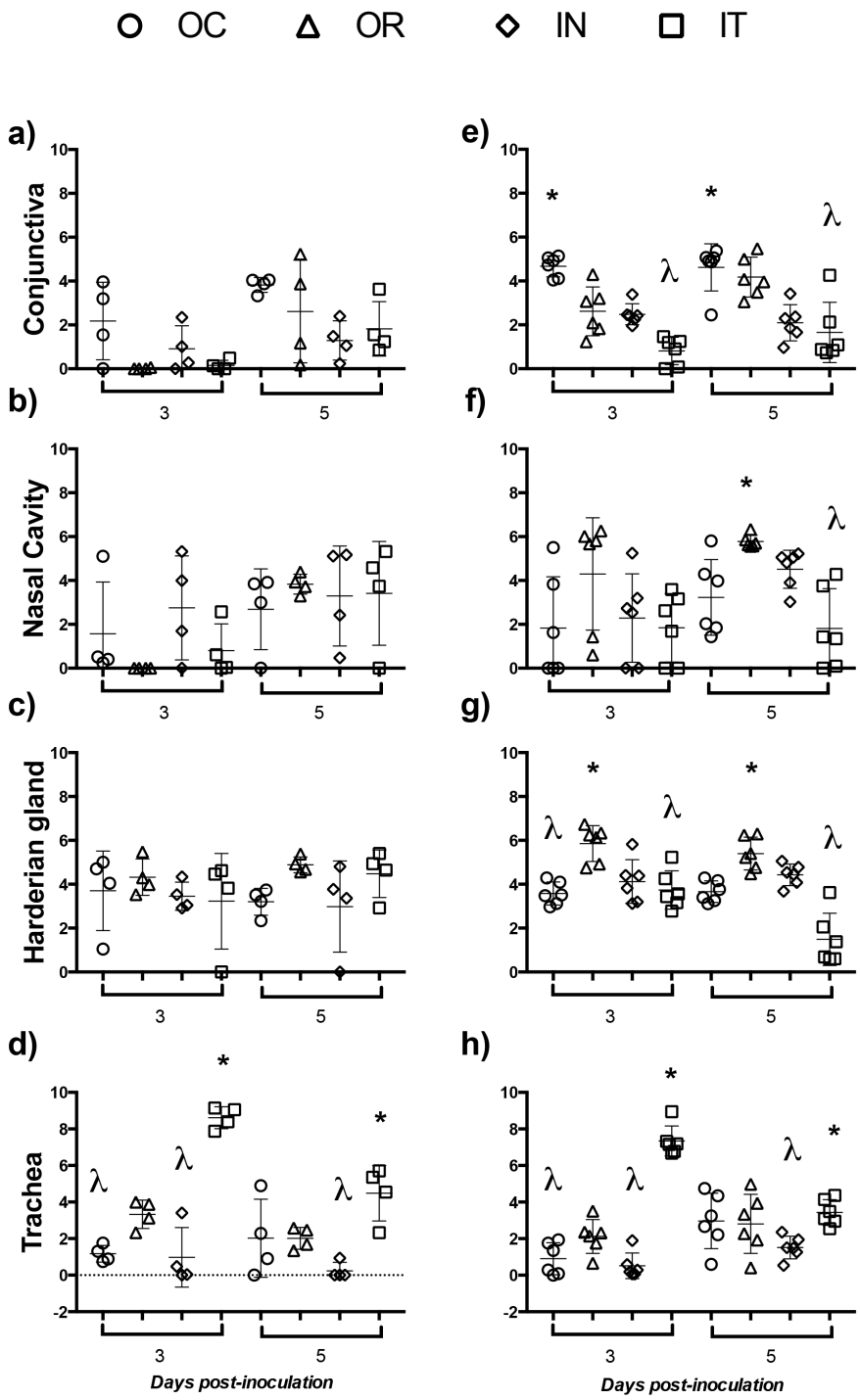

Figure 3.3. Individual genome load of pathogenic ILTV strain 63140 and CEO vaccine when deliver via the ocular (OC), oral (OR), intranasal (IN) or intratracheal (IT) routes. Individual genome load ($Log_{10} 2^{-\Delta\Delta Ct}$) of 63140 (Figure 3.3a to 3.3d) and CEO vaccine (Figure 3.3e to 3.3h)

at 3 and 5 days post-inoculation. Genome load of 63140 or CEO vaccine for each tissue were compared among routes of inoculation (OC, OR, IN, IT) at day 3 and 5 post-inoculation by the one-way analysis of variance Kruskal-Wallis. Significant differences ($P < 0.05$) in genome load detected among routes of inoculation are showed. Significantly lower genome load is indicated by lambda symbol (λ). Significantly higher genome load is indicated by asterisk (*). Mean genome load per tissue is depicted by an horizontal line and standard-deviation is depicted by a vertical line.

CHAPTER 4

Cell-mediated immune responses in the eye associated lymphoid tissues of chickens during vaccination or infection with Infectious laryngotracheitis virus (ILTV)

Gabriela Beltrán[1], David J. Hurley, Susan M. Williams, Carmen F. Jerry, Leah R. Read, Shayan Sharif, Robert M. Gogal, Daniel A. Maekawa, Sylva M. Riblet and Maricarmen García. To be submitted to *Veterinary Research.*

ABSTRACT

The aim of this study was to assess the cellular dynamics associated to the local cell immune responses elicited by infectious laryngotracheitis virus (ILTV) after ocular stimulation with the CEO vaccine and the virulent 63140 strain. Dynamics of lymphocyte populations, assessment of MHC class I and MHC class II^{Hi} expression, and transcription of cytokines genes that favor the cell-mediated immune responses were investigated in conjunctiva associated lymphoid tissues (CALT) and Harderian gland (HG). After CEO stimulation a timely immune response resulted in the increase transcription of IFN-γ and Granzyme A genes by day 3 post-inoculation (pi) followed by increase of $CD8^+$ cells between days 5 and 7 and in the CALT. On the contrary after 63140 stimulation upregulation of the IL-12p40 and IFN-γ genes by day 1 pi, was indicative of a tardy innate response. Furthermore, the decrease in $MHCI^+/MHCII^{Hi+}$ and IgM^+ B cells suggested that antigen presentation was compromised in the CALT after 63140 stimulation. In the HG increases in $CD4^+$ T and IgM^+ B cells at late stage of virus replication was indicative of B cell proliferation and the increased transcription of IFN-γ and granzyme A indicates that in the HG unaltered numbers of resident $CD8^+$ cells contributed to the cytotoxic response against ILTV. Overall this study confirmed the essential role of the local cell mediated immune response to disease resistance and provided a first glimpse that ILTV can circumvent the local immunity by delaying innate responses and downregulating MHC class II expression.

INTRODUCTION

Infectious laryngotracheitis (ILT) is a highly contagious acute respiratory disease of chickens caused by the avian alphaherpesvirus *Gallid alpha herpesvirus 1* (GaHV-1), commonly known as infectious laryngotracheitis virus (ILTV). The disease has a worldwide distribution and occurs frequently in densely populated poultry production areas. Intervention strategies to control the disease rely on implementation of biosecurity measures and vaccination with live-attenuated and/or recombinant viral vector vaccines expressing ILTV proteins (García et al., 2013). Among live-attenuated vaccines there are two main types; the tissue culture origin (TCO) vaccine (Gelenczei & Marty, 1965); and chicken embryo origin (CEO) vaccines (Samberg et al., 1971). Both, CEO and TCO vaccines are administered through the ocular, oral and intranasal mucosal routes to elicit local immunity (Gelenczei & Marty, 1964; Fulton et al., 2000) and are capable of protecting chickens against clinical signs, mortality, and suppressing replication of the challenge virus (Vagnozzi et al., 2012). However, it has been demonstrated both live attenuated vaccine strains, particularly the CEO vaccines can easily regain virulence if allowed to circulate in naïve chickens, given rise to outbreak related viruses such as the virulent strain 63140 (García et al., 2013). Although live attenuated vaccines are routinely used in the field, a dearth of knowledge exists on the components associated with vaccine-induced protection.

Early seminal studies demonstrated the central role of the cell-mediated arm of the immune system. In particular the roles of T cell subsets play in vaccine protection and resistance against the disease (Fahey et al., 1983; Fahey et al., 1984; Honda et al., 1994). More recently gathered evidence suggests that the inflammatory processes contribute to the pathology of the disease and eventually modulate the adaptive immune response to facilitate viral replication (Coppo et al., 2013). Furthermore the latest findings indicate that ILTV down-regulates type I interferon

transcription and delays the early transcription of inflammatory genes to favor initial virus replication in the trachea (Coppo et al., 2018; Vagnozzi et al., 2018).

Different from the mammalian immune system, the avian immune system lacks lymph nodes; in mammals these are the primary sites where antigen presentation takes place (Balic et al., 2014). Instead chickens have an immune network consisting of mucosal-associated lymphoid tissues (MALT) (Balic et al., 2014). The head-associated lymphoid tissue (HALT) is comprised by the nasal-associated lymphoid tissue (NALT), the eye associated lymphoid tissues organized in the conjunctiva-associated lymphoid tissue (CALT) and the Harderian gland (HG). Despite the lack of direct anatomic connection with the respiratory system, the HG, CALT, and NALT are associated with generation of local immunity in the upper respiratory airways. Cells identified as antigen-presenting cells (APC) in the NALT were capable of up taking Newcastle disease virus (NDV) coated beads after intranasal administration (de Geus et al., 2015). Van Ginkel et al., (2009) demonstrated that the amount of IgA and IgG producing cells were elevated in the HG after ocular inoculation of an adenovirus 5 vector expressing the avian influenza H5 protein. T effector cells ($CD3^+$, $CD44^+$) were detected in the HG and the CALT after infectious bronchitis virus (IBV) ocular inoculation (Gurjar et al., 2013). Little is known about the components of the cell immune responses associated with resistance against the disease in the eye associated lymphoid tissue. Recent findings indicate that the mucosal route of viral entry can greatly influence lytic replication and lymphocyte infiltration in the conjunctiva and trachea. While in the Harderian gland no apparent viral lytic replication or massive lymphocytic infiltration could be detected, and only viral antigen was associated with potential mononuclear cells. From this study it was concluded that interactions of ILTV with the head associated lymphoid tissues dictate the outcome of lytic replication and that the Harderian gland may serve

as an exclusive site of virus uptake within the eye associated lymphoid tissue (Beltrán et al., 2017).

Therefore, assessing the changes in immune cell populations within the eye associated lymphoid tissues (CALT and HG) after ILTV exposure may help identifying important features of the local cell mediated immune response that are involved in ILTV pathobiology. To this end, the objective of the current study was to assess differences in cell-mediated immune responses by monitoring T and B lymphocytes, MHC class I and MHC class II^{Hi} antigen surface expression, and transcript profiling of cytokine genes that are associated with the generation of cell mediated immune responses (i.e. interleukin (IL)-12p40, interferon (IFN) -γ, and granzyme A genes) in the CALT and HG after ocular inoculation with CEO vaccine and the virulent strain 63140.

MATERIALS AND METHODS

Experimental design

A total of 215 specific pathogen free (SPF) fertile eggs obtained from Charles River (Norwich, CT.) were incubated and hatched at the Poultry Diagnostic Research Center (PDRC, Athens, GA), University of Georgia hatchery facilities. One-day-old chicks were housed in isolation units, with filtered air and negative pressure, and provided with feed and water *ad libitum*. At five weeks of age chickens were divided in three groups. One group of chickens was inoculated with virulent strain 63140 (n=75); a second group was inoculated with the chicken embryo origin (CEO) vaccine strain (n=75). Both virus strains were administered via the ocular route at $10^{3.5}$ tissue culture infective dose ($TCID_{50}$) in 60 μL volume, 30 μL per eye. The third group of chickens (n=65) was mock-inoculated with cell culture media in a similar fashion and used as negative control. At 1, 3, 5, 7, and 9 days post-inoculation (dpi) conjunctival-associated lymphoid tissue (CALT) of the lower eyelids, Harderian gland (HG) from both eyes, and upper trachea sections were collected from five chickens that received the virulent strain 63140, five chickens that received the CEO vaccine strain and five mock-inoculated chickens. CALT and HG samples were used for flow cytometry analysis, while the upper trachea sections were used to determine viral genome load by real-time PCR. Additionally, CALT and HG samples were collected from 4 to 6 chickens per group at 1, 3, 5, 7, and 9 dpi and utilized to assess viral genome load and host cytokines genes transcription levels. At 1, 3, 5, and 7 dpi conjunctiva samples were collected from five chickens from each group for histopathology examination.

Samples collection

Chickens were euthanized by CO_2 gas inhalation for one minute. The CALT tissues from both lower eyelids and HG from each eye were aseptically removed and immediately placed in

15 mL conical tubes containing 8 mL of ice-cold transport medium (calcium and magnesium-free PBS with 0.5% bovine serum albumin) (Thermo Fisher Scientific, Waltham, MA). Samples were kept on ice until the tissues were processed for flow cytometry analysis. The upper trachea was collected and immediately placed in 1 ml of sterile phosphate-buffered saline solution (HyClone, Logan, UT) with 2% antibiotic-antymicotic 100X (Gibco, Grand Island, NY), and 2% fetal bovine serum (Atlanta®, Biological, Flowery Branch, GA). Tubes were immediately stored at -80 °C until processing for DNA extraction. CALT and HG samples were collected for RNA and DNA extraction. Upon collection tissues were placed in tubes containing 1.4 mm ceramic spheres (Lysing matrix D, MP Biomedical, Santa Ana, CA) containing 1 ml of TRIzol® (Thermo Fisher, Waltham, MA), incubated for 30 min on ice and homogenized using a FastPrep-24™5G kits (MP Biomedical, Santa Ana, CA). Tubes were immediately stored at -80 °C until processing for RNA and DNA extraction.

Histopathological examination of conjunctiva tissues

Conjunctiva sections collected at 1, 3, 5, and 7 days post ocular inoculation with CEO or 63140 were placed in 10% buffered natural formalin and fixed for 24 hours at room temperature. Four-micrometer sections stained with haematoxilin and eosin (H&E) were subjected to microscopic examination for the signs of ILTV lytic replication, indicated by the presence of syncytial cell formation and eosinophilic intranuclear inclusion bodies.

Single cell suspension preparation

Immediately after collection single cell suspension from CALT and HG tissues were obtained by mechanical disruption using a 60 μm wire screen mesh (Sigma-Aldrich, St. Luis, MO). During tissue disruption, to avoid excessive cell damage, the screen mesh was submerged

in transport media at all times. CALT cell suspensions were passed once through a 70 μm cell strainer (Thermo Fisher Scientific, Waltham, MA) to remove connective tissue. CALT cells were washed once with transport medium and centrifuged at 250 xg for 7 min at 4 °C. The HG cell suspension was passed once through a 70 μm and twice through a 40 μm cell strainer to remove connective tissue fragments. The cells were washed twice as described above. Following washes CALT cells were re-suspended in 1 mL and HG in 2 mL of ice-cold transport medium. Cells were enumerated and viability was determined using trypan blue exclusion on a Cellometer Mini (Nexcelcom Bioscience, Lawrence, MA) with final cell dilutions set at $1x10^5$ cells/100 μL for CALT and $4x10^5$ cells/100 μL for HG.

Antibody dilutions and staining procedures

Lymphocyte populations from each tissue were evaluated using four staining combinations of monoclonal antibody: 1) Allophycocyanin (APC) conjugated to mouse anti-chicken CD45, a pan leukocyte marker alone (Clone LT40, Southern Biotech, Birmingham, AL); 2) Phyocoerythrin (PE)- conjugated to mouse anti-chicken CD4 (Clone CT-4) paired with fluorescein isothiocyanate (FITC)-conjugated to mouse anti-chicken CD8α (Clone CT8) and APC conjugated mouse anti-chicken CD45; 3) PE-conjugated mouse anti-chicken IgM (Clone M-1) paired with FITC-conjugated mouse anti-chicken IgA (Clone A-1, Southern Biotech, Birmingham, AL) and APC conjugated mouse anti-chicken CD45; 4) PE-conjugated mouse anti-chicken MHCII (Clone 2G11) paired with FITC-conjugated mouse anti-chicken MHCI (Clone F21-2, Southern Biotech, Birmingham, AL) and APC conjugated mouse anti-chicken CD45. Antibody concentrations were optimized to the minimum saturating and cross-talk (between colors) concentration in prior trials. The APC-CD45 was used at a concentration of 0.05 μg per reaction. The PE-CD4 and the FITC-CD8 were diluted to a final concentration per

reaction of 0.25 μg and 0.5 μg, respectively. The PE-IgM and the FITC-IgA antibodies were utilized at a final concentration per reaction of 0.5 μg and 1 μg, respectively. While, the PE-MHCII and the FITC-MHCI antibodies were used at a final concentration per reaction of 0.125 μg and 0.5 μg, respectively. Working dilutions of antibodies were performed in FACS buffer (calcium and magnesium-free PBS, 0.5% bovine serum albumin, with 0.1% sodium azide). Final cell dilutions for each tissue suspension were distributed in round bottom 96-well plates, 100 μL per well. Cells were incubated with 100 μL of antibody combinations as indicated above on a plate shaker for 30 minutes at 4 ^{o}C. After incubation, the plates were centrifuged at 4 ^{o}C for 7 minutes at 250 xg, cell pellets were washed once with 200 μL of FACS buffer at 4 ^{o}C for 5 minutes at 250 xg. Cells were then re-suspended in 100 μL of FACS buffer and 100 μL of IC fixation buffer (Thermo Fisher Scientific, Waltham, MA) and stored overnight at 4 ^{o}C. Before flow cytometry analysis, fixed cells were further diluted with 200μL of calcium and magnesium-free PBS.

Flow cytometry strategy

Flow cytometry analysis was performed on a BD Accuri C6 Flow Cytometer (San Jose, CA). Gating for leukocyte populations in HG and CALT and the establishment of control windows for staining and double staining were determined beforehand. Briefly, primary gating was based on size consistency and single cells using forward scatter height versus forward scatter area (FSC-H vs FSC-A) (Figure 4.1a). These cells were subjected to CD45 assessment and established the leukocyte population in this primary gate (Figure. 4.1b). Then forward angle and right angle scatter (FSC-A vs SSC-A) relative to $CD45^{+}$ expression was used to identify the lymphocyte population and exclude macrophages from the analysis (Figure. 4.1c). The $CD45^{+}$ lymphocytes in this gate were then evaluated for $CD4^{+}$, $CD8^{+}$ (Figure. 4.1d), IgM^{+}, IgA^{+} (Figure.

4.1e), and MHC class I^{+}, MHC class II^{Hi+} antigen expression. In the lymphocyte gate 4,000 events per CALT, and 3,000 events per HG were collected due to the limited number of lymphocytes each preparation contained.

DNA and RNA extraction from tissues

Total DNA was extracted from upper trachea tissues using the MagaZorb® DNA extraction mini-prep 96 well kit as previously described (Vagnozzi. et al., 2010). In addition, immediately after homogenization of CALT and HG samples in 1 mL of TRIzol, 200 µL of chloroform were added followed by centrifugation at 4°C for 15 minutes at 12,000 xg to separate the aqueous and organic phases of the homogenate. Total RNA was extracted from the upper aqueous phase using the RNeasy kit (QIAGEN, Valencia, CA) as described by Vagnozzi *et al*., (2018). To eliminate DNA contamination the eluted RNA was treated with TURBO DNA-free™ (2 to 4 units/per reaction) (Ambion, Carlsbad, CA) for 30 minutes at 37°C. The DNase was inactivated with 5 µL of DNase inactivation buffer for 2 minutes at room temperature. After DNA digestion a total of 80 units of RNase inhibitor (RNase OUT™, Invitrogen, Carlsbad, CA) was added per sample. Optical density ratios (260/280 and 260/230) were obtained using the NanoDrop™ 2000c (Thermo Fisher Scientifics, Waltham, MA) to assess the purity and concentration of RNA per sample. To ensure the absence of residual genomic DNA, a Syber green real time PCR reaction that amplifies the chicken β-actin gene was performed using primers previously described by Vagnozzi *et al*., (2018). The amplification reaction was performed in a 20 µL volume, 10 µL of Syber® Select Master Mix (2X) (Life Technologies, Carlsbad, CA), 1 µL of 5 µM of each primer, 5 µL of template and 3 µL of nuclease free water. The cycling profile was 50 °C for 2 minutes; 95 °C for 2 minutes; 40 cycles of 95 °C for 15

seconds; and 60 °C for 1 minute. Eluted RNA was stored at -80 °C until further host cytokine gene quantification. Total DNA from CALT and HG was extracted from the organic phenol phase of the TRIzol® homogenate following the manufacturer´s recommendations (Thermo Fisher, Waltham, MA). Briefly, 300 µL of absolute ethanol was added to the phenol phase, followed by centrifugation at 2,000 xg for 5 minutes at 4 °C. The pellet was washed twice with 1 M sodium citrate in 10% ethanol and once with 75% ethanol and centrifuged at 2,000 xg for 5 minutes at 4 °C. The pellet was then re-suspended in 200 µL of 8 mM sodium hydroxide. Further DNA purification was performed using the MagaZorb® DNA extraction mini-prep 96 well kit following the manufacturer´s recommendations (Promega, Madison, WI). Eluted DNA was stored at -80 °C until further viral DNA quantification.

cDNA synthesis

Complementary DNA (cDNA) synthesis was done using total RNA purified from CALT and HG samples. Briefly, reverse transcription was performed with 500 nanograms of RNA from CALT and 250 nanograms of RNA from HG samples. The reverse transcription reaction was performed in a volume of 20 µL using 200 units of reverse transcriptase (SuperScriptIII™ RT Invitrogen Life Technologies, Carlsbad, CA) and 200 nM oligo (dT) 15 primers (Sigma-Aldrich, St. Louis, MO) per reaction. The reverse transcription was performed following the First-Strand Synthesis System protocol as recommended by manufacturer's (Invitrogen Life Technologies, Carlsbad, CA).

Transcription of host cytokine genes

Quantification of interleukin (IL)-12p40, interferon (IFN)-γ and granzyme A transcripts was done using CALT and HG. Briefly, a 20 μL reaction containing LightCycler 480 SYBR Green I Master (Roche Diagnostics GmbH) 0.25 μM of each gene-specific primer set, the chicken β-actin primer set and 5 μL of a 1:10 dilution of previously produced cDNA was assembled in 384-well plates (Roche Diagnostics, Indianapolis, IN). Real-time PCRs were performed in the LightCycler 480II instrument (Roche Diagnostics, Indianapolis, IN). Primers, amplification reaction parameters and efficiencies for each reaction are shown in Table 4.1. Fold changes in IL-12p40, IFN-γ and granzyme A transcripts in CALT and HG extracts from CEO and 63140 inoculated groups of chickens were determined based on relative changes to the mock-inoculated group using the chicken β-actin transcript as an endogenous control at each time point post-inoculation (1, 3, 5, 7, and 9 dpi) and presented as $2^{-\Delta\Delta Ct}$ median fold change (Livak & Schmittgen, 2001) and its 95% confidence interval.

Virus genome load

Detection of ILTV genomes in samples was determined by a duplex probe-based-Real-time PCR (Vagnozzi et al., 2012). The duplex assay amplifies the UL44 (gC) viral gene and a fragment of the chicken α2-collagen gene. The relative amount of viral DNA per samples was expressed as $\log_{10} 2^{-\Delta\Delta Ct}$ value.

Clinical signs

Clinical sings were recorded from 6 to 7 chickens within the mock, CEO vaccine, and 63140 virulent strain inoculated groups of chickens. Signs of respiratory distress, lethargy and

conjunctivitis were recorded from 2 to 7 days post inoculation. Clinical signs were scored as previously described (A. Vagnozzi, Zavala, et al., 2012). Briefly, signs of dyspnea, conjunctivitis and lethargy were scored on a scale of 0 to 3, normal (0), mild (1), moderate (2), and severe (3). A score of six was given to any encountered mortality. Total clinical sign scores per chicken were calculated, and the mean clinical sign score per time point per group was also calculated.

Statistical analysis

The non-parametric Mann-Withney U test ($p < 0.05$) was utilized to evaluate differences between CEO and 63140 genome load in conjunctiva, Harderian gland and trachea at each time point post-inoculation. Mean and media did not show differences, thus the results are presented as mean with standard deviation (SD). The pairwise percentage expression of either $CD4^+$ and $CD8^+$ or $IgM^+$and IgA^+ or $MHCI^{+/}MHCII^{Hi+}$ in CALT and HG from mock-inoculated chickens after 1, 3, 5, 7 and 9 days post-inoculation were compared by the one-way analysis of variance Kruskal-Wallis test and the Dunn´s multiple comparison test. No significant differences in percentage expression of $CD4^+$, $CD8^+$, IgM^+, IgA^+ or $MHCI^{+/}MHCII^{Hi+}$ in the CALT and HG from mock-inoculated chickens were detected between 1 to 9 days post-inoculation. Therefore, percentage expression for each cell marker from days 1 to 9 pi were pooled to obtain a wider representation of the basal percentage of lymphocytes levels in CALT and HG from mock-inoculated chickens. The one-way analysis of variance Kruskal-Wallis test and the Dunn´s multiple comparison test was utilized to compare the percentage expression of $CD4^+$, $CD8^+$, IgM^+, IgA^+ and $MHCI^{+/}MHCII^{Hi+}$ in CALT and HG collected from 63140 and CEO inoculated groups at 1, 3, 5, 7, and 9 dpi, and the pool mock-inoculated (1 to 9 days pi). Data is reported as mean ± standard deviation (SD).

The Kruskal-Wallis and the Dunn´s multiple comparison tests were used to detect differences in host cytokine gene transcription in CALT and HG tissues collected at 1, 3, 5, 7, and 9 dpi from either CEO (n=4 to 6) or 63140 (n=4 to 6) inoculated chickens. Statistical analysis of the data was conducted using the Prism 7 (GraphPad, Software Inc. San Diego, CA, USA).

Ethical statement

All animal experiments conducted in this study were performed under the Animal Use Proposal A2018 06-009-Y1-A0 approved by the Animal Care and Use Committee (IACUC) in accordance with regulations of the Office of the Vice President for Research at the University of Georgia.

RESULTS

Clinical signs

No chickens needed to be sacrificed due to the severity of clinical signs, and mortalities were not detected after ocular inoculation with either the CEO vaccine or the virulent 63140 strain. For both, CEO and 63140 inoculated groups the highest mean clinical signs score was detected at day 5 post-inoculation (pi) (Figure 4.2a). From days 4 to 7 pi the group of chickens inoculated with the virulent 63140 strain showed significantly higher clinical signs scores as compared to chickens inoculated with the CEO vaccine (Figure 4.2a).

Viral load

Viral load of CEO and 63140 in the CALT (Figure 4.2b) were markedly higher compared to those detected in Harderian gland (Figure 4.2c) and trachea (Figure 4.2d) throughout the infection. In the CALT, at 1 dpi the CEO mean viral load (2.34) was significantly lower than that of 63140 (5.76) (Figure 4.2b). From days 3 to 9 pi no differences in CEO or 63140 viral load were detected. The highest viral load in the CALT for both CEO (5.78) and 63140 (6.0) were detected by day 3 pi. Both CEO and 63140 viral loads began declining by day 5, and by day 9 pi dropped to 1.75 and 2.20 for CEO and 63140, respectively (Figure 4.2b). In the Harderian gland at day 1 pi the CEO viral load was nominal, whereas viral load of 63140 was significantly higher (3.85), by day 3 pi the viral load for both 63140 and CEO reached its highest level. Strain 63140 had a viral load of (5.3) which was significantly higher than that of the CEO strain (4.19). By day 5 pi both CEO and 63140 viral load began declining and by days 7 and 9 nominal genome load of CEO or 63140 were detected in the HG (Figure 4.2c). In the trachea, viral loads for both CEO (1.76) and 63140 (1.50) could be quantified as early as day 3 pi, and increased by day 5 pi to (2.48) CEO and (4.20) 63140. Both CEO and 63140 viral loads persisted in the trachea from

days 7 to 9 pi (Figure 4.2d). No viral loads were quantified in any of the tissues collected from mock-inoculated groups of chickens.

Histopathological changes in the conjunctival epithelium

By day 1 pi, despite evidence of a significant amount of 63140 genome vial load in the CALT (Figure 4.2b), only minimal tissue damage and lack of lytic replication (syncytial cell formation and eosinophilic intranuclear inclusion bodies) was observed in the conjunctival epithelium of the 63140 (Figure 4.3b) or CEO inoculated chickens (Figure 4.3a). However, at day 3 pi the conjunctival epithelium from both the CEO and 63140 (Figures 4.3c & 4.3d) inoculated chickens showed focal syncytia cell formations with eosinophilic intranuclear inclusions, mild to moderate heterophilic infiltration and low numbers of lymphocyte infiltrations in the epithelium and sub-epithelium connective tissue. At day 5 pi numerous syncytial cells with eosinophilic intranuclear inclusion bodies were present in the conjunctival epithelium from both CEO and 63140 inoculated chickens (Figures 4.3e & 4.3f). In addition, at 5 dpi mild multifocal heterophilic infiltrates were observed in conjunctiva sections collected from CEO inoculated chickens (Figure 4.3e), while moderate infiltrates of lymphocytes and heterophils, degeneration, necrosis and sloughing of epithelial cells were observed in the conjunctiva collected from 63140 inoculated chickens (Figure 4.3f). Microscopic examination of conjunctiva sections collected at day 7 pi from CEO inoculated chickens showed multifocal necrotic epithelial cells, moderate infiltrates of heterophils and lymphocytes with no evidence of ILTV lytic replication (Figure 4.3g), whereas conjunctiva sections from 63140 inoculated chickens showed evidence of ILTV lytic replication, marked necrosis and sloughing of the mucosal epithelium and mild heterophilic infiltrate (Figure 4.3h).

CALT $CD4^+$, $CD8^+$, IgM^+, $MHCI^+/MHCII^{Hi+}$ cell percentages

The percentage of $CD4^+$, $CD8^+$, IgM^+, $MHCI^+/MHCII^{Hi+}$ cells in CALT after inoculation with the CEO vaccine and virulent strain 63140 are shown in Figure 4.4. In the CALT of CEO vaccinated chickens the average percentage of $CD4^+$ T cells at 3 days pi (15.41%) was significantly lower ($p \leq 0.01$) than the 33.52% $CD4^+$ cells detected in the mock-inoculated group, but significantly higher ($p \leq 0.05$) 35.25% by day 9 pi (Figure 4.4a). A similar situation was observed in chickens inoculated with virulent strain 63140. The percentage of $CD4^+$ T cell at day 3 pi (15.55%) was significantly lower ($p \leq 0.05$) as compared to the mock-inoculated group of chickens (33.52%), and significantly increased ($p \leq 0.01$) to 38.9% by day 7 pi (Figure 4.4b). The average percentage expression of $CD8^+$ cells in the CALT of CEO vaccinated chickens at 5 (14.86%) and 7 (14.83%) days pi were significantly higher ($p \leq 0.05$) compared to 9.0% $CD8^+$ cells in the mock-inoculated group of chickens (Figure 4.4c). On the other hand, the average percentage of $CD8^+$ cells in the CALT of 63140 inoculated chickens from day 1 (9.7%) to day 9 (11.92%) pi did not show any significant fluctuations (Figure 4.4d). The average percentage of IgM^+ B cells in the CALT of CEO vaccinated chickens at day 3 pi (61.01%) was significantly ($p \leq 0.01$) higher compared to 39.92% IgM^+ cells in the mock-inoculated group of chickens (Figure 4.4e), but IgM^+ cells were significantly lower ($p \leq 0.05$) compared to mock inoculated levels by day 9 pi. A similar tendency was observed in 63140 infected chickens where the percentage of IgM^+ cells in CALT at 3 dpi (63.78%) was significantly higher ($p \leq 0.05$) as compared to IgM^+ cells in the mock-inoculated groups of chickens, but 31.36% of IgM^+ cells was significantly lower ($p \leq 0.01$) relative to those found in mock-inoculated chickens at day 7 pi (Figure 4.4f). After CEO inoculation, the average percentage of $MHCI^+/MHCII^{Hi+}$ cells at day 1 pi was 46.56%. By day 3 pi (66.91%) was significantly ($p \leq 0.01$) higher compared to 47.14% found in

the mock-inoculated group of chickens. By days 5 to 9 pi the expression of $MHCI^{+}/MHCII^{Hi+}$ showed no significant fluctuations maintaining an average range from 47.03% to 52.74% (Figure 4.4g). A similar trend was observed in the CALT of 63140 infected chickens where the percentage of $MHCI^{+}/MHCII^{Hi+}$ expressing cells in CALT at day 1 pi was 48.19%, increased to 69.21% by 3 dpi and then significantly decreased to 32.25% ($p \leq 0.001$) and 41.7% ($p \leq 0.05$) by days 7 and 9 pi, respectively (Figure 4.4h).

Harderian gland $CD4^{+}$, $CD8^{+}$, IgM^{+}, $MHCI^{+}/MHCII^{Hi+}$ cell percentages

The percentage of $CD4^{+}$, $CD8^{+}$, IgM^{+}, $MHCI^{+}/MHCII^{Hi+}$ cells in HG after inoculation with the CEO vaccine and virulent strain 63140 are shown in Figure 4.5. In the Harderian gland from CEO vaccinated chickens the percentage of $CD4^{+}$ T cell population at day 5 pi (29.72%) was significantly higher ($p \leq 0.01$) compared to the mock-inoculated group (15.56%), but significantly decreased ($p \leq 0.05$) to 13.42% by day 7 pi, and recovered to 26.46% by day 9 pi (Figure 4.5a). Strikingly no significant changes were quantified for $CD4^{+}$ T cell population in the HG of 63140 inoculated chickens from day 1 (22.16%) to day 9 (21.7%) pi (Figure 4.5b). Compared to mock-inoculated chickens (32.85%) no significant differences were observed in the percentage of $CD8^{+}$ cells in the HG of CEO vaccinated (Figure 4.5c) and 63140 infected chickens from days 1 to 9 pi in (Figure 4.5d). The percentage of IgM^{+} cells in the HG of CEO vaccinated chickens at day 1 pi was 22.77% and significantly increased ($p \leq 0.05$) to 35.84% by day 7 pi, but decreased to levels similar to those detected in the mock- inoculated group by day 9 pi (Figure 4.5e). The percentage of IgM^{+} cell population in the HG from 63140 infected chickens showed no significant fluctuations from days 1 to 9 pi (25 .01% to 36.36%) (Figure 4.5f). The average percentage of $MHCI^{+}/MHCII^{Hi+}$ cells in the HG of CEO vaccinated chickens did not

show any significant changes during days 1 through 9 pi and ranged from 19.06% to 32.91%. The average percentage of $MHCI^{+}/MHCII^{Hi+}$ expressing cells in mock-inoculated chickens was (26.41%) (Figure 4.5g). The average percentage of $MHCI^{+}/MHCII^{Hi+}$ expressing cells in the HG of 63140 inoculated chickens (ranged from 26.31% to 31.74%) and also showed no significant fluctuations from day 1 to 9 (Figure 4.5h).

CALT and Harderian gland IgA^{+} B cell percentages

The percentage of IgA^{+} cells in CALT and HG after inoculation with the CEO vaccine and virulent strain 63140 are shown in Figure 4.6. In the CALT of CEO vaccinated and 63140 infected chickens the average percentage of IgA^{+} B cells ranged from 0.30% to 0.78% from days 1 to 7 pi. The percentage of IgA^{+} cell population was significantly increased to an average of 1% in CEO vaccinated ($p \leq 0.05$) as compared to 0.52% in mock-inoculated chickens by day 9 pi (Figure 4.6a). For 63140 infected chickens the percentage IgA^{+} cells increased to an average of 1% by day 9 pi which was significantly higher ($p \leq 0.01$) than the 0.3% detected earlier at days 5 and 7 pi (Figure 4.6b). In the HG the percentage of IgA^{+} B cells from CEO vaccinated chickens significantly decreased ($p \leq 0.01$) to a nominal 0.19% by day 5 pi but increased to 1.42% by day 7 and 1.07% by day 9 pi (Figure 4.6c). Significant decrease ($p \leq 0.01$) in the percentage of IgA^{+} cells (0.27%) were quantified at day 9 pi in the HG from 63140 inoculated chickens relative to the 1.21% quantified in the mock-inoculated groups of chickens (Figure 4.6d).

CALT relative quantitation of cytokine gene transcription

The relative quantification of cytokine transcripts (IL-12p40, IFN-γ and granzyme A) in CALT tissues collected from CEO and 63140 inoculated chickens are presented in Figure 4.7a to

4.7f. The IL-12p40 gene transcription median fold change for CEO vaccinated chickens was 0.57 by day 1 pi, it significantly increased ($p \leq 0.05$) to 5.81 by day 3 pi, decreased to 1.80 by day 5 pi, to 0.77 by day 7 pi ($p \leq 0.05$), and rebounded to 2.79 by day 9 pi (Figure 4.7a). In stark contrast to the transcription of IL-12p40 gene for CEO vaccinated chickens, the IL-12p40 gene transcription median fold change at day 1 pi in the CALT for 63140 infected chickens was as high as 43.41, it decreased to 6.42 by day 3 pi, followed by a significant decrease ($p \leq 0.05$) to 0.88 by day 7 pi, and rebounded to 1.29 by day 9 pi (Figure 4.7b).

The IFN-γ gene transcription for CEO vaccinated chickens at day 1 pi had a median fold change of 0.04, by 5 days pi it significantly increased ($p \leq 0.05$) to 9.31, decreased to 2.71 by day 7 pi, and rebounded to 4.18 by day 9 pi (Figure 4.7c). Different than the CEO vaccinated chickens, at day 1 pi the median fold change of the IFN-γ gene transcription for 63140 infected chickens was as high as 6.45, it increased to 12.15 by day 3 pi, to 8 by day 5 pi followed by 4.52 by day 7 pi and then significantly decreased ($p \leq 0.05$) to 2.85 by day 9 pi (Figure 4.7d).

The granzyme A gene transcription median fold change for CEO vaccinated chickens at day 1 pi was 1.97, and it significant increased ($p \leq 0.01$) to 513.6 and 519 by days 3 and 5 pi, respectively; decreased to 13.79 by day 7 pi, and rebounded to 57.21 by day 9 pi (Figure 4.7e). The granzyme A gene transcription median fold change at day 1 pi for 63140 infected chickens was 30.70, and although not statistically different, it increased to 517.3 by day 3 pi, declined to 290 by day 5 pi, and compared to fold changes at days 3 and 5 pi it significantly decreased ($p \leq 0.05$) to 14.54 and 26.20 at days 7 and 9 pi, respectively (Figure 4.7f).

Harderian gland relative quantitation of cytokine gene transcription

The relative quantification of cytokine (IL-12p40, IFN-γ and granzyme A) gene transcripts in the HG collected from CEO and 63140 inoculated chickens are presented in Figure 4.7g to 4.7L. The IL-12p40 gene transcription for the CEO vaccinated group of chickens had a median fold change of 0.3 by day 1 pi, it significantly increased ($p \leq 0.05$) by day 3 pi to 9.69, significantly decreased ($p \leq 0.05$) to 0.31 by day 5 pi, and rebounded to 0.71 and 1.36 by days 7 and 9 pi, respectively (Figure 4.7g). In the 63140 infected chickens the transcription of the IL-12p40 gene was similar to that induced by CEO vaccination, at day 1 pi had a median fold change of 3.37, it increased to 14.3 by day 3 pi, significant decreased ($p \leq 0.05$) to 0.57 by day 5 pi, and increased to median fold changes of 1.59 and 1.78 by days 7 and 9 pi, respectively (Figure 4.7h).

The IFN-γ gene transcription for CEO vaccinated chickens at day 1 pi had a median fold change of 0.43, it increased to 1.36 by day 3 pi, significantly decreased ($p \leq 0.05$) to 0.2 by day 5 pi, rebounded to 0.9 by day 7 pi, and significantly increased ($p \leq 0.01$) to 2.74 by day 9 pi (Figure 4.7i). The IFN- γ gene transcription profile for 63140 infected chickens was very similar to that of CEO vaccinated chickens with the exception of a second IFN-γ gene transcription increase by day 9 pi. At day 1 pi the median fold change was 0.9, it increased to 4.01 by day 3 pi, significantly decreased ($p \leq 0.05$) to 0.16 by day 5, and significantly rebounded ($p \leq 0.05$) to 1.74 and 1.38 by days 7 and 9 pi, respectively (Figure 4.7j). The granzyme A gene transcription in the CEO vaccinated group of chickens had a median fold change of 0.92 by day 1 pi, it increased to 10.36 by day 3 pi, compared to median fold change at day 1 pi it significantly increased ($p \leq 0.01$) to 126.2 by day 5 pi, followed by a decreased to 67.32 by day 7 pi and 11.49 by day 9 pi (Figure 4.7k). Although the median fold changes of the granzyme A gene transcripts

in 63140 infected chickens were higher than those detected in the HG of CEO vaccinated chickens, similar transcription profiles were observed for both groups of chickens. The granzyme A gene transcription at day 1 pi had a median fold change of 3.80, it increased to 51.70 by day 3 pi, compared to the median fold change at day 1 pi a significant increase ($p \leq 0.05$) of 886.1 was detected by day 5 pi, followed by a gradual decrease to 177.6 by day 7 pi, and a significant decrease ($p \leq 0.05$) to 12.42 by day 9 pi (Figure 4.7L).

DISCUSSION

It has been previously documented that resistance against ILT is generated by the cell-associated arm of the immune system, however not much is known about the components that mediate the local cell immune responses and provide resistance against the disease. In an intent to unmask key components connected to local immune responses that contribute to disease resistance changes in (i) lymphocyte populations and (ii) transcriptional levels of interleukin (IL)-12, interferon gamma (IFN-γ), and granzyme A genes were monitored in the eye-associated lymphoid tissue (CALT and HG) after ocular inoculation with CEO and 63140 strains. In parallel clinical sign of the disease, viral lytic replication in the conjunctiva epithelium, and viral genome load in CALT, HG and trachea were assessed from days 1 to 9 post-inoculation. The lymphocyte composition of the CALT in unstimulated five-week-old SPF chickens showed an average of 33.52% $CD4^+$ T cells, 9.04% $CD8^+$ cells, 39.92% IgM^+ B cells (Figure 4.4) and 0.52% IgA^+ B cells (Figure 4.6). After stimulation, an evident $CD4^+$ T to IgM^+ B cell population shift occurred at day 3 pi. The percentage of $CD4^+$ T cells was significantly decreased from a 31.6% to an average of 15.4% while the percentage of IgM^+ B cells significantly increased from 44.4% to an average of 62.30% in the CALT of both CEO and 63140 stimulated chickens. Although avian B cells are not considered to be professional APCs, B cells present antigen to effector $CD4^+$ T cells to generate an antigen-specific antibody response (Kaiser & Stäheli, 2014). The increase in IgM^+ B cells in the CALT by day 3 pi coincided with an increased percentage expression of $MHCI^+$ $MHCII^{Hi+}$ cells suggesting that B cells were primed as antigen presenting cells. However, at day 3 pi the percentage of $CD4^+$ T cells in the CALT significantly decreased for both CEO and 63140 stimulated chickens (Figure 4.4). The decrease in $CD4^+$ T cells in the CALT by day 3 pi occurred concurrently with the peak of CEO and 63140 lytic replication (Figure 4.2). Whether the decrease in $CD4^+$ T cells at day 3 pi is due to migration of these cells

from the CALT to the upper and lower respiratory epithelium needs to be investigated. A second lymphocyte population shift occurred in the CALT of 63140 stimulated group of chickens. In this instance an increase in $CD4^+$ T by day 7 pi was accompanied by an abrupt decrease from days 7 to 9 pi of IgM^+ B cells and cells expressing $MHCI^+/MHCII^{Hi+}$ (Figure 4.4). Whether infection with 63140 down regulated $MHCI^+/MHCII^{Hi+}$ expression consequently disturbing antigen presentation by B cells and negatively impacting a time sensitive production of IgA or IgG antibodies in the CALT merits further investigation. Nevertheless, despite the decrease in IgM^+ B cells and cells expressing $MHCI^+/MHCII^{Hi+}$, IgA^+ B cells augmented in the CALT of CEO and 63140 stimulated chickens by day 9 pi (Figure 4.6). Although in the current study the antigen specificity of the IgA^+ B cells was not determined, these results suggest that a local antibody response was mounted in the CALT after ILTV stimulation. However, the increase in IgA^+ B cells occurred after the decline of virus lytic replication in the conjunctival epithelium by day 9 pi (Figure 4.2). This result is in agreement with York *et al*., (1989), who found that IgA^+ producing cells in the trachea after ILTV inoculation peak by day 7 pi when virus replication was no longer detected. Therefore, both studies imply that ILTV stimulation of local antibodies in trachea or conjunctiva may not be sufficiently swift enough to effectively block virus replication at peak times.

Activated APCs modulate early adaptive immune responses through the production of IL-12, which stimulate natural killer (NK) and T cells to produce IFN- γ. In humans and mice bioactive IL-12 is composed by two subunits, p40 and p35. Subunit p35 is expressed by many cell types, whereas p40 is expressed mainly by APCs (Balu & Kaiser, 2003). Similar to activated $CD8^+$ cells, activated NK cells are capable of inducing cytotoxic activity by the production of serine proteases such as granzyme A (Sarson et al., 2008). More pertinent, NK cells participate in the maturation of professional APCs, enhance antigen specific cytotoxic $CD8^+$ T cell

responses, assists in the polarization of $CD4^+$ T cells (Lam & Lanier, 2017), and in the absence of a $CD4^+$ T cells can participate as helpers in the genesis of functional $CD8^+$ T cell responses (Nandakumar et al., 2008; Morandi et al., 2009). Increased transcription of IL-12p40, IFN-γ, and granzyme A genes occurred in the CALT of 63140 stimulated chickens from days 1 to 3 pi, while increased transcription of these genes in the CALT of CEO stimulated chickens was delayed and occurred at day 3 pi (Figure 4.7). The elevated transcription of the IL-12p40, IFN-γ, and granzyme A genes observed at day 1 after 63140 stimulation, but not after CEO stimulation, suggests that the 63140 strain may slowdown local immune responses, while the CEO vaccine probably precipitated the expression of these cytokines before day one pi.

Chicken $CD8^+$ T and NK cells share the CD8 alpha chain (Jansen et al., 2013); therefore the percentage of $CD8^+$ cells reported in this study represents populations of both NK and $CD8^+$ T cells. In the CALT of 63140 stimulated chickens the $CD8^+$ cells population remained unchanged throughout the infection. While in CEO vaccinated chickens a sustained increase in $CD8^+$ cells was observed from days 5 to 7 pi (Figure 4.4) which coincided with clearance of CEO cytolytic replication in the conjunctival epithelium by day 7 pi (Figure 4.2). More complete phenotyping of these $CD8^+$ cells will be necessary to more accurately identify their effector role in limiting vaccine virus lytic replication.

The lymphocyte composition of the unstimulated HG was 32.85% $CD8^+$ cells, 27.43% IgM^+ B cells, followed by 15.56% $CD4^+$ T cells (Figure 4.5), and 1.21% IgA^+ B cells (Figure 4.6). The HG lymphocyte composition is in contrast to the CALT where 33.52% were identified as $CD4^+$ T cells and only a 9.02% corresponded to $CD8^+$ cells. Although $CD8^+$cells were the predominant population in the HG of unstimulated chickens, remarkably no major fluctuations in

$CD8^+$ cells were detected after stimulation with CEO and 63140 (Figure 4.5). In the HG of 63140 stimulated chickens the $CD4^+$, IgM^+ B, and $MHCI^+/MHCII^{Hi+}$ cell population remained unchanged throughout the infection. In CEO stimulated chickens the $CD4^+$ T and IgM^+ B cells increased between days 5 and 7 pi while the percentage expression of $MHCI^+/MHCII^{Hi+}$ remained unaffected (Figure 4.5). Even though the $CD8^+$ cell population in CEO and 63140 stimulated groups of chickens remained unaltered (average 23 to 30%) (Figure 4.5), increased transcription of the IFN-γ (day 3 pi) and granzyme A (day 5 pi) genes (Figure 4.7) suggests that activated resident $CD8^+$ cells were responsible the increased transcription of these genes. Other sign of the HG involvement in the ILTV immune response was evidenced by a decrease in IgA^+ B cell population by day 5 pi after CEO and 63140 stimulation (Figure 4.6), an indication that the gland serve as a site where IgA^+ B cells are produced and probably migrate to influence the humoral immune response in other mucosal sites (Akaki et al., 1997).

In the present study the dynamics of γδ T cells were not monitored. Chickens have high frequencies of γδ T in the blood and tissues such as spleen, cecum, thymus, and bursa (Cooper et al., 1991). These cells have a role of immunological surveillance and it has been demonstrated that can produce IFN-γ early after infection with Marek´s disease virus (MDV) establishing an appropriate environment for the activation of Th1 responses (Laursen et al., 2018). For future studies it would be prudent to include a measure of γδ T cell dynamics.

In summary similar lymphocyte population dynamics were detected in the CALT by day 3 pi after CEO or 63140 stimulation (decrease $CD4^+$ T, increase IgM^+ B and $MHCI^+/MHCII^{Hi+}$) and by day 7 pi an opposing shift in lymphocyte populations were observed only after 63140 stimulation (increase $CD4^+$ T, decrease IgM^+ B $MHCI^+/MHCII^{Hi+}$). The $CD8^+$ cell population

increased in the CALT after CEO stimulation, but not after 63140 stimulation. To the contrary, in the HG the percentage of $CD8^+$ cells remained unchanged after stimulation with either CEO or 63140, while changes of $CD4^+$ T and IgM^+ B cells were unique to the HG of CEO stimulated chickens. These opposing trends in lymphocyte changes observed in the CALT and HG are a reflection of their inherent different lymphoid composition. However, differences in the CALT and HG responses were also greatly influenced by the viral strain. This was best supported by the differences in transcription profiles stimulated by the CEO vaccine and the 63140 strain in particular for the IL-12p40 gene. The delayed stimulation of IL-12p40 gene transcription in both CALT and HG at day 1 after 63140 stimulation but not observed after CEO stimulation, suggests that the 63140 strain maybe hampering the innate immune response of the eye associated lymphoid tissues. Previous transcription analysis of the CALT and HG innate immune related genes after ocular stimulation with the virulent strain 63140 showed significant downregulation of Toll like receptors (TLR) 3, 7, 21 genes transcription between 12 to 24 hours post inoculation, and reduced transcription of IFN-γ, α, and β genes as early as 6 hours pi (Beltrán et al., 2017). Comparison of CALT and HG early cytokine transcription profiles after 63140 and CEO ocular stimulation is warranted.

On the whole, primarily this study confirmed the role of the local mucosal cell mediated immunity and its contribution to disease resistance and/or disease outcome, secondly it provided evidence that the CALT and HG play different roles during ILTV immune responses and, finally it revealed that a virulent strain of ILTV can circumvent the local immune response by probably delaying innate responses and downregulating MHC class II expression.

REFERENCES

Akaki, C., Simazu, M., Baba, T., Tsuji, S., Kodama, H., Mukamoto, M., & Kajikawa, T. (1997). Possible migration of harderian gland immunoglobulin a bearing lymphocytes into the caecal tonsil in chickens. Zentralblatt fur Veterinarmedizin. Reihe B. *Journal of veterinary medicine*. Series B*, 44*, 199-206.

Balic, A., Garcia-Morales, C., Vervelde, L., Gilhooley, H., Sherman, A., Garceau, V., Gutowska, M. W., Burt, D. W., Kaiser, P., Hume, D. A., Sang, H.M. (2014). Visualisation of chicken macrophages using transgenic reporter genes: Insights into the development of the avian macrophage lineage. *Development, 141*, 3255-3265.

Balu, S., & Kaiser, P. (2003). Avian interleukin-12beta (p40): Cloning and characterization of the cdna and gene. *Journal of Interferon & Cytokine Research, 23*, 699-707.

Beltrán, G., Williams, S.M., Zavala, G., Guy, J.S., & García, M. (2017). The route of inoculation dictates the replication patterns of the infectious laryngotracheitis virus (ILTV) pathogenic strain and chicken embryo origin (CEO) vaccine. *Avian Pathology, 46*, 585-593.

Beltrán Gabriela, Riblet, S.M., Read, L., Sharif, S., & García, M. (2017). Local innate responses in conjunctiva, harderian gland and trachea after ocular or oral inoculation with a virulent strain of infectious laryngotracheitis virus (ILTV). *Annual meeting of the American Association of Avian Pathologists (AAAP)*.

Brisbin, J.T., Gong, J., Parvizi, P., & Sharif, S. (2010). Effects of lactobacilli on cytokine expression by chicken spleen and cecal tonsil cells. *Clinical and Vaccine Immunology, 17*, 1337-1343.

Coppo, M.J., Hartley, C.A., & Devlin, J.M. (2013). Immune responses to infectious laryngotracheitis virus. *Developmental and Comparative Immunology, 41*, 454-462.

Coppo, M.J.C., Devlin, J.M., Legione, A.R., Vaz, P.K., Lee, S.W., Quinteros, J.A., Gilkerson, J. R., Ficorilli, N., Reading, P. C., Noormohammadi, A. H., Hartley, C.A. (2018). Infectious laryngotracheitis virus viral chemokine-binding protein glycoprotein g alters transcription of key inflammatory mediators in vitro and in vivo. *Journal of Virology, 92* e01534-17.

Cooper, M.D., Chen, C.-L.H., Bucy, R.P., & Thompson, C.B. (1991). Avian T cell ontogeny. *Advances in Immunology, 50*, 87-117.

de Geus, E.D., Degen, W.G., van Haarlem, D.A., Schrier, C., Broere, F., & Vervelde, L. (2015). Distribution patterns of mucosally applied particles and characterization of the antigen presenting cells. *Avian Pathology, 44*, 222-229.

Fahey, K.J., Bagust, T.J., & York, J.J. (1983). Laryngotracheitis herpesvirus infection in the chicken: The role of humoral antibody in immunity to a graded challenge infection. *Avian Pathology, 12*, 505-514.

Fahey, K.J., York, J.J., & Bagust, T.J. (1984). Laryngotracheitis herpesvirus infection in the chicken. Ii. The adoptive transfer of resistance with immune spleen cells. *Avian Pathology, 13*, 265-275.

Fulton, R.M., Schrader, D.L., & Will, M. (2000). Effect of route of vaccination on the prevention of infectious laryngotracheitis in commercial egg-laying chickens. *Avian Diseases, 44*, 8-16.

García, M., Spatz, S., & Guy, J. (2013). Infectious laryngotracheitis. In D. E. Swayne, J. R. Glisson, L. R. McDougland, L.K. Nolan, D. L. Suarez & V. L. Nair (Eds.), *Diseases of poultry 13th edn* (pp. 161-179): Ames, Iowa: Wiley-Blackwell.

Gelenczei, E.F., & Marty, E.W. (1964). Studies on a tissue-culture-modified infectious laryngotracheitis virus. *Avian Diseases, 8*, 105-122.

Gelenczei, E.F., & Marty, E.W. (1965). Strain stability and immunologic characteristics of a tissue-culture-modified infectious laryngotracheitis virus. *Avian Diseases, 9*, 44-56.

Gurjar, R.S., Gulley, S.L., & van Ginkel, F.W. (2013). Cell-mediated immune responses in the head-associated lymphoid tissues induced to a live attenuated avian coronavirus vaccine. *Developmental and Comparative Immunology, 41*, 715-722.

Honda, T., Okamura, H., Taneno, A., Yamada, S., & Takahashi, E. (1994). The role of cell-mediated immunity in chickens inoculated with the cell-associated vaccine of attenuated

infectious laryngotracheitis virus. *The Journal of Veterinary Medical Science, 56*, 1051-1055.

Jansen, C.A., de Geus, E.D., van Haarlem, D.A., van de Haar, P.M., Londt, B.Z., Graham, S.P., Gobel, T. W., van Eden, W., Brookes, S. M., Vervelde, L. (2013). Differential lung NK cell responses in avian influenza virus infected chickens correlate with pathogenicity. *Scientific Reports, 3*, 2478.

Kaiser, P., & Stäheli, P. (2014). Chapter 10 - avian cytokines and chemokines *Avian immunology (second edition)* (pp. 189-204). Boston: Academic Press.

Lam, V.C., & Lanier, L.L. (2017). Nk cells in host responses to viral infections. *Current Opinion in Immunology, 44*, 43-51.

Laursen, A.M.S., Kulkarni, R.R., Taha-Abdelaziz, K., Plattner, B.L., Read, L.R., & Sharif, S. (2018). Characterizaton of gamma delta t cells in marek's disease virus (gallid herpesvirus 2) infection of chickens. *Virology, 522*, 56-64.

Livak, K.J., & Schmittgen, T.D. (2001). Analysis of relative gene expression data using real-time quantitative pcr and the 2(-delta delta c(t)) method. *Methods, 25*, 402-408.

Morandi, B., Mortara, L., Carrega, P., Cantoni, C., Costa, G., Accolla, R.S., Mingari, M. C., Ferrini, S., Moretta, L., Ferlazzo, G. (2009). NK cells provide helper signal for cd8+ t

cells by inducing the expression of membrane-bound il-15 on dcs. *International Immunology, 21*, 599-606.

Nandakumar, S., Woolard, S.N., Yuan, D., Rouse, B.T., & Kumaraguru, U. (2008). Natural killer cells as novel helpers in anti-herpes simplex virus immune response. *Journal of Virology, 82*, 10820-10831.

Samberg, Y., Cuperstein, E., Bendheim, U., & Aronovici, I. (1971). The development of a vaccine against avian infectious laryngotracheitis. Iv. Immunization of chickens with a modified laryngotracheitis vaccine in the drinking water. *Avian Diseases, 15*, 413-417.

Sarson, A.J., Abdul-Careem, M.F., Read, L.R., Brisbin, J.T., & Sharif, S. (2008). Expression of cytotoxicity-associated genes in marek's disease virus-infected chickens. *Viral Immunology, 21*, 267-272.

St. Paul, M., Paolucci, S., Barjesteh, N., Wood, R.D., Schat, K.A., & Sharif, S. (2012). Characterization of chicken thrombocyte responses to toll-like receptor ligands. *PLoS ONE, 7*, e43381.

Vagnozzi, A., Riblet, S.M., Zavala, G., & García, M. (2012). Optimization of a duplex real-time pcr method for relative quantitation of infectious laryngotracheitis virus. *Avian Diseases, 56*, 406-410.

Vagnozzi, A., Zavala, G., Riblet, S.M., Mundt, A., & Garcia, M. (2012). Protection induced by commercially available live-attenuated and recombinant viral vector vaccines against infectious laryngotracheitis virus in broiler chickens. *Avian Pathology, 41*, 21-31.

Vagnozzi, A.E., Beltran, G., Zavala, G., Read, L., Sharif, S., & Garcia, M. (2018). Cytokine gene transcription in the trachea, harderian gland, and trigeminal ganglia of chickens inoculated with virulent infectious laryngotracheitis virus (ILTV) strain. *Avian Pathology*, 1-12.

Vagnozzi., García, M., Riblet, S., & Zavala, G. (2010). Protection induced by infectious laryngotracheitis virus vaccines alone and combined with newcastle disease virus and/or infectious bronchitis virus vaccines. *Avian Diseases, 54*, 1210-1219.

van Ginkel, F.W., Tang, D.C., Gulley, S.L., & Toro, H. (2009). Induction of mucosal immunity in the avian harderian gland with a replication-deficient ad5 vector expressing avian influenza h5 hemagglutinin. *Developmental and Comparative Immunology, 33*, 28-34.

York, J.J., Young, J.G., & Fahey, K.J. (1989). The appearance of viral antigen and antibody in the trachea of naive and vaccinated chickens infected with infectious laryngotracheitis virus. *Avian Pathology, 18*, 643-658.

TABLES

Table 4.1. List of primers and the reaction conditions used for quantitation of host genes expression by real-time PCR.

			Real time PCR reaction					
Gene		*Primers (5'-3')*	*Den*[c]	*Ann*[d]	*Ext*[e]	*Cycles*	*Eff*[f]	*Reference*
β-actin	Fw[a]	CAACACAGTGCTGTCTGGTGGTA	95C (10s)	60C (5s)	72C (10s)	45	2	(Brisbin et al., 2010)
	Rv[b]	ATCGTACTCCTGCTTGCTGATCC						
IFN-γ	Fw	ACACTGACAAGTCAAAGCCGCACA	95C (10s)	60C (5s)	72C (10s)	45	1.98	(Brisbin et al., 2010)
	Rv	GTCGTTCATCGGGAGCTTGGC						
Granzyme	Fw	TGGGTGTTAACAGCTGCTCATTGC	95C (10s)	55C (5s)	72C (10s)	50	2.02	(Sarson et al., 2008)
	Rv	CACCTGAATCCCCTCGACATGAGT						
IL12p40	Fw	CCAAGACCTGGAGCACACCGAAG	95C (10s)	60C (5s)	72C (10s)	50	2.0	(St. Paul., et al., 2012)
	Rv	CGATCCCTGGCCTGCACAGAGA						

[a] Forward primer; [b] Reverse primers; [c] Denature temperature; [d] Annealing temperature; [e] Extension temperature; f Efficiency.

FIGURES

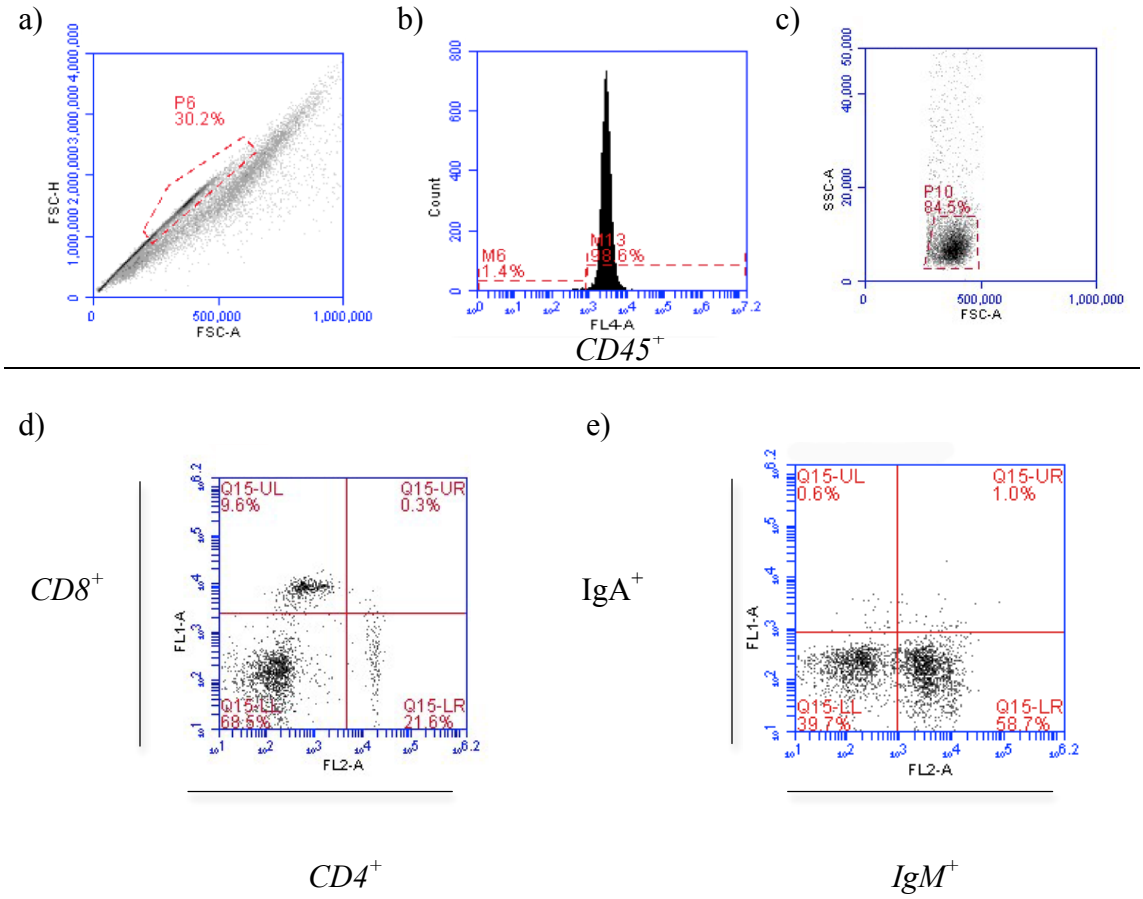

Figure 4.1. Gating strategy of the lymphocyte population. Primary gating was based on size consistency and single cell using forward scatter height versus forward scatter area (FSC-H vs FSC-A) (a), and subjected to CD45 assessment (b). Representative flow cytometric forward angle and right angle scatter (FSC-A vs SSC-A) relative to $CD45^+$ expression was used to identify the lymphocyte population (c). The $CD45^+$ lymphocytes population was subjected to $CD4^+$, $CD8^+$ (d), IgM^+, IgA^+ (e) assessment.

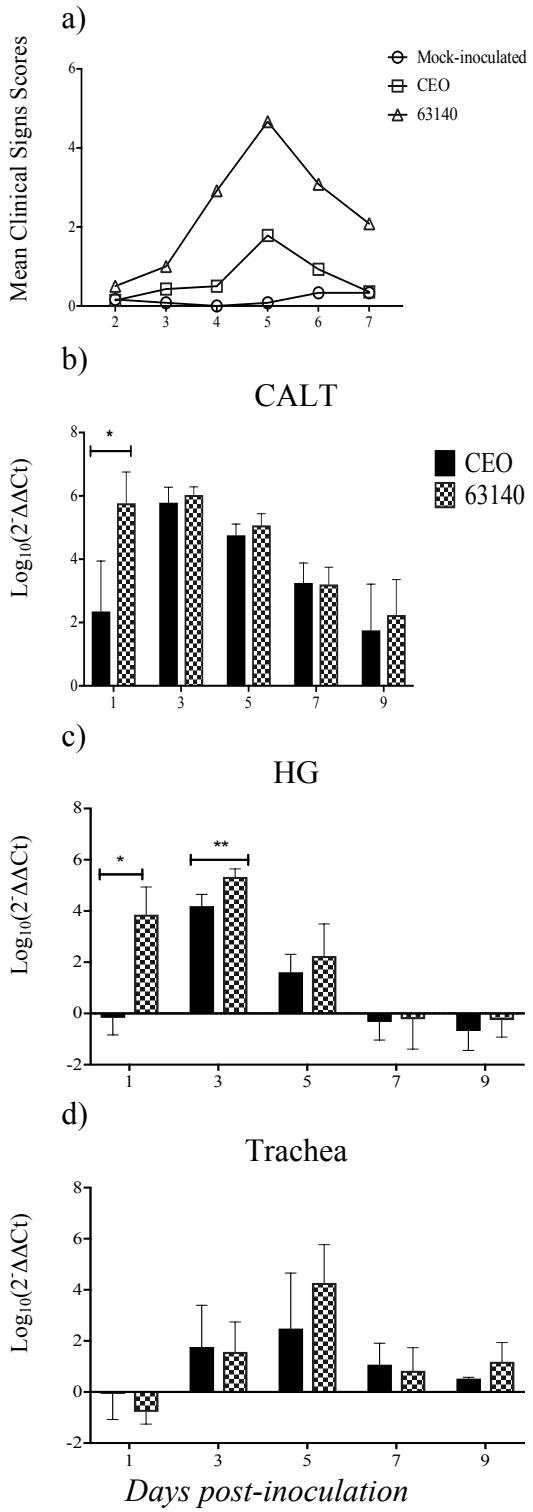

Figure 4.2. Mean clinical sign scores and genome load ($Log_{10}2^{-\Delta\Delta Ct}$) of the CEO vaccine and 63140 virulent strain in the CALT, Harderian gland (HG) and trachea after ocular inoculation. a) Mean clinical sign scores recorded from 2 to 7 dpi (n = 6 to 7). Mean clinical

sign scores are indicated by geometrical symbols. Mean viral genome load in CALT (b), HG (c), and trachea (d) at 1, 3, 5, 7 and 9 days post-inoculation. Mean and media did not show differences, thus the results are presented as mean and standard deviation (SD). The bars represent the mean genome viral load and the vertical lines indicate the standard deviation per tissue. Significant genome load differences between strains per tissue at each time point are indicated ($p \leq 0.0332$ (*), $p \leq 0.0021$(**).

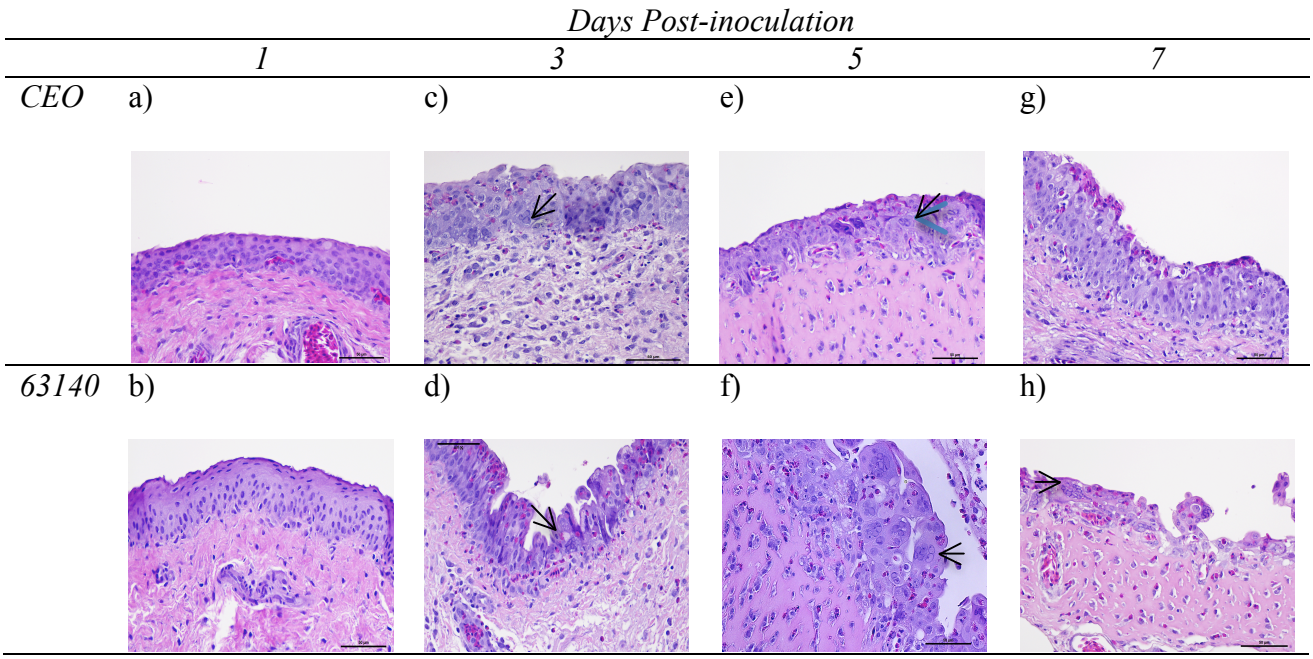

Figure 4.3. Photomicrographs of conjunctiva sections stained with haematoxilin and eosin (H&E) after ocular vaccination with CEO vaccines or infection with virulent 63140 ILTV strain. Conjunctiva sections from CEO vaccinated chickens collected at 1 (a), 3 (c), 5 (e), and 7 (g) days post-inoculation. Conjunctiva sections from 63140 ocular inoculated chickens collected at 1 (b), 3(d), 5(f), and 7 (h) days post-inoculation. An arrowhead indicates evidence of ILTV lytic replication.

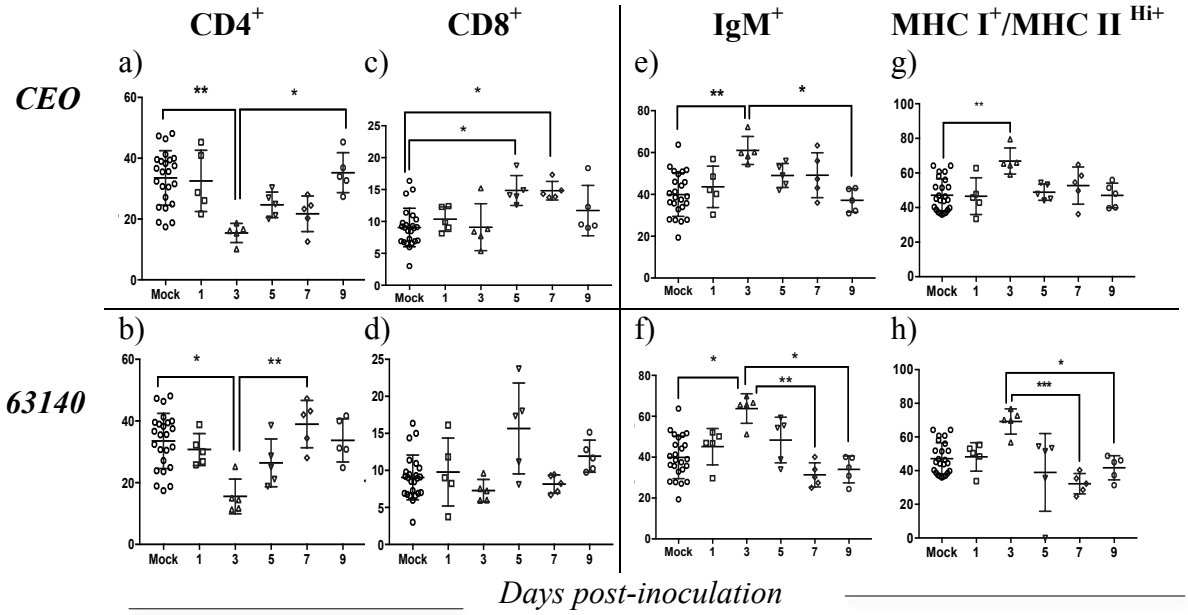

Figure 4.4. CALT CD4$^+$, CD8$^+$, IgM$^+$ and MHC I$^+$/MHC II $^{Hi+}$ percentage expression after CEO vaccine and virulent strain 63140 ocular inoculation. Percentage expression of CD4$^+$ (a), CD8$^+$ (c), IgM$^+$ (e), MHC I$^+$/MHC II^{Hi+} (g) in CALT at days 1 to 9 post CEO vaccination. Percentage expression of CD4$^+$ (b), CD8$^+$ (d), IgM$^+$ (f), MHC I$^+$/MHC II^{Hi+} (h) at days 1 to 9 post 63140 infection. Percentage expression of CD4$^+$, CD8$^+$, IgM$^+$ and MHC I$^+$/MHC II $^{Hi+}$ in the CALT of CEO vaccinated, 63140 infected, and mock-inoculated chickens were compared by one-way analysis of variance Kruskal-Wallis test and Dunn´s multiple comparison test. Individual percentages are depicted by geometric characters, and the mean ± standard deviation are depicted by horizontal and vertical lines, respectively. Statistical differences are indicated with asterisks: $p \leq 0.05$ (*), $p \leq 0.01$ (**), $p \leq 0.001$ (***).

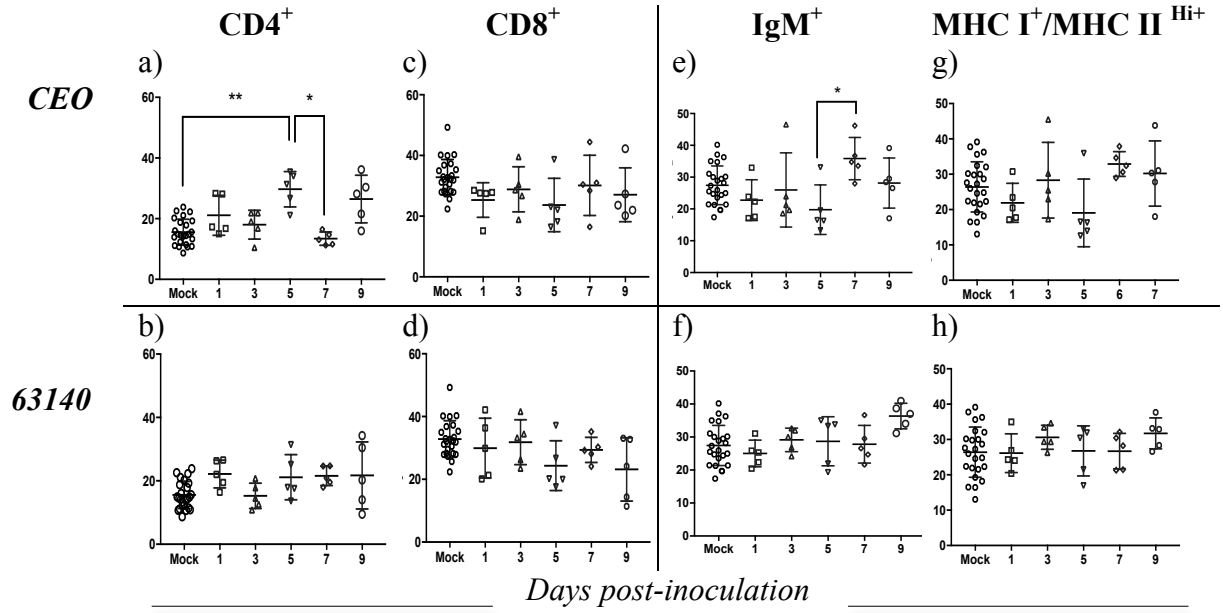

Figure 4.5. Harderian gland CD4$^+$, CD8$^+$, IgM$^+$ and MHC I$^+$/MHC II $^{Hi+}$ percentage expression after CEO vaccine and virulent strain 63140 ocular inoculation. Percentage expression of CD4$^+$ (a), CD8$^+$ (c), IgM$^+$ (e), MHC I$^+$/MHC II^{Hi+} (g) in HG at days 1 to 9 post CEO vaccination. Percentage expression of CD4$^+$ (b), CD8$^+$ (d), IgM$^+$ (f), MHC I$^+$/MHC II^{Hi+} (h) in HG at days 1 to 9 post 63140 infection. Percentage expression of CD4$^+$, CD8$^+$, IgM$^+$ and MHC I$^+$/MHC II $^{Hi+}$ in the HG of CEO vaccinated, 63140 infected, and mock-inoculated chickens were compared by one-way analysis of variance Kruskal-Wallis test and Dunn´s multiple comparison test. Individual percentages are depicted by geometric characters, and the mean ± standard deviation are depicted by horizontal and vertical lines, respectively. Statistical differences are indicated with asterisks: $p \leq 0.05$ (*), $p \leq 0.01$ (**), $p \leq 0.001$ (***).

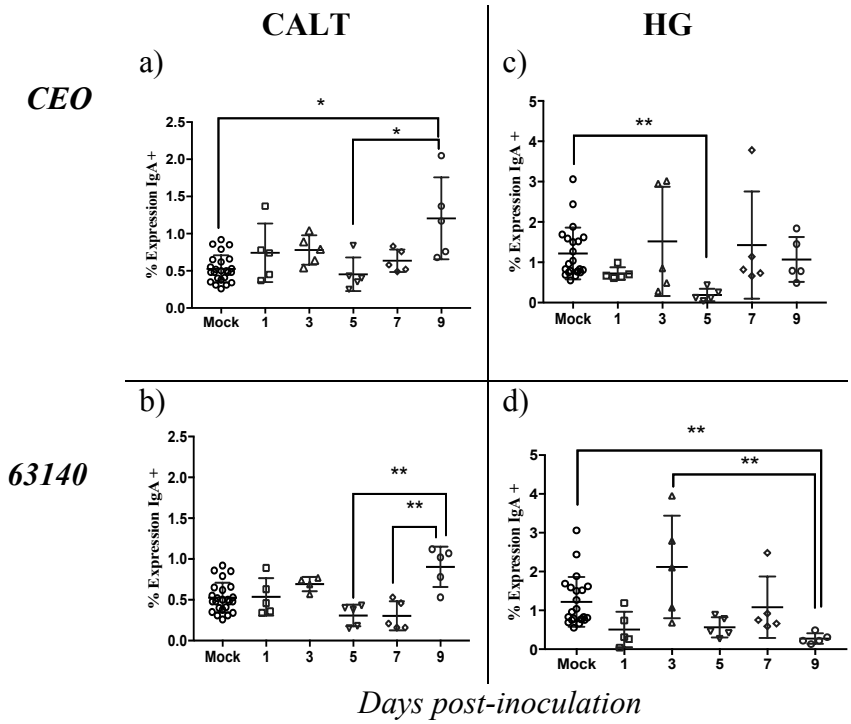

Figure 4.6. CALT and Harderian gland (HG) IgA$^+$ percentage expression after CEO vaccine and virulent 63140 strain ocular inoculation. Percentage expression of IgA$^+$ cells in the CALT of CEO vaccinated (a) and 63140 infected chickens (b); percentage expression of IgA$^+$ cells in the HG of CEO vaccinated (c) and 63140 infected chickens (d) collected from day 1 to 9 pi. Percentage expression of IgA$^+$ cells in the CALT and HG of CEO vaccinated, 63140 infected, and mock-inoculated chickens were compared by one-way analysis of variance Kruskal-Wallis test and Dunn´s multiple comparison test. Individual percentages are depicted by geometric characters, and the mean ± standard deviation are depicted by horizontal and vertical lines, respectively. Statistical differences are indicated with asterisks: $p \leq 0.05$ (*), $p \leq 0.01$ (**).

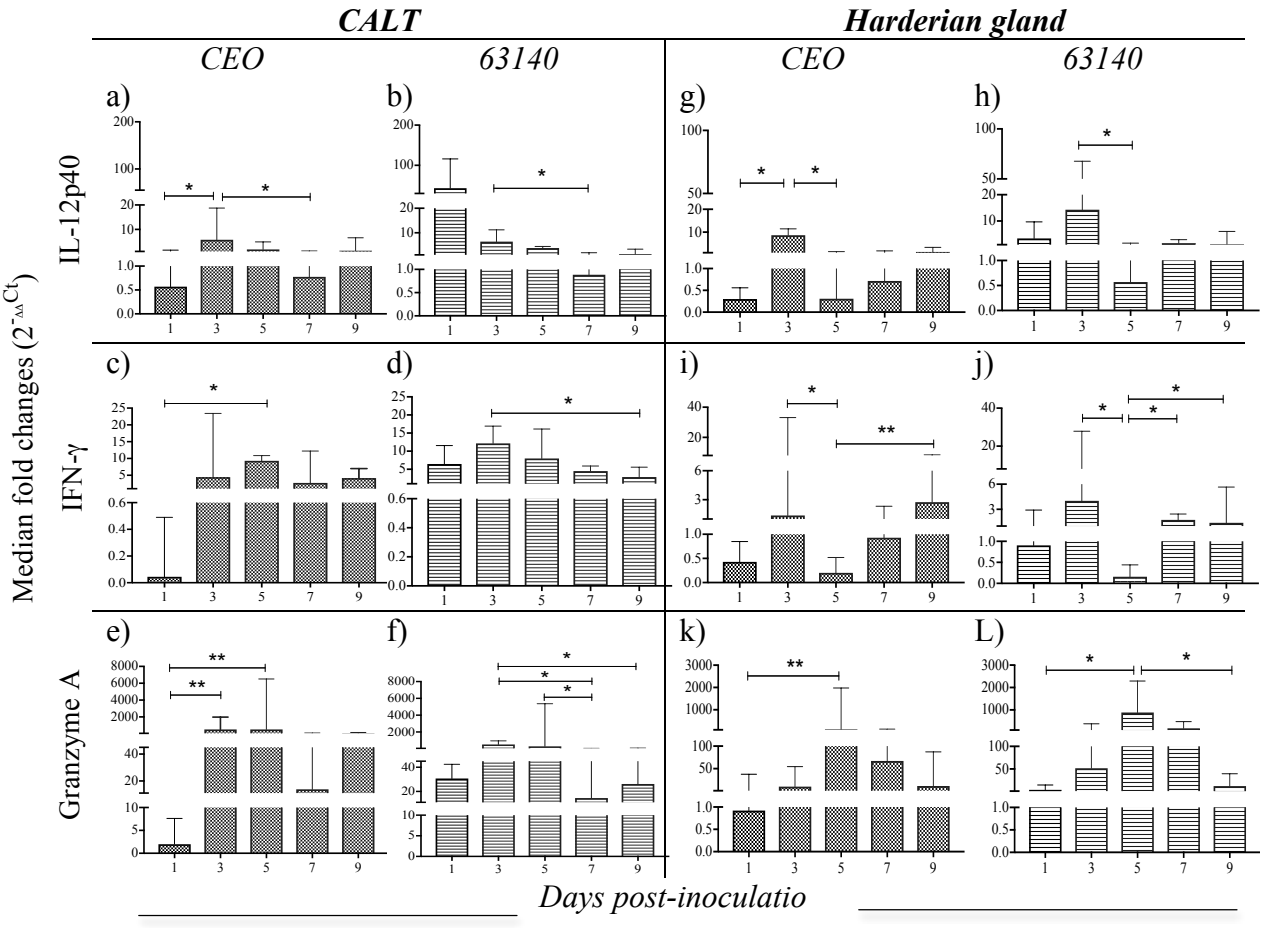

Figure 4.7. Gene transcription median fold changes ($2^{-\Delta\Delta Ct}$) in CALT and Harderian gland (HG) after CEO vaccine and virulent strain 63140 ocular inoculation. Median fold gene transcription changes in CALT for IL12p40 (a & b), IFN-γ (c & d) and granzyme A (e & f) at days 1, 3, 5, 7, and 9 pi. Median fold gene transcription changes in HG for IL12p40 (g & h), IFN-γ (i & j) and granzyme A (k & L) at days 1, 3, 5, 7, and 9 pi. Bar graphs indicate the median fold changes and vertical lines the 95% confidence interval of the median. The cytokine gene transcription median fold changes for each tissue were compared at 1, 3, 5, 7 and 9 dpi. Significant differences in cytokine gene transcription expression are indicated with asterisks ($p \leq 0.05$ *, $p \leq 0.01$ **, $p \leq 0.001$ ***).

CHAPTER 5

The mononuclear phagocyte composition of the eye associated lymphoid tissues of chickens after ocular vaccination or infection with Infectious laryngotracheitis virus (ILTV)

Gabriela Beltrán[1], David J. Hurley, Robert M. Gogal, Sylva M. Riblet, Carlos A. Loncoman, and Maricarmen García. To be submitted to *Avian Diseases*

ABSTRACT

In this study the mononuclear phagocyte (MNP) composition of the CALT and HG of unstimulated and Infectious laryngotracheitis virus (ILTV) stimulated five-week-old specific pathogen free (SPF) chickens was evaluated. Chickens were inoculated via the ocular route with live-attenuated chicken embryo origin (CEO) vaccine and the virulent strain 63140 strain. The MNP populations were characterized by surface expression of the chicken colony stimulating factor 1 receptor (CSF1R) and the major histocompatibility complex (MHC) II. The ability of the CEO and 63140 strains to infect and induce apoptosis in cultures of chicken monocyte-derived macrophages (MDMs) was evaluated. The MNP composition of the CALT and the HG in unstimulated chickens showed two distinct cell populations, $CSF1R^{+}/MCH\text{-}II^{Lo+}$ and $CSF1R^{+}/MCH\text{-}II^{Hi+}$, both expressed in higher percentages in the HG than in the CALT. Stimulation with either CEO or 63140 induced an early increase of both MNP populations in the CALT and a reduction in the HG. Compared to the 63140 virulent strain, the CEO vaccine induced a higher and enhanced expression of both $CSF1R^{+}/MCH\text{-}II^{Lo+}$ and $CSF1R^{+}/MCH\text{-}II^{Hi+}$ cell populations in the CALT. In the HG, ILTV stimulation with either CEO or 63140 induced a sustained decrease of both cell populations. In MDMs both CEO and 63140 strains established a semi-productive infection and inhibited apoptosis of infected MDMs. This latter finding together with the abrupt decrease of $CSF1R^{+}/MCH\text{-}II^{Lo+}$ and $CSF1R^{+}/MCH\text{-}II^{Hi+}$ populations in the HG suggest that upon ILTV stimulation the gland may be a source of infected MNPs which facilitate virus spread while evading the host immune response to ultimately establish latency.

INTRODUCTION

In poultry production chickens are subjected to strict vaccination protocols. A vast majority of the vaccination strategies against respiratory diseases of poultry use the mucosal surface of the respiratory tract and the conjunctival mucosa as portals to deliver antigens. The oral, nasal and ocular are the preferred routes to induce mucosal immunity against Infectious laryngotracheitis (ILT) as laryngotracheitis virus (ILTV) live-attenuated chicken embryo origin (CEO) vaccines are administered either via eye drop or by mass vaccination via the drinking water or coarse spray, whereas the tissue culture origin (TCO) vaccine is only administered via eye drop (Gelenczei & Marty, 1964; Fulton *et al*., 2000).

Different from mammals, chickens lack lymph nodes and lymphatic vessels; instead a network system consisting of mucosal-associated lymphoid tissues (MALT) has been described in the intestinal tract, the respiratory tract, and the eye region (Balic *et al*., 2014). The Harderian gland (HG), and the conjunctiva-associated lymphoid tissue (CALT) are highly developed mucosal-associated lymphoid tissues located in the eye region of chickens. They are sites where primary immune responses are developed after antigen stimulation (van Ginkel *et al*., 2009; Gurjar *et al*., 2013).

Development of immune responses at the mucosal surfaces is required to protect the host against invading pathogens. This process is under the control of a complex network of mononuclear phagocytes (MNP) (Paul, 2013). In mammals the mononuclear phagocyte (MNP) system includes blood monocytes, macrophages, and conventional dendritic cells. Although the respiratory tract in chickens differ significantly from that in mammals, recent studies have demonstrated that similar to mammals, the avian respiratory tract is also guarded by

macrophages and dendritic cells that can up take antigen (de Geus *et al*., 2012; de Geus *et al*., 2015). Chicken dendritic cells (DC) and macrophages are specialized cells that can recognize antigens through pathogen recognition receptors (PRR) such as Toll-like receptors (TLR) and C-type lectin receptors (CLR). Chicken DCs can internalize antigen and present it to naïve T cells subsequently driving their differentiation into Th1, Th2 and Th17 cell subset (Degen *et al*., 2005; Goto et al., 2014; Wu & Kaiser, 2011). Similar to avian DCs, avian macrophages also express PRRs and play key role in clearance of invading pathogens and as antigen-presenting cells (APCs) (Wu & Kaiser, 2011). Based on marker expression $CD11^{+}$, $MHCII^{Hi+}$, $MHCII^{Lo+}$, and $CD80^{+}$ different subset of macrophages and dendritic cells were identified in the lungs of unstimulated chickens (de Geus *et al*., 2012). In mammals, the differentiation, proliferation and survival of macrophages are mainly controlled by the cytokine macrophage colony-stimulating factor (CSF1) when it interacts with its receptor (CSF1R) also known as CD115 (Balic *et al*., 2014). It was recently revealed that different to mammals in chickens the CSF1R is expressed not only by macrophages but also by dendritic cells (Sutton *et al*., 2018a), and at low levels in heterophils (Balic *et al*., 2014).

Upon ILTV infection productive viral lytic replication occurs in the respiratory epithelium lining the upper respiratory tract and the conjunctival epithelium of chickens (Beltrán *et al*., 2017). Whereas a semi-productive infection was described in cultures of chicken monocytes- derived macrophages as indicated by the expression of viral antigens, increased transcription of viral genes, detection of cytopathic effect but absence of virus release to culture supernatants (Calnek *et al*., 1986; Loudovaris *et al*., 1991; Coppo *et al*., 2018). In the current study, we first investigated the mononuclear phagocyte (MNP) composition based on CSF1R and MHC-II surface expression in the CALT and HG of unstimulated five-week-old specific

pathogen free chickens and after ocular stimulation with CEO vaccine or virulent strain 63140. Additionally, cultures of monocyte-derived macrophages (MDM) were evaluated in their ability to support productive replication of the CEO vaccine and the strain 63140, also the potential of these ILTV strains to induce apoptosis in MDMs was assessed. Knowledge of the dynamics of mononuclear phagocyte cells in the eye associated-lymphoid tissues after ILTV stimulation would provide a better understanding on how the local cell mediated immune responses are initiated after ILTV stimulation. This knowledge is necessary for the development of improved ILTV vaccines and vaccination strategies that could effectively trigger local specific responses after mucosal administration (eye-drop, spray, drinking water).

MATERIALS AND METHODS

Experimental design

A total of 220 specific pathogen free (SPF) fertile eggs, Charles River, Norwich, CT.) were incubated and hatched at the Poultry Diagnostic Research Center (PDRC, Athens, GA), University of Georgia hatchery facilities. One-day-old chicks were housed in isolation units, with filtered air and negative pressure, provided with feed and water *ad libitum.* At five weeks of age chickens were divided in three groups. One group of chickens was inoculated with virulent strain 63140 (n=75); a second group was inoculated with the chicken embryo origin (CEO) vaccine strain (n=75) via the ocular route. Both virus strains were administered at $10^{3.5}$ tissue culture infective dose ($TCID_{50}$) in 60 μL volume, 30 μL per eye. The third group of chickens (n=65) was mock-inoculated with cell culture media and used as negative control. At days 1, 3, 5, 7, and 9 post-inoculation (pi) five chickens that received the 63140 virulent strain, five chickens that received the CEO vaccine strain and five mock-inoculated chickens were euthanized by CO_2 gas inhalation for one minute. The conjunctival-associated lymphoid tissue (CALT) of the lower eyelids and Harderian gland (HG) from both eyes, were aseptically removed and immediately placed in 15 mL conical tubes containing 8 mL of ice-cold transport medium (calcium and magnesium-free PBS with 0.5% bovine serum albumin) (Thermo Fisher Scientific, Waltham, MA), Samples were kept on ice until the tissue was processed for flow cytometry analysis.

Single cell suspension preparation

Immediately after collection single cell suspension of tissues were obtained from CALT and HG by mechanical disruption using a 60 μm wire screen mesh (Sigma-Aldrich, St. Luis, MO). To avoid excessive cell damage, the screen mesh was submerged in transport media at all times during tissue disruption. CALT cell suspensions were passed once through a 70 μm cell

strainer (Thermo Fisher Scientific, Waltham, MA) to remove connective tissue. CALT cells were washed once with transport medium and centrifuged at 250 xg for 7 min at 4 °C. The HG cell suspension was passed once through a 70 µm and twice through a 40 µm cell strainer to remove connective tissue fragments. The cells were washed twice as described above. Following washes the CALT cells were suspended in 1 mL and the HG cells in 2 ml of ice-cold transport medium. Cells were enumerated and viability was determined using trypan blue exclusion on a Cellometer Mini (Nexcelcom Bioscience, Lawrence, MA) with final cell dilutions set at $1x10^5$ cells/100 µL CALT and $4x10^5$ cells/100 µL HG.

Antibody dilutions and staining procedures of CALT and HG cell suspension

The mononuclear phagocyte (MNP) composition in CALT and HG was evaluated by cell surface marker expression using two staining combinations of monoclonal antibody: 1) Allophycocyanin (APC) conjugated to mouse anti- chicken CD45, a pan leukocyte marker alone (Clone LT40, Southern Biotech, Birmingham, AL), and 2) Alexa Fluor 488 (AF488)-conjugated to mouse anti-chicken CSF1R (CD115, Clone ROS-AV170, Bio-Rad, Hercules, CA) paired with phyocoerythrin (PE)- conjugated to mouse anti-chicken MHCII (Clone 2G11, Southern Biotech, Birmingham, AL). Antibody concentrations were optimized to the minimum saturating and cross-talk (between colors) concentration in prior trials. The APC-CD45 was used at a concentration of 0.05 µg per reaction. The AF488-CSF1R and the PE-MHCII were diluted to a final concentration per reaction of 0.125 µg and 0.25 µg, respectively. Working dilutions of antibodies were performed in FACS buffer (calcium and magnesium-free PBS, 0.5% bovine serum albumin, with 0.1% sodium azide). One hundred microliter per cell suspension was distributed in round bottom 96-well plates. Cells were incubated with 100 µL of antibody combinations as indicated above on a plate shaker for 30 minutes at 4 ^oC. After incubation, the

plates were centrifuged at 4 ^{o}C for 7 minutes at 250 xg, cell pellets were washed once with 200 µL of FACS buffer at 4 ^{o}C for 5 minutes at 250 xg. Following washing, cells were re-suspended in 100 µL of FACS buffer and 100 µL of IC fixation buffer (Thermo Fisher Scientific, Waltham, MA) and stored overnight at 4 ^{o}C. Before flow cytometry analysis, fixed cells were further diluted with 200µL of ice-cold calcium and magnesium-free PBS. Flow cytometry analysis was performed on a BD Accuri C6 Flow Cytometer (San Jose, CA).

Flow cytometry strategy for identification of MNPs in CALT and HG

Primary gating was based on size uniformity and exclusion of cell doublets and clusters using forward scatter height versus forward scatter area (FSC-H vs FSC-A) (Figure 5.1a). Cells in forward angle and right angle scatter (FSC-A vs SSC-A) (Figure 5.1b) were subjected to CD45 assessment (Figure 5.1c) and established the leukocyte population. The $CD45^{+}$ leukocytes were then evaluated for CSF1R and MHCII surface expression (Figure 5.1d). In the leukocyte gate (Figure 5.1b) 4,000 events were collected per sample from CALT preparations, and 3,000 events from HG preparations. Two cell populations were detected based on the expression of CSF1R and MHCII: 1) $CSF1R^{+}$/ $MHCII^{Lo+}$, 2) $CSF1R^{+}$/$MHCII^{Hi+}$(Figure 5.1d).

Isolation and culture of monocyte-derived-macrophages

Heparanized blood was collected from 2 to 5 month old SPF chickens. To obtain an optimum number of macrophages, five chickens were bled and approximately 25 mL of blood was pooled and utilized in the assay. Blood was diluted 1:1 with transport medium. Four milliliters of diluted blood was layered onto 3 mL of Ficoll-paque Plus (Sigma-Aldrich, St. Luis, MO), and centrifuged at 400 xg for 30 minutes at 18 °C with no break. Peripheral blood mononuclear cells (PBMC) were harvested from the Ficoll interface and washed twice with

transport medium and centrifuged at 250 xg for 7 min at 4 °C. Following washes PBMCs were re-suspended in culture medium containing DMEM (HyClone, Logan, UT), 10% fetal bovine serum (Atlanta®, Biological, Flowery Branch, GA), 50 μg/mL ampicillin, 5 μg/mL amphotericin B (Gibco, Grand Island, NY), and 50 μg/mL gentamicin (Sigma-Aldrich, St. Luis, MO). The PBMCs were enumerated and viability was determined using trypan blue exclusion. The PBMCs were set to a final concentration of 2 $x10^6$ cells/ml in 12-well plates (Corning, Thermo Fisher Scientific, Waltham, MA) and utilized for assessment of CEO vaccine and virulent strain 63140 replication. Additionally, PBMCs at a concentration of $1x10^7$ cells/ml were plated in 75 cm^2 culture flasks (Corning, Thermo Fisher Scientific, Waltham, MA) and used for apoptosis assessment. The cells were incubated at 37 °C in 5% CO_2. At 24 hours of incubation the non-adherent cells (enriched lymphocytes) were removed, fresh culture medium was added and adherent cells were incubated for an additional 24 hours. Forty-eight hours from the initial seeding the adhered cells were mainly monocyte-derived-macrophages (MDM).

Flow cytometry monocyte-derived macrophage apoptosis assay

Adherent MDMs were inoculated with CEO vaccine and the virulent 63140 strain at a multiplicity of infection (MOI) of 0.05, otherwise cells remained unstimulated and used as negative control. Cells were incubated at 39 °C in 5% CO_2 for 48 hours. In addition, an apoptosis positive control was generated by inoculating MDMs with 2 nM of Staurosporine (Sigma-Aldrich, St. Luis, MO) followed by incubation at 39 °C for 12 hours. MDMs were detached from the plates using Accutase® (Innovative cell technologies, San Diego, CA) for 10 minutes incubation at room temperature. Once MDMs were detached, they were enumerated using trypan

blue exclusion on the Cellometer Mini (Nexcelcom Bioscience, Lawrence, MA). Final MDMs concentration was adjusted at $2x10^6$ cells/100 μL.

Purity of the MDM population was evaluated by expression of CSF1R using the Alexa Fluor 647-conjugated mouse anti-chicken antibody (Clone ROS-AV170, Bio-Rad, Hercules, CA). In addition, the ability of ILTV to ablate expression of CSF1R was assessed in MDMs after stimulation with either CEO vaccine or virulent strain 63140. Staining of CSF1R was conducted as described above. Staining with Annexin V (AnnV) was performed as recommended by the manufacturer (Biogmes, Westlake Village, CA) with several modifications. Briefly, final cell dilution from non-stimulated, Staurosporine treated, CEO and 63140 inoculated MDMs were distributed in round bottom 96-well plates, 100 μL per well. MDMs were incubated with 5 μL of Ann V at 1:10 dilution and incubated on a plate shaker for 40 minutes at room temperature. Cells were washed once with 200 μL of Ann V binding buffer (Biogmes, Westlake Village, CA) and centrifuged at 250 xg for 7 min at 4 °C. MDMs were then re-suspended with Ann V binding buffer and incubated with 5 μL of 7-amino actinomycin D (7-AAD) solution on a plate shaker for 15 minutes at room temperature. Before flow cytometry analysis, stained MDMs were further diluted with 400μL of Ann V binding buffer. Primary gating of CEO, 63140 or mock-inoculated MDMs was based on size consistency and single cells using forward scatter height versus forward scatter area (FSC-H vs FSC-A) (Figure 5.3a). Cells in forward angle and right angle scatter (FSC-A vs SSC-A) (Figure 5.3b) from unstimulated (Figure 5.3c), and CEO or 63140 stimulated (Figure 5.3d & 5.3e) were subjected to CSF1R surface marker analysis. Percentage expression of $CSF1R^+$ MDMs was separate into three populations based on dual fluorescent staining with phycoerythrin labeled Ann-V and 7-AAD (Figure 5.3f to 5.3h).

Virus genome load in MDMs and LMH cells

Adherent MDM cells were either mock-inoculated with cell culture media and used as negative control, inoculated with CEO vaccine or virulent strain 63140 as described above. After absorption for 1 hour, the inoculum was removed, fresh PBMC medium was added and incubated at 39 °C in 5% CO_2 for 48 hours. Supernatant and MDM cell lysate (n=3) were harvested at 0, 6, 12, 24 and 48 hours pi and stored in -80 °C until DNA extraction. LMH cells were inoculated with either CEO vaccine or 63140 at MOI of 0.002 and supernatant was harvested at 0, 6, 12, 24 and 48 hours pi and stored in -80 °C until DNA extraction was conducted.

DNA extraction

Total DNA was extracted from supernatant and cell lysate of MDMs inoculated, supernatant of LMH inoculated, and mock-inoculated LMH and MDMs using the MagaZorb® DNA extraction mini-prep 96 well kit following the manufacturer´s recommendations (Promega, Madison, WI).

ILTV genome load

Detection of ILTV genome in MDM and LMH cells was determined by duplex Real-time PCR as previously described (Vagnozzi *et al*., 2016). The duplex assay targets the UL44 (gC) viral gene and a fragment of the chicken α2-collagen gene. The relative amount of viral DNA per samples was expressed as $\log_{10} 2^{-\Delta\Delta Ct}$ value.

Statistical analysis

The percentage expression of $CSF1R^{+}/MHCII^{Lo+}$, and $CSF1R^{+}/ MHCII^{Hi+}$ in CALT and HG from mock-inoculated chickens at days 1, 3, 5, 7, and 9 pi were compared by the one-way analysis of variance Kruskal-Wallis test and Dunn´s multiple comparison test. No significant differences in percentage expression of $CSF1R^{+}/MHCII^{Lo+}$, and $CSF1R^{+}/MHCII^{Hi+}$ in the CALT or HG from mock-inoculated chickens were detected between 1 to 9 days post-inoculation (pi). Therefore, percentage expression for each cell marker from days 1 to 9 pi were pooled to obtain a wider representation of the basal percentage of MNPs in CALT and HG from mock-inoculated chickens. The one-way analysis of variance Kruskal-Wallis test and Dunn´s multiple comparison test was utilized to compare the percentage expression of $CSF1R^{+}/MHCII^{Lo+}$, and $CSF1R^{+}/MHCII^{Hi+}$ in CALT and HG collected from 63140 and CEO inoculated groups of chickens and the pool mock-inoculated at days 1, 3, 5, 7, and 9 pi. The Kruskal-Wallis and Dunn´s multiple comparison tests were used to compare mean genome viral genome load of the CEO vaccine and virulent strain 63140 in the supernatant and cell lysate of MDM at 0, 6, 12, 24, and 48 hours post-inoculation. Data is reported as mean ± standard deviation (SD). The two-way ANOVA was utilized to highlight differences in mean viral genome load detected in the supernatant and cell lysate of CEO or 63140 inoculated MDM and LMH cells at 0, 6, 12, 24, and 48 hours post-inoculation. Statistical analysis of the data was conducted using the Prism 7 (GraphPad, Software Inc. San Diego, CA, USA).

Ethical statement

All animal experiments conducted in this study were performed under the Animal Use Proposal A2018 06-009-Y1-A0 approved by the Animal Care and Use Committee (IACUC) in

accordance with regulations of the Office of the Vice President for Research at the University of Georgia.

RESULTS

CSF1R^{+}/MHCII $^{Lo+}$, and CSF1R^{+}/MHCII $^{Hi+}$ in CALT

The percentage of cells expressing CSF1R^{+}/MHCII^{Lo+} and CSF1R^{+}/MHCII^{Hi+} in CALT and HG are shown in Figure 5.2. In the CALT of CEO vaccinated chickens the average percentage of cells expressing CSF1R^{+}/MHCII^{Lo+} by day 1 pi was 6.46%, which was significantly higher ($p \leq 0.001$) compared to an average of 1.09 % detected for the mock-inoculated group of chickens. By day 3 pi the percentage of cells expressing CSF1R^{+}/MHCII^{Lo+} dropped to 1.41% and the expression was maintained at average 1.47% to 2.22% until day 9 pi (Figure 5.2a). A 3.78% of the CALT cells expressed CSF1R^{+}/MHCII^{Hi+} by day 1 pi that was significantly ($p \leq 0.001$) higher compared to 0.85% expression detected in the mock-inoculated group of chickens. By days 3 to 7 the expression decreased to levels similar to those detected for the mock-inoculated chickens (1.32% to 1.81%) and by day 9 pi an average of 2.02% of the cells expressed CSF1R^{+}/MHCII^{Hi+} which was significantly ($p \leq 0.05$) higher as compared to the mock-inoculated group of chickens (0.85%) (Figure 5.2b).

In the CALT of 63140 infected chickens, the average percentage of CSF1R^{+}/MHCII^{Lo+} cells by day 1 pi was 3.68%, which was significantly ($p \leq 0.01$) higher than an average 1.09% detected in the mock-inoculated group of chickens. By days 3 to 7 the percentage of cells expressing CSF1R^{+}/MHCII^{Lo+} decreased to similar levels as those observed in the mock-inoculated group (ranging from 1.45 % to 1.86 %), by day 9 pi it significantly ($p \leq 0.05$) increased to an average of 4.85% (Figure 5.2c). Average 2.09% and 2.27% cells expressing CSF1R^{+}/ MHCII^{Hi+} were detected in the CALT of 63140 inoculated at days 1 and 3 pi, in both instances the percentages of cells expressing CSF1R^{+}/ MHCII^{Hi+} were significantly ($p \leq 0.05$ day

1 and $p \leq 0.01$ day 3) higher than those detected in mock-inoculated chickens (0.85%). From days 5 to 7 percentage of cells expressing $CSF1R^{+}$/ $MHCII^{Hi+}$ decreased to 0.98% by day 5 and to 1.03% by day 7, and it significantly ($p \leq 0.01$) recovered to a 3.35 % by day 9 pi (Figure 5.2d).

$CSF1R^{+}$/$MHCII^{Lo+}$, and $CSF1R^{+}$/$MHCII^{Hi+}$ in HG

In the HG of CEO vaccinated chickens the average percentage of cells expressing $CSF1R^{+}/MHCII^{Lo+}$ fluctuated between 7.18% and 7.59% from days 1 to 3 pi. At day 5 pi the average percentage significantly ($p \leq 0.001$) decreased to 1.04% as compared to an average of 13.32% of cells expressing $CSF1R^{+}/MHCII^{Lo+}$ detected in the mock-inoculated groups of chickens. By days 7 and 9 pi the percentage of cells expressing $CSF1R^{+}/MHCII^{Lo+}$ rebounded to 5.84% and 4.74% (Figure 5.2e). The average percentage of $CSF1R^{+}/MHCII^{Hi+}$ cells in the HG of CEO inoculated chickens remained lower from days 1 to 9 pi as compared to an average of 5.3% $CSF1R^{+}/MHCII^{Hi+}$ cells detected for the mock-inoculated group of chickens. At days 1 and 3 pi the average percentage was 2.02% and 1.92% and it significantly ($p \leq 0.05$) decreased to 0.2% by day 5 pi followed by an increase to 3.10% by day 7 pi, and a significant ($p \leq 0.001$) decrease to 1.28% by day 9 pi (Figure 5.2f).

In the HG of 63140 infected chickens the average percentage of cells expressing $CSF1R^{+}$/ $MHCII^{Lo+}$ by day 1 pi was 6.57% and 8.43% by day 3 pi. Although lower, these percentages were not significant different than the average 13.32% of $CSF1R^{+}$/ $MHCII^{Lo+}$ cells detected in the mock-inoculated group of chickens. However by days 5, 7, and 9 pi the $CSF1R^{+}$/ $MHCII^{Lo+}$ cell population significantly decreased to 2.67%, 2.91%, 3.03% ($p \leq 0.01$),

respectively (Figure 5.2g). An average percentage of 2.15% $CSF1R^{+}$/ $MHCII^{Hi+}$ expressing cells were observed in the HG of 63140 infected chickens at day 1 pi, which was not different to the average percentage of $CSF1R^{+}$/ $MHCII^{Hi+}$ cells observed in the mock-inoculated group of chickens (5.33%). Whereas at day 3 and 5 pi the percentage of $CSF1R^{+}$/ $MHCII^{Hi+}$ expressing cells significantly decreased to 1.03% ($p \leq 0.01$) and 1.10% ($p \leq 0.05$), by day 7 pi $CSF1R^{+}$/ $MHCII^{Hi+}$ expressing cells slightly increased to 2.37%, and significantly dropped again to 1.31% ($p \leq 0.01$) by day 9 pi (Figure 5.2h).

Apoptosis of ILTV infected MDMs

To determine whether virus induced apoptosis was involved in the decrease of MNPs observed in the HG after ILTV stimulation, populations of unstimulated and stimulated MDMs were analyzed for the binding of PE-conjugated AnnV and 7-AAD to discriminate whether MDMs were in early apoptosis or late stages of apoptotic and necrotic processes. Percentage expression of $CSF1R^{+}$ in unstimulated MDMs was 88.2% (Figure 5.3c), in CEO inoculated it was 99.2% (Figure 5.3d), and in 63140 inoculated it was 90.3% (Figure 5.3e). Three cell populations were detected by the AnnV and 7-AAD cytometry analysis: $AnnV^{+}$ and 7-AAD $^{-}$ (early apoptotic cells), $AnnV^{+}$ and $7\text{-}AAD^{+}$(membrane compromise late apoptotic or necrotic cells), and $AnnV^{-}$ and $7\text{-}AAD^{+}$ (necrotic cells). In unstimulated MDMs, 32.4% of the cell population was early apoptotic, 13.7% was in late apoptotic or necrotic stage, and 4.3% was necrotic (Figure 5.3f). In MDMs inoculated with CEO vaccine 8.8% of the cell population was in early apoptotic stage, 1.1% was late apoptotic or necrotic stage, and 1.7% was necrotic (Figure 5.3g). In MDMs inoculated with virulent strain 63140 18.8% of the cell population was in an early apoptotic stage, 2.2% was late apoptotic or necrotic, and 2.1% was necrotic (Figure 5.3h).

Viral genome load in MDM and LMH cells

The mean viral genome load in the supernatant of CEO inoculated MDMs after 1 hour post absorption at 0 hrs pi was 4.15, from 6 to 48 hrs pi the CEO genome load fluctuated from 4.33 to 3.77 showing a significant decreased to 3.77 ($p \leq 0.05$) by 48 hrs pi (Figure 5.4a). The mean viral genome load in the cell lysate of CEO inoculated MDMs showed a similar trend to that observed in the supernatant. At 0 hours pi the mean viral genome load was 4.43, at 6 hours pi it slightly increased to 4.45, at 12 hours pi it dropped to 4.26, at 24 hours pi increased to 4.30 and at 48 hours pi it significantly decreased to 4.08 ($p \leq 0.05$) (Figure 5.4c). The mean viral genome load in the supernatant and cell lysate of 63140 inoculated MDMs did not show significant changes. In the supernatant the mean viral genome load fluctuated from 3.65 to 4.05 (Figure 5.4b), whereas in the cell lysate mean viral genome of 63140 oscillated from 3.96 to 4.28 (Figure 5.4d). ILTV cytopathic effect was detected in MDMs at 48 hours pi with either CEO vaccine (Figure 5.4f) or virulent strain 63140 (Figure 5.4g). No cytopathic effect was observed in mock-inoculated MDMs (Figure 5.4h).

The replication kinetics of CEO vaccine and virulent 63140 in the supernatant of LMH cells showed a different trend. At 0 hours pi mean viral genome load of CEO in the supernatant was 3.83, it decreased to 2.87 at 6 hours pi, at 12, 24, and 48 hours pi it increased to 3.18, 4.03, and 4.95, respectively. CEO genome load significantly ($p \leq 0.05$) increased to 4.95 as compared to 6 hours pi (2.87) (Figure 5.4e). Mean viral genome load of 63140 at 0 hours pi was 2.20, decreased to 1.79 by 6 hours pi with subsequent increase to 2.65, 3.25, 4.87 by 12, 24, and 48 hours pi, respectively. By 48 hours pi it significantly ($p \leq 0.05$) increase to 4.87 as compared to 1.79 detected at 6 hours pi (Figure 5.4e).

DISCUSSION

In this study the mononuclear phagocyte (MNP) composition based on surface expression of CSF1R and MHC II was evaluated in the CALT and HG of unstimulated chickens and after ocular stimulation with the live-attenuated CEO vaccine or virulent 63140 ILTV strain. In addition, we evaluated the ability of chicken monocyte-derived macrophages (MDM) to support productive replication of the CEO vaccine and the virulent strain 63140 and assessed the ability of these ILTV strains to induce apoptosis in MDMs.

Assessment of MNP composition of the CALT and the HG in unstimulated and ILTV stimulated chickens consistently showed two distinct cell populations, one expressing $CSF1R^{+}/MCH\text{-}II^{Lo+}$ and a second expressing $CSF1R^{+}/MCH\text{-}II^{Hi+}$. Both cell populations identified in this study showed a steady surface expression of the CSF1R (Figure 5.1d). It has been previously indicated that following ligand binding the chicken CSF1R is internalized and degraded, thus making the receptor inaccessible to binding by the antibody (Garcia-Morales *et al*., 2014). Therefore, it implies that the steady surface expression of the CSF1R observed in our study was due to the binding of the antibody before receptor internalization. On the other hand, the MHCII expression was distinctly separated by the $MHCII^{Hi+}$ and $MHCII^{Lo+}$. This MHCII phenotypic feature has been previously associated with different subsets of resident macrophages and dendritic cells in the lung of unstimulated chickens that also express $CD11^{+}$ and $CD80^{+}$ (de Geus *et al*., 2012).

Recently, using transgenic chickens expressing a reporter gene under the control of the CSF1R promoter and enhancer ($CSF1R\text{-}transgene^{+}$), lymphoid aggregates were visualized in the air sacs, lungs and trachea from day 18 of embryonation through 63 weeks in healthy chickens.

CSF1R-transgene^{+} cells were detected in the bronchi associated lymphoid tissue (BALT) as early as 1 week of age, and in the trachea lymphoid aggregates were highly organized from 4 weeks onward (Sutton *et al*., 2018b). In this study a 1.09% expression of CSF1R^{+}/MCH-II^{Lo+} cells and 0.85% expression of CSF1R^{+}/MCH-II^{Hi+} cells were detected in the CALT of five-week-old SPF chickens. Therefore, under unstimulated conditions similar to the BALT, the CALT harbors mononuclear phagocytes, which reside in these tissues to ensure an effective and timely cellular defense against antigens that trespass the eye mucosa. Either the CEO vaccine or the virulent strain 63140 stimulated an increase of CSF1R^{+}/MCH-II^{Lo+} and CSF1R^{+}/MCH-II^{Hi+} expressing cells in the CALT by day 1 pi indicative of immune activation in this site. However, the percentage expression of CSF1R^{+}/MCH-II^{Lo+} (Figures 5.2a & 5.2b) and CSF1R^{+}/MCH-II^{Hi+} (Figures 5.2c & 5.2d) detected by day 1 pi after CEO vaccination was higher than percentages detected after 63140 stimulation. Furthermore, the increased expression of CSF1R^{+}/MCH-II^{Hi+} cells (2.09 to 2.27%) in the CALT of 63140 inoculated chickens was sustained until day 3 pi (Figure 5.2d). It is possible that the restricted expression of CSF1R^{+}/MCH-II^{Lo+} and CSF1R^{+}/MCH-II^{Hi+} observed after stimulation with 63140 is associated with failure of macrophages to function properly in early virus clearance or to effectively present antigen, consequently compromising the generation of a timely adaptive immune response (Chapter 4). On the other hand, the higher percentage and timely appearance of both CSF1R^{+}/MCH-II^{Lo+} and CSF1R^{+}/MCH-II^{Hi+} cell populations in the CALT of CEO vaccinated chickens suggests an effective response to CEO stimulation. This data is supported by the increase of CD8^{+} cells in the CALT after CEO vaccination, which correlated with clearance of CEO cytolytic replication from the conjunctiva epithelium after ocular vaccination (Chapter 4). For both, CEO vaccinated and 63140 infected chickens the percentage of CSF1R^{+}/MCH-II^{Lo+} and CSF1R^{+}/MCH-II^{Hi+} in

the CALT decreased to levels comparable to those detected in unstimulated chickens by day 3 to 5 pi.

In the HG of unstimulated chickens the average percentage of cells expressing $CSF1R^{+}/MCH\text{-}II^{Lo+}$ and $CSF1R^{+}/MCH\text{-}II^{Hi+}$ were higher than those detected in the CALT of unstimulated chickens. The HG of unstimulated chickens harbor a 13.32% and 5.33% of cells expressing $CSF1R^{+}/MCH\text{-}II^{Lo+}$ and $CSF1R^{+}/MCH\text{-}II^{Hi+}$, respectively. As early as day 1 pi, following stimulation with either CEO vaccine or virulent strain 63140 the percentage of both cell populations markedly decreased reaching their lowest levels by day 5 pi. Particularly, levels of cells expressing $CSF1R^{+}/MCH\text{-}II^{Hi}$ remained significantly low up to day 9 pi as compared to levels detected in the HG of unstimulated chickens. In a previous study following ocular, oral, and intratracheal inoculation with ILTV, the viral antigen detected in the HG was associated with potential mononuclear cells. This finding was indicative that the gland lymphoid tissue might serve as a main site for virus uptake and immune stimulation (Beltrán *et al*., 2017). In this study the sustained reduction of cells expressing $CSF1R^{+}/MCH\text{-}II^{Lo+}$ and $CSF1R^{+}/MCH\text{-}II^{Hi+}$ after ILTV stimulation suggests that both vaccine and virulent strains dampen the immune response of MNPs in the HG. Whether the reduction of cells expressing $CSF1R^{+}/MCH\text{-}II^{Lo+}$ and $CSF1R^{+}/MCH\text{-}II^{Hi+}$ is due to migration of these cells from the HG to other sites or to virus induced apoptosis warrant further analysis. There is evidence to support that early after ILTV infection monocyte-derived macrophages (MDM) express viral antigens, but do not support productive viral replication (Calnek *et al*., 1986; Loudovaris *et al*., 1991). It has been suggested, but not tested that macrophages and/or other immune cells can transport viral particles to non-respiratory sites (Oldoni *et al*., 2009). Recently although presence of cytopathic effect and syncytia formation were observed in cultures of MDMs after inoculation with attenuated and

virulent ILTV strains, very low levels of virus were released into the culture supernatant (Calnek *et al*., 1986; Coppo *et al*., 2018). In agreement with Coppo *et al*., (2018) we observed that both CEO and 63140 strains induced marked cytophatic effect in MDMs. However, viral genomes of either the CEO or 63140 strains were present in the cell culture supernatants indicating that virus was released from infected cells. The replication kinetics of both CEO and 63140 in MDMs, as determined by viral genome load, showed that neither strain followed the exponential increase expected from a cell associated or cell free productive virus infection as observed in LMH cells (Figure 5.4e). Therefore, it was concluded that in agreement with an earlier study (Calnek *et al*., 1986) both ILTV strains establish a semi-productive infection in MDMs. Apoptosis analysis showed that compared to a 32.4% of unstimulated MDMs only 8.8% of the CEO and 18.8% of the 63140 infected MDMs where undergoing early apoptosis suggesting that both the CEO vaccine and the virulent strain 63140 may persist in MDMs through the inhibition of apoptotic pathways. Furthermore, neither the CEO vaccine nor the 63140 virulent strain ablated the surface expression of CSF1R. This indicates that ILTV infection does not deregulate surface expression of CSF1R, allowing development, and maintenance of MDMs.

Overall the results from this study reveal that the CALT and HG of chickens harbor mononuclear phagocyte (MNP). MNPs composition of the CALT and the HG in unstimulated chickens showed two distinct cell populations, $CSF1R^{+}/MCH\text{-}II^{Lo+}$ and $CSF1R^{+}/MCH\text{-}II^{Hi+}$, which were expressed in higher percentages in the HG than in the CALT. Stimulation with either CEO or 63140 induced an early increase of both MNP populations in the CALT and a reduction in the HG. In the CALT the CEO vaccine induced a rapid increase of $CSF1R^{+}/MCH\text{-}II^{Lo+}$ and $CSF1R^{+}/MCH\text{-}II^{Hi+}$ cell populations. In the HG, ILTV stimulation induced a sustained significant decrease of $CSF1R^{+}/MCH\text{-}II^{Lo+}$ and $CSF1R^{+}/MCH\text{-}II^{Hi+}$ cells. Inhibition of apoptosis

accompanied with evidence of a semi-productive infection of MDMs by CEO and 63140, raised the possibility that the abrupt decrease of $CSF1R^{+}$/MCH-II^{Lo+} and $CSF1R^{+}$/MCH-II^{Hi+} cells in the HG may be a mechanism by which the virus spreads via infected MNPs while evading the host immune surveillance ultimately allowing the establishment of a latent infection.

REFERENCES

Balic, A., Garcia-Morales, C., Vervelde, L., Gilhooley, H., Sherman, A., Garceau, V., Gutowska, M. W., Burt, D. W., Kaiser, P., Hume, D. A., Sang, H.M. (2014). Visualisation of chicken macrophages using transgenic reporter genes: Insights into the development of the avian macrophage lineage. *Development, 141*, 3255-3265.

Beltrán, G., Williams, S.M., Zavala, G., Guy, J.S., & García, M. (2017). The route of inoculation dictates the replication patterns of the infectious laryngotracheitis virus (iltv) pathogenic strain and chicken embryo origin (CEO) vaccine. *Avian Pathology, 46*, 585-593.

Calnek, B.W., Fahey, K.J., & Bagust, T.J. (1986). In vitro infection studies with infectious laryngotracheitis virus. *Avian Diseases, 30*, 327-336.

Coppo, M.J.C., Devlin, J.M., Legione, A.R., Vaz, P.K., Lee, S.W., Quinteros, J.A., Gilkerson, J. R., Ficorilli, N., Reading, P. C., Noormohammadi, A. H., Hartley, C.A. (2018). Infectious laryngotracheitis virus viral chemokine-binding protein glycoprotein g alters transcription of key inflammatory mediators in vitro and in vivo. *Journal of Virology, 92*.

de Geus, E.D., Degen, W.G., van Haarlem, D.A., Schrier, C., Broere, F., & Vervelde, L. (2015). Distribution patterns of mucosally applied particles and characterization of the antigen presenting cells. *Avian Pathology, 44*, 222-229.

de Geus, E.D., Jansen, C.A., & Vervelde, L. (2012). Uptake of particulate antigens in a nonmammalian lung: Phenotypic and functional characterization of avian respiratory phagocytes using bacterial or viral antigens. *Journal of Immunology, 188*, 4516-4526.

Degen, W.G., Daal, N., Rothwell, L., Kaiser, P., & Schijns, V.E. (2005). Th1/th2 polarization by viral and helminth infection in birds. *Veterinary Microbiology, 105*, 163-167.

Fulton, R.M., Schrader, D.L., & Will, M. (2000). Effect of route of vaccination on the prevention of infectious laryngotracheitis in commercial egg-laying chickens. *Avian Diseases, 44*, 8-16.

Garcia-Morales, C., Rothwell, L., Moffat, L., Garceau, V., Balic, A., Sang, H.M., Kaiser, P., Hume, D.A. (2014). Production and characterisation of a monoclonal antibody that recognises the chicken csf1 receptor and confirms that expression is restricted to macrophage-lineage cells. *Developmental and Comparative Immunology, 42*, 278-285.

Gelenczei, E.F., & Marty, E.W. (1964). Studies on a tissue-culture-modified infectious laryngotracheitis virus. *Avian Diseases, 8*, 105-122.

Goto, Y., Panea, C., Nakato, G., Cebula, A., Lee, C., Diez, Marta G., Ivanov, Ivaylo I. (2014). Segmented filamentous bacteria antigens presented by intestinal dendritic cells drive mucosal Th17 cell differentiation. *Immunity, 40*, 594-607.

Gurjar, R.S., Gulley, S.L., & van Ginkel, F.W. (2013). Cell-mediated immune responses in the head-associated lymphoid tissues induced to a live attenuated avian coronavirus vaccine. *Developmental and Comparative Immunology, 41*, 715-722.

Loudovaris, T., Calnek, B.W., Yoo, B.H., & Fahey, K.J. (1991). Genetic susceptibility of chicken macrophages to in vitro infection with infectious laryngotracheitis virus. *Avian Pathology, 20*, 291-302.

Oldoni, I., Rodriguez-Avila, A., Riblet, S.M., Zavala, G., & García, M. (2009). Pathogenicity and growth characteristics of selected infectious laryngotracheitis virus strains from the united states. *Avian Pathology, 38*, 47-53.

Paul, W.E. (2013). Fundamental immunology. *Philadelphia : Wolters Kluwer Health/Lippincott Williams & Wilkins,*.

Sutton, K., Borowska, D., Katrina, M., Balic, A., & Vervelde, L. (2018a). Identification and characterisation of antigen-presenting cells in the chicken spleen. *XV Avian Immunology Research Group (AIRG) Meeting*.

Sutton, K., Costa, T., Alber, A., Bryson, K., Borowska, D., Balic, A., Kaiser, P., stevens, M., Vervelde, L. (2018b). Visualisation and characterisation of mononuclear phagocytes in the chicken respiratory tract using csf1r-transgenic chickens. *Veterinary Research, 49*, 104.

Vagnozzi, A., Riblet, S., Zavala, G., Ecco, R., Afonso, C.L., & Garcia, M. (2016). Evaluation of the transcriptional status of host cytokines and viral genes in the trachea of vaccinated and non-vaccinated chickens after challenge with the infectious laryngotracheitis virus. *Avian Pathology, 45*, 106-113.

van Ginkel, F.W., Tang, D.C., Gulley, S.L., & Toro, H. (2009). Induction of mucosal immunity in the avian harderian gland with a replication-deficient ad5 vector expressing avian influenza H5 hemagglutinin. *Developmental and Comparative Immunology, 33*, 28-34.

Wu, Z., & Kaiser, P. (2011). Antigen presenting cells in a non-mammalian model system, the chicken. *Immunobiology, 216*, 1177-1183.

FIGURES

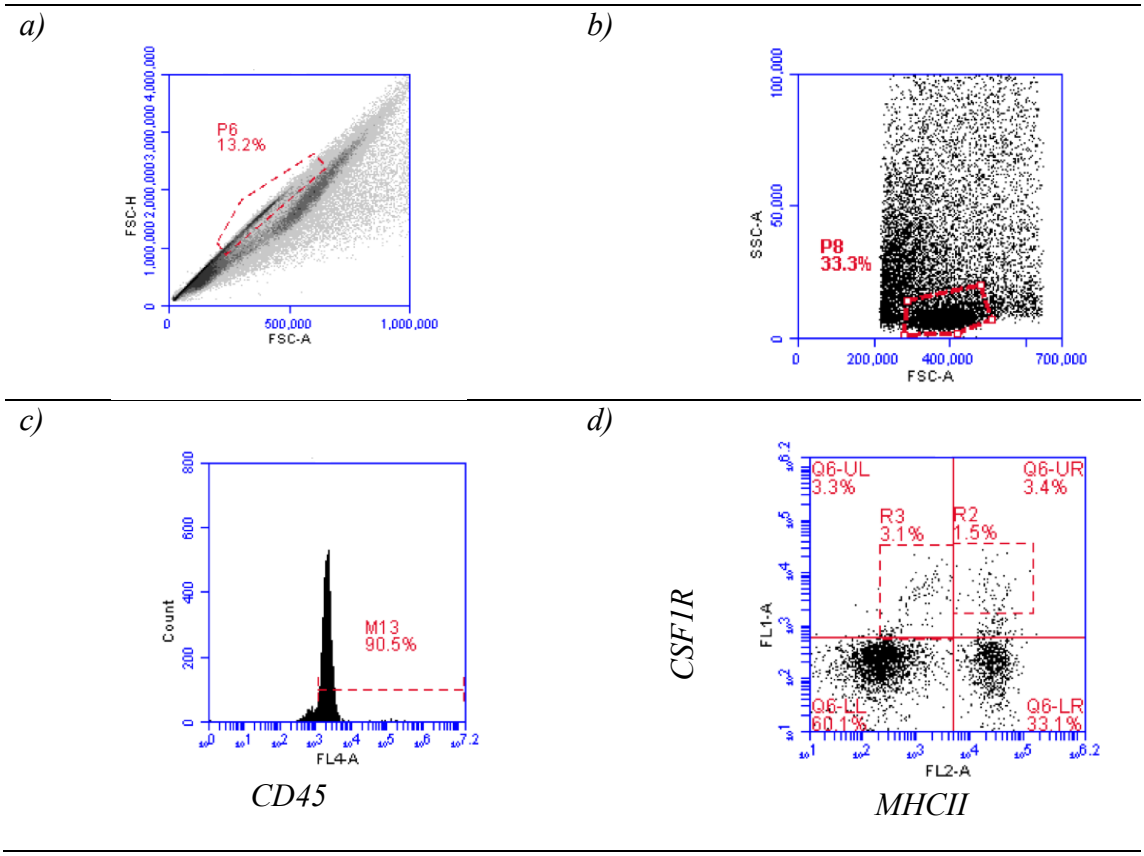

Figure 5.1. Gating strategy for the detection of mononuclear phagocytes CSF1R^{+}, MHCII^{+} in CALT and HG after vaccination and virulent strain 63140 infection. Primary gating was based on size consistency and single cells using forward scatter height versus forward scatter area (FSC-H vs FSC-A) (Figure 5.1a) followed by forward angle and right angle scatter (FSC-A vs SSC-A) (Figure 5.1b). Assessment of CD45^{+} (Figure 51c) and CSF1R^{+}/MHCII^{+} surface expression (Figure 5.1d). Two cell populations expressing CSF1R and MHCII were detected: 1) CSF1R^{+}/ MHCII^{Lo+} (R3), and 2) CSF1R^{+}/MHCII^{Hi+} (R2) (Figure 5.1d).

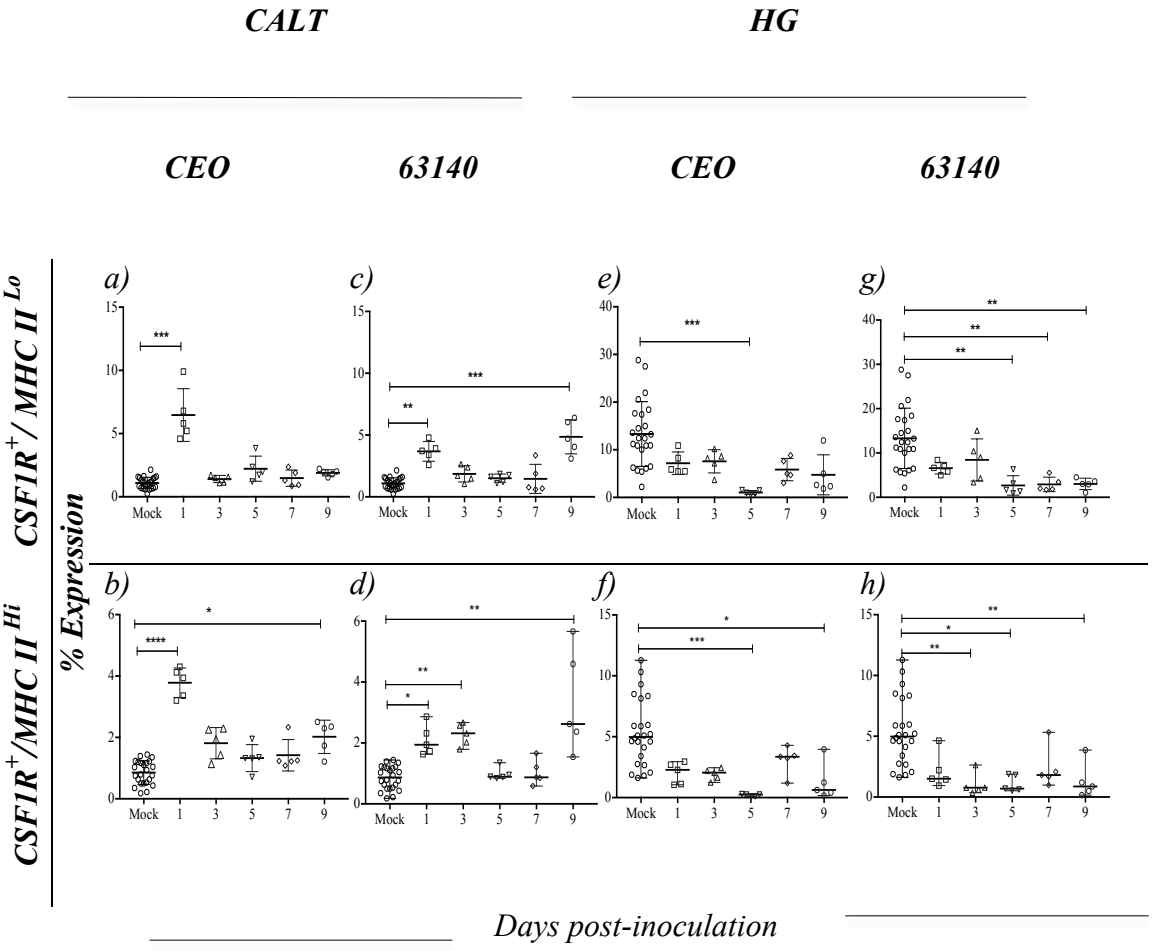

Figure 5.2. CSF1R^{+}/MHCII^{Lo}, and CSF1R^{+}/MHCII^{Hi} in CALT and HG after vaccination and virulent strain 63140 infection. Percentage expression of CSF1R^{+}/MHCII^{Lo} in the CALT of CEO vaccinated (a), and 63140 infected chickens (c); percentage expression of CSF1R^{+}/MHCII^{Hi} in the CALT of CEO vaccinated (b), and 63140 infected chickens (d) collected from day 1 to 9 pi. Percentage expression of CSF1R^{+}/MHCII^{Lo} in HG of CEO vaccinated (e), and 63140 infected chickens (g); percentage expression of CSF1R^{+}/MHCII^{Hi} in the HG of CEO vaccinated (f), and 63140 infected chickens (h) collected from day 1 to 9 pi. Percentage expression of CSF1R^{+}/MHCII^{Lo} and CSF1R^{+}/MHCII^{Hi} in the CALT and HG from

CEO vaccinated, 63140 infected, and mock-inoculated chickens were compared by one-way analysis of variance Kruskal-Wallis test and Dunn´s multiple comparison test. Individual percentages are depicted by geometric characters, and the mean ± standard deviation are depicted by horizontal and vertical lines, respectively. Statistical differences are indicated with asterisks: $p \leq 0.05$ (*), $p \leq 0.01$ (**), $p \leq 0.001$ (***), $p \leq 0.0001$ (****).

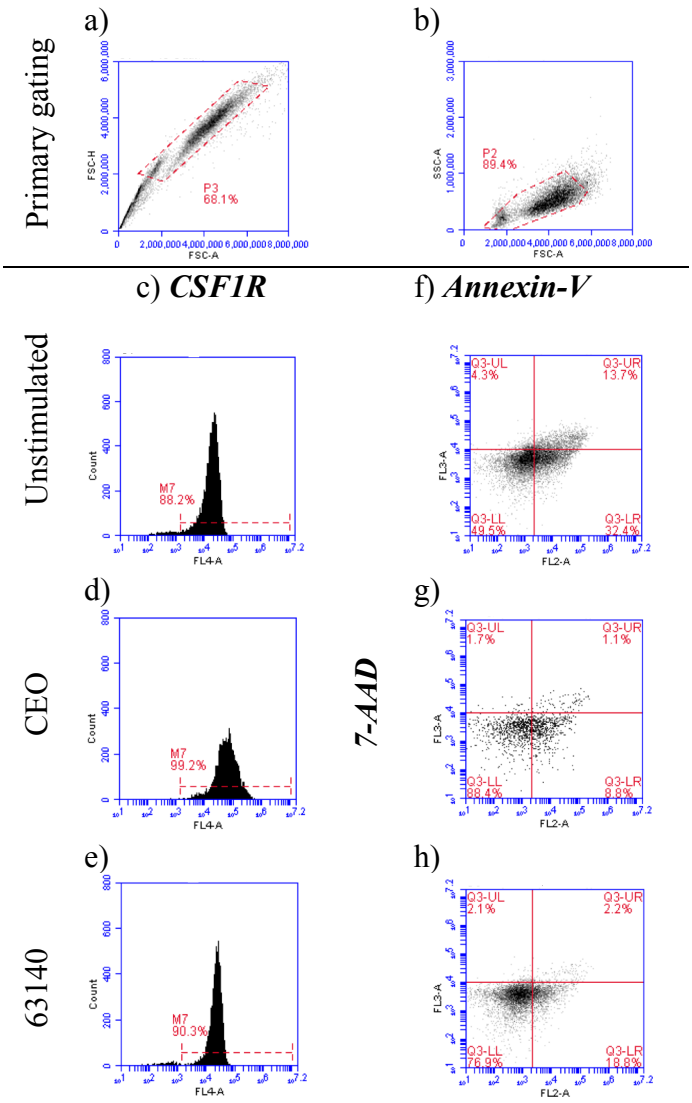

Figure 5.3. Evaluation of apoptosis by Annexin-V (AnnV) and 7-AAD staining in monocyte-derived macrophages (MDMs) after inoculation with CEO vaccine and virulent strain 63140. Primary gating of CEO, 63140 or mock-inoculated MDMs was based on size consistency and single cells using forward scatter height versus forward scatter area (FSC-H vs FSC-A) (Figure 5.3a). Cells in forward angle and right angle scatter (FSC-A vs SSC-A) (Figure 5.3b) were subjected to CSF1R surface marker analysis. Percentage expression of $CSF1R^{+}$ in unstimulated was 88.2% (Figure 5.3c), 99.2% CEO (Figure 5.3d), and 90.3% for 63140 (Figure 5.3e) inoculated MDMs. Based on dual fluorescent staining with phycoerythrin labeled Ann-V

(FL-2A) and 7-amino actinomycin D (7-AAD) (FL-3A), unstimulated MDMs (Figure 5.3f), and CEO (Figure 5.3g), 63140 (Figure 5.3h) stimulated MDMs separated into three populations. Cells with surface exposed phosphatidylserine ($AnnV^+$) and non-permeable cell membrane ($7\text{-}AAD^-$), cells with exposed phosphatidylserine ($AnnV^+$) and permeable cell membrane ($7\text{-}AAD^+$), and cells with permeable cell membrane ($7\text{-}AAD^+$), but without exposed phosphatidylserine ($AnnV^-$). In unstimulated MDMs the percentage expression of $CSF1R^+$ was 88.2% (Figure 5.3c), the percentage expression of $AnnV^+$ was 32.4%, $AnnV^+/7\text{-}AAD^+$ was 13.7%, and the percentage expression of $7\text{-}AAD^+$ was 4.3% (Figure 5.3f). In CEO stimulated MDMs the percentage expression of $CSF1R^+$ was 99.2% (Figure 5.3d), the percentage expression of $AnnV^+$ was 8.8%, $AnnV^+/7\text{-}AAD^+$ was 1.1%, and the percentage expression of $7\text{-}AAD^+$ was 1.7% (Figure 5.3g). In 63140 stimulated MDMs the percentage expression of $CSF1R^+$ was 90.3% (Figure 5.3e), the percentage expression of $AnnV^+$ was 18.8%, $AnnV^+/7\text{-}AAD^+$ was 2.2%, and the percentage expression of $7\text{-}AAD^+$ was 2.1% (Figure 5.3h).

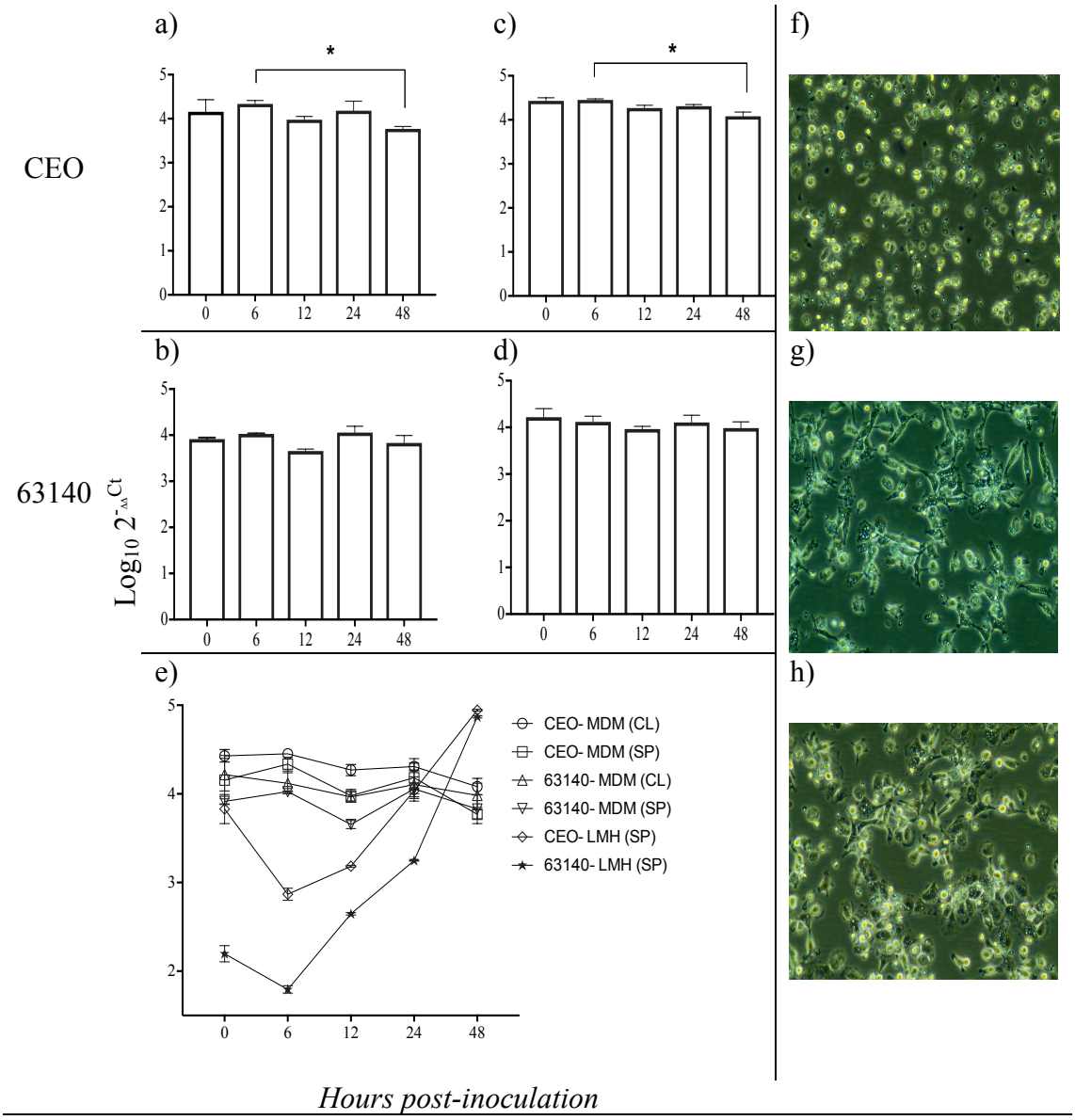

Figure 5.4. Growth kinetics of ILTV vaccine strain CEO and virulent strain 63140 in monocyte-derived macrophages (MDM) and LMH cells. Mean viral genome load in MDM supernatant after CEO (a) or 63140 (b) inoculation, and in the cell lysate after CEO (c) or 63140 (d) inoculation at 0, 6, 12, 24, and 48 hours pi. Growth kinetics comparison of the CEO vaccine and virulent strain 63140 in the supernatant (SP) and cell lysate (CL) of MDM cells versus in the supernatant (SP) of LMH cells at 0, 6, 12, 24, and 48 hours pi (e). Absence of ILTV cytopathic

effect in MDMs (f), syncytial cell formation in MDMs inoculated with CEO vaccine (g) or 63140 (h).

CHAPTER 6

GENERAL DISCUSSION

Infectious larynotracheitis (ILT) is one of the most economically significant respiratory diseases in the poultry industry. The disease is caused by the avian *alphaherpesvirus Gallid alpha herpesvirus 1* (GaHV-1) also known as infectious laryngotracheitis virus (ILTV). Currently the disease is controlled by vaccination with live-attenuated and/or recombinant viral vector vaccines. The two ILTV live-attenuated vaccines used in the field are the chicken embryo origin (CEO) vaccines and the tissue culture origin (TCO) vaccine. Both, the CEO and TCO vaccines are administered through the mucosal routes inducing effective protection against the disease (Gelenczei & Marty, 1964; Fulton et al., 2000). However, despite their efficacy these vaccines can establish latency (Bagust et al., 1986; Hughes et al., 1991) and failure to uniformly vaccinate flocks, particularly with CEO vaccine, can enhance the potential for virus shedding, virus circulation in the field and consequently regain virulence by selection of vaccine subpopulations that become established as vaccine revertants when allowed to circulate in the field (Fulton et al., 2000; Garritty, 2008). On the other hand, two types of recombinant viral vector vaccines carrying ILTV glycoproteins are commercially available: the fowl-pox virus (FPV) and herpesvirus of turkey (HVT). Different from live attenuated vaccines, recombinant viral vector do not regain virulence, they do not reactivate from latency and do not transmit bird-to-bird (Garcia, 2016). However, it has been suggested that recombinant viral vector vaccines induce weak mucosal immune responses (Gimeno et al., 2011), and have a limited ability to decrease shedding of challenge virus as compared to the CEO vaccine (Vagnozzi et al., 2012). Understanding the mechanism by which antigen presenting cells (APCs) in the eye associated

lymphoid tissue are activated and/or inhibited after stimulation with ILTV antigens would reveal key components of the innate immune responses and their role in directing the adaptive immunity. This knowledge is necessary for the development of viral vector, or subunit vaccines, and adjuvants that could effectively trigger virus specific T cell responses after mucosal vaccination via eye-drop, the drinking water or spray.

The hypothesis behind this work was that the local immune responses in the head-associated lymphoid tissues (HALT) of chickens will dictate the level of ILTV replication in the upper and lower respiratory tract and consequently will influence the outcome of infection. This research concentrated in deciphering: (1) the level of CEO vaccine and virulent strain 63140 replication in the conjunctiva, Harderian gland, the upper and lower respiratory tract after delivering the virus through different mucosal routes of administration (ocular, intranasal, oral, and intratracheally); (2) to determine key components and changes of the immune cell populations in the eye associated lymphoid tissue after ocular stimulation with a CEO vaccine and a virulent strain of ILTV. How these changes may contribute and/or influence in the outcome of the disease are discussed.

The objective of the first study (Chapter 3) was to investigate how the route of viral entry ocular, oral, intranasal or intra-tracheal influences the pattern of replication for virulent strain 63140 and the CEO vaccine in the conjunctiva, Harderian gland, nasal cavity and trachea. From this study it was determined that the mucosal route of viral entry of both strains, CEO vaccine and 63140 virulent strain, greatly influenced patterns of lytic replication in the conjunctiva and trachea but did not disturbed viral lytic replication in the nasal cavity. In contrast, in the Harderian gland, independently of the route of inoculation, neither microscopic lesions

characteristic of lytic replication nor massive lymphocytic infiltration were detected. Whereas viral genomes of the CEO and 63140 strain were detected and viral antigen was identified in potential mononuclear cells. Overall from these results it was concluded that interactions of the virus with the head associated lymphoid tissues (HALT), mainly in the NALT and CALT, direct the outcome of infection after mucosal entry of the virus. Also in the absence of ILTV lytic replication, the Harderian gland may serve as an exclusive site of virus uptake within the eye associated lymphoid tissue.

The objective of the second study (Chapter 4) was to assess the cellular dynamics associated to the local cell immune response that contribute to disease protection and/or influence the outcome of the disease after ocular stimulation with ILTV CEO vaccine and the virulent 63140 strain. To this end, dynamics of lymphocyte populations and assessment of cytokines that favor the cell-mediated immune response were investigated in CALT and HG after ocular inoculation of five-week-old specific pathogen free (SPF) chickens with CEO and 63140 strains. Overall this study confirmed an important role of the local cell-mediated immunity and its contribution to disease resistance and/or disease outcome. This was supported by the increase in $CD8^+$ cells, interferon gamma and granzyme A in CALT which occurred in parallel to CEO vaccine clearance from the conjunctiva epithelium. While in later stages of ILTV replication, of either the CEO vaccine or 63140 virulent strain, an increase in IgA^+ B cells occurred indicating that local antibody response did not played a role in clearance of the vaccine or the virulent strains. This study provided evidence of the different roles that the CALT and HG play during ILTV immune responses. Different from CALT, in ILTV stimulated HG increases in $CD4^+$ T and IgM^+ B lymphocytes were detected in later stages of ILTV replication, which was indicative of B cell proliferation. Also unlike in the CALT, in the HG $CD8^+$ cell populations

remained unaltered. However increased transcription of IFN-γ and granzyme A was evidence that the HG also played a role in the cytotoxic response after ILTV stimulation. Additionally, this study revealed the ability of ILTV, in particular the virulent strain 63140, to circumvent the immune response by delaying transcription of IL-12 and downregulating expression of the major histocompatibility complex (MHC) II^{Hi+}. The CEO vaccine and the 63140 strain induced an abrupt decrease in $CD4^+$ cells in the CALT early post-infection. Whether this $CD4^+$ T cells decrease was a result of immune evasion by either viral strains or resulted from the migration of $CD4^+$ T cell from the CALT to the conjunctiva epithelium or other respiratory epithelium needs to be investigated. On the whole, this study confirmed the essential role of the local cell mediated immune response to disease resistance, underscored the distinctive roles of CALT and HG when stimulated, and provided a first glimpse that ILTV can circumvent local immunity by delaying innate responses and downregulating MHC class II cellular expression.

In the interest of attaining a wider representation of the local cell-mediated immunity elicited by ILTV a third study was conducted. It´s objective was to determine the mononuclear phagocyte (MNP) composition of the CALT and HG of unstimulated and ILTV stimulated chickens by assessing the surface expression of colony stimulating factor 1 receptor (CSF1R) and MHC II expression. Five-week-old specific pathogen free (SPF) chickens were inoculated via the ocular route with CEO vaccine and the virulent strain 63140. Also the ability of the CEO and 63140 strains to infect and induce apoptosis in chicken monocyte-derived macrophages (MDM) was evaluated. In general, the results from this study demonstrated that MNP composition of the CALT and the HG showed two distinct cell populations, $CSF1R^+/MCH\text{-}II^{Lo+}$ and $CSF1R^+/MCH\text{-}II^{Hi+}$, which were expressed in higher percentages in the HG than in the CALT. Upon stimulation with either CEO vaccine or virulent strain 63140 an increase in both

populations was observed in the CALT, while in the HG, a sustained reduction was observed from day 1 pi onwards. In the CALT, the CEO vaccine induced a higher expression of $CSF1R^{+}/MCH\text{-}II^{Lo+}$ and $CSF1R^{+}/MCH\text{-}II^{Hi+}$ cell populations than the 63140 strain. This finding was indicative of a robust immune activation generated by the vaccine strain. As a further test of viral-MNP interaction, monocyte-derived macrophages (MDM) cultures were used to assess the replication of CEO vaccine and 63140 virulent strains and to determine if these strains induced apoptosis. In MDMs both CEO and 63140 strains established a semi-productive infection and inhibited apoptosis. Taken together evidence of a semi-productive infection and inhibition of apoptosis of MDMs accompanied with the abrupt decrease of MNPs ($CSF1R^{+}/MCH\text{-}II^{Lo+}$ and $CSF1R^{+}/MCH\text{-}II^{Hi+}$) in the HG after CEO and 63140 stimulation raises the possibility that semi-productive infected MNPs leave the gland and facilitate virus spread while evading the host immune response to ultimately establish latency. These studies most importantly provided a glimpse on the potential relevance that antigen presentation play in the outcomes of cellular immune responses to ILTV. Understanding how APCs in the eye-associated lymphoid tissues are activated and/or inhibited after stimulation with ILTV antigens would reveal key components of the innate immune responses and their role in directing the adaptive immunity. The assessment of the cell dynamics of the eye-associated lymphoid tissues after ILTV stimulation provided a reliable system to assess the local immune response at the mucosal level. Further work will require detailed phenotyping of antigen presenting cells and lymphocyte subsets and their respective stages of activation after stimulation with ILTV vaccines. This knowledge is necessary for the development of viral vector, or subunit vaccines, and adjuvants that could effectively trigger virus specific T cell responses after mucosal vaccination via eye-drop, the drinking water or spray.

REFERENCES

Bagust, T.J., Calnek, B.W., & Fahey, K.J. (1986). Gallid-1 herpesvirus infection in the chicken. 3. Reinvestigation of the pathogenesis of infectious laryngotracheitis in acute and early post-acute respiratory disease. *Avian Diseases, 30*, 179-190

Fulton, R.M., Schrader, D.L., & Will, M. (2000). Effect of route of vaccination on the prevention of infectious laryngotracheitis in commercial egg-laying chickens. *Avian Diseases, 44*, 8-16.

Garcia, M. (2016). Current and future vaccines and vaccination strategies against infectious laryngotracheitis (ILTV) respiratory disease of poultry. *Veterinary Microbiology, 206*, 157-162.

Garritty, A.D. (2008). ILTV vaccination-challenging the dogma. *The Poultry Informed Professional*, 1-5.

Gelenczei, E.F., & Marty, E.W. (1964). Studies on a tissue-culture-modified infectious laryngotracheitis virus. *Avian Diseases, 8*, 105-122.

Gimeno, I.M., Cortes, A.L., Guy, J.S., Turpin, E., & Williams, C. (2011). Replication of recombinant herpesvirus of turkey expressing genes of infectious laryngotracheitis virus in specific pathogen free and broiler chickens following in ovo and subcutaneous vaccination. *Avian Pathology, 40*, 395-403.

Hughes, C.S., Williams, R.A., Gaskell, R.M., Jordan, F.T., Bradbury, J.M., Bennett, M., & Jones, R.C. (1991). Latency and reactivation of infectious laryngotracheitis vaccine virus. *Archives of Virology, 121*, 213-218.

Vagnozzi, A., Zavala, G., Riblet, S.M., Mundt, A., & Garcia, M. (2012). Protection induced by commercially available live-attenuated and recombinant viral vector vaccines against infectious laryngotracheitis virus in broiler chickens. *Avian Pathology, 41*, 21-31.